PLZF as a Novel Regulator of Dopamine D1 Receptor Signaling

Deserae Ball

Thesis submitted to the University of Ottawa in partial fulfillment of the requirements for the M.Sc. degree in Neuroscience

Department of Cellular and Molecular Medicine

Faculty of Medicine

University of Ottawa

Abstract

G protein-coupled receptors (GPCRs) represent the largest and most diverse family of transmembrane receptors, mediating a wide range of physiological processes through the activation of intracellular signaling cascades. Among these, dopamine receptors (DARs) play a central role in regulating critical neurological functions such as movement, cognition, and reward. The D1-class dopamine receptors (D1R and D5R), particularly the D1R, have been implicated in several neurological disorders such as Parkinson's Disease (PD) and Levodopa-Induced Dyskinesia (LID). Therefore, more research is needed to better understand novel methods to be able to treat these dysfunctions. A major topic in D1R signaling is the role of proteins that interact with the receptor intracellular domains. The Promyelocytic Leukemia Zinc Finger (PLZF) protein was previously identified through yeast two-hybrid screening in the Tiberi lab as a novel interacting partner of the D1-class receptors. Unpublished studies in our lab found that PLZF, a multifunctional nuclear protein and transcriptional regulator with major roles in brain development, exerts subtype-specific effects on D1-class signaling and trafficking. Previous studies have also shown that PLZF forms a complex with both the agonist-stimulated GPCR AT_2R and the constitutively activated Gαo subunit. However, its mechanistic role in D1R signaling and the desensitization process remains poorly understood.

In this thesis, I investigate the phosphorylation of the proximal cytoplasmic tail (CT) residues of the D1R, focusing on the contribution of the more distal CT domains in addition to complex formation with PLZF. Using HEK293 cells transfected with Flag-tagged wild-type or truncated D1R constructs (fVal388-STOP, fSer417-STOP, fSer431-STOP), receptor phosphorylation was assessed at specific proximal residues (Thr354 and Ser372/Ser373) through immunoprecipitation studies following dopamine stimulation. The results demonstrate that truncation of the distal domains of the D1R CT sequentially impairs phosphorylation of upstream residues, suggesting a hierarchical phosphorylation pattern. Co-expression of HA-tagged PLZF with D1R significantly decreases phosphorylation at these proximal sites, and this

effect was modulated in truncated receptors, indicating that PLZF-mediated regulation occurs via specific distal domains of the CT.

Furthermore, GST pulldown assays revealed that PLZF interacts with both the IL3 and CT domains of D1R, with PLZF exhibiting a stronger affinity for the CT. Additionally, co-immunoprecipitation studies show that PLZF displays dynamic recruitment to the IL3 and CT, with truncation of either IL3 domain modulating the degree of binding under basal and dopamine-stimulated states, as well as retainment of recruitment with complete removal of the CT. Collectively, this work identifies PLZF as a key regulator of D1R signaling and provides new insight into the molecular mechanisms controlling dopaminergic receptor responsiveness. These novel findings may provide a better understanding of the molecular underpinnings involved in disorders compromising the dopaminergic system and potentially inform future therapeutic strategies for dopaminergic dysfunction in neurological disorders.

Table of Contents

List of Figures

List of Abbreviations

AA: Ascorbic acid

AADC: Amino acid decarboxylase

AC: Adenylyl cyclase

AD: Alzheimer's disease

AngII: Angiotensin II

AP-2: Adaptor protein-2

APL: Acute promyelocytic leukemia

ASD: Autism spectrum disorder

ATRA: all-trans retinoic acid

AT1R: Angiotensin II type 1 receptor

AT2R: Angiotensin II type 2 receptor

ATP: Adenosine triphosphate

Barkor: Beclin 1-associated autophagy-related key regulator

BCS: Bovine calf serum

Bmax: Maximal binding capacity

BSA: Bovine serum albumin

BTB: Bric a brac, tramtrack and broad

Ca2+: Calcium

CAMKII: Calmodulin-dependent kinase II

cAMP: Cyclic adenosine monophosphate

CDK: Cyclin-dependent kinase

CK: Casein kinase

CNS: Central nervous system

Co-IP: Co-immunoprecipitation

COMT: Catechol-O-methyltransferase

CREB: cAMP response element-binding protein

CT: Carboxyl-terminus

Cul3: Cullin-3

Cys: Cysteine

DARRP-32: Dopamine and cAMP-regulated phosphoprotein 32

D1R: Dopamine D1 receptor

D2R: Dopamine D2 receptor

D3R: Dopamine D3 receptor

D4R: Dopamine D4 receptor

D5R: Dopamine D5 receptor

DA: Dopamine

DAG: Diacylglycerol

DAR: Dopamine Receptor

DARPP-32: DA and cAMP-regulated phosphoprotein 32

DAT: Dopamine transporter

DHX: Dihydrexidine

DMEM: Dulbecco's modified eagle medium

DRIP: Dopamine receptor interacting protein

DRN: Dorsal raphe nucleus

EDTA: Ethylenediaminetetraacetic acid

EGFR: Epidermal growth factor receptor

EL: Extracellular loop

ELISA: Enzyme-linked immunosorbent assay

EMEM: Eagle's minimal essential medium

ENTH: Epsin NH2 terminal homology

ER: Endoplasmic reticulum

ERK: Extracellular signal regulated kinase

FBS: Fetal bovine serum

FGF: Fibroblast growth factors

G-protein: Guanine nucleotide-binding protein

GDNF: Glial cell - derived neurotrophic factor

GDP: Guanosine diphosphate

GEF: Guanine nucleotide exchange factor

GP: Globus pallidus

GPCR: G protein-coupled receptor

GRK: GPCR kinase

GSK3β: Glycogen synthase kinase 3 beta

GST: Glutathione-S-transferase

GTP: Guanosine triphosphate

HB-EGF: Heparin-binding epidermal-like growth factor

HD: Huntington's disease

HDAC: Histone deacetylase

HEK293: Human embryonic kidney 293

HEPES: 4-(2-hydroxyethyl)-1-piperazineethanesulfonic acid

HRP: Horseradish peroxidase

H8: Helix 8 domain

IB: Immunoblot

IL: Intracellular loop

IP3: Inositol triphosphate

L-DOPA: L-3,4-dihydroxyphenylalnine

LID: Levodopa-induced dyskinesia

MAO: Monoamine oxidase

MAPK: Mitogen activated protein kinase

MCAO: Middle cerebral artery occlusion

MEF: Mouse embryonic fibroblast

MEK: Mitogen-activated protein kinase kinase

mGluR5: Metabotropic glutamate receptor 5

MSNs: Medium spiny neurons

mTORC: Mammalian TOR complex

N-CoR: Nuclear corepressors

NAc: Nucleus accumbens

NF-M: Neurofilament-M

NMDAR: N-methyl-D-aspartate receptor

NPC: Neural progenitor cell

NPY: Neuropeptide Y

NSC: Neural stem cell

NSF: N-ethylmaleimide-sensitive factor

N-CoR: Nuclear corepressors

NT: Amino-terminus

PBS: phosphate-buffered saline

PD: Parkinson's disease

PDZ: PSD-95-Disc large Zonula occludens-1

PFC: Prefrontal cortex

PIP2: Phosphatidylinositol biphosphate

PI3K: Phosphoinositide 3-kinase

PKA: Protein kinase A

PKC: Protein kinase C

PLC: Phospholipase C

PLZF: Promyelocytic leukemia zinc finger

PML: Promyelocytic leukemia protein

PMSF: Phenylmethylsulphonyl fluoride

POZ: Poxvirus and zinc finger

PP1: Protein phosphatase 1

PP2B: Protein phosphatase 2B

PSD-95: Post synaptic density 95

PTX: Pertussis toxin

PVDF: Polyvinylidene fluoride

RARE: Retinoic acid response elements

RAMP: Receptor Activity-Modifying Protein

RARα: Retinoic acid receptor alpha

RAS: Renin-angiotensin system

RD2: Repression domain 2

Redd1: Regulated in development and DNA damage responses 1

RER: Renin/prorenin receptor

RGS: Regulators of G-protein signaling

ROC1: Regulator of cullins-1

SAP102: Synapse-associated protein 102

SDS-PAGE: Sodium dodecyl sulfate-polyacrylamide gel electrophoresis

Ser: Serine

Shh: Sonic hedgehog gene

SNc: Substantia nigra pars compacts

SNr: Substantia nigra pars reticulata

snRNP: Small nuclear ribonucleoprotein

SPC: Spermatogonial progenitor cells

STAT3: Signal Transducer and Activator of Transcription 3

STN: Subthalamic nucleus

SUMO: Small ubiquitin-like modifier

TBS-T: Tris-buffered saline containing Tween 20

TCM: Ternary complex model

TH: Tyrosine hydroxylase

Thr: Threonine

TM: Transmembrane

TPA: 12-*O*-tetradecanoylphorbol-13-acetate

ULK1: Unc-51 like autophagy activating kinase 1

Val: Valine

VMAT: Vesicular monoamine transporters

VTA: Ventral tegmental area

Y2H: Yeast two-hybrid

Zbtb16: Zinc finger and bric a brac, tramtrack and broad BTB domain containing 16

ZFP145: Zinc finger protein 145

β1-AR: β1-adrenergic receptor

β2-AR: β2-adrenergic receptor

Acknowledgements

Completion of this thesis would not be possible without the support of many people around me. First and foremost, this research would not be possible without my thesis supervisor, Dr. Mario Tiberi, whose guidance and upmost support throughout my M.Sc. degree I am especially grateful for. Also, I'd like to thank the members of my thesis advisory committee, Dr. Stephen Ferguson and Dr. Diane Lagace, for the helpful advice they have given me during each of our meetings.

I would like to thank all present and former members of the Tiberi laboratory for being so helpful and encouraging. Thank you to Dr. Bassam Albraidy and Bradley Mischuk for your mentorship and for dedicating your time to teaching me new techniques in the lab. Thank you to Patricia Bilodeau for all your technical assistance as well as your constant encouragement. Thank you to Sophie Bechkos for your work with the D5R project as well as Ngoc Dung Ngo for your assistance with the GST-protein purification and pulldown assays. Thank you to Raina Barara, Pierre-Olivier Charette, Victoria Puzej, Étienne Sirois and Reeja Syed for always providing such an enjoyable working environment in the lab. It has been a pleasure to work alongside all of you. Also, thank you to my best friends Mohreet and William for your continuous moral support throughout my degree.

Last but certainly not least, thank you to my parents, Jacquie and Stuart, for your relentless love and support for my success. There is no doubt in my mind that I would not have been able to complete this thesis without your unwavering faith in my abilities. This thesis is dedicated to both of you.

1. Introduction

In this section of my thesis, I will begin by providing an overview of the G-Protein Coupled Receptors (GPCRs), the largest and most diverse family of transmembrane receptors. As these receptors are broadly implicated in physiology and disease, they represent appealing drug targets for the treatment of numerous pathophysiological conditions in humans (Rehman et al., 2023). I will then focus this section on dopamine, an essential neurotransmitter for the regulation of various central nervous system (CNS) functions, which exerts its effects upon binding to GPCRs through several different pathways. Finally, I will finish this section by discussing the Promyelocytic Leukemia Zinc Finger (PLZF), which the Tiberi lab has previously identified as a novel interacting protein with the D1-class (D1R and D5R) of dopamine receptors.

1.1. G Protein-Coupled Receptors

1.1.1. Transmembrane Receptors

The human body is a dynamic system that is constantly receiving signals from the external and internal environment. The plasma membrane requires cell surface or transmembrane receptors to be able to transduce these signals into the cell, which it achieves through the activation of various downstream signaling pathways and responses. There exist three types of transmembrane receptors that can be categorized according to their structure, biological function and ligand: ligand-gated ion channels, enzyme-linked receptors and G protein-coupled receptors (GPCR) (Uings and Farrow, 2000). GPCRs constitute the largest and most versatile family of transmembrane receptors and their signaling plays key roles in mediating numerous physiological functions including vision, olfaction, gustation, neurotransmission, hormone regulation, cellular growth and differentiation (Schiöth and Fredriksson, 2005; Luttrell, 2008). GPCRs are activated by a wide range of endogenous agonists including peptides, hormones, odorants, growth factors and even light (Flower, 1999; Schiöth and Fredriksson, 2005). GPCRs are also implicated in several hereditary disorders including neurological and cardiovascular diseases. In addition, mutated GPCRs were found in 30% of human thyroid tumors, suggesting a link between GPCRS and cancer in humans (Marinissen and Gutkind, 2001). It is understandable why then

over 50% of all therapeutic agents on the market are targeted at GPCRs as well as why their signaling mechanisms are such an important topic of study (Flower, 1999).

1.1.2. Structure of GPCRs

GPCRs have been characteristically classified by their physiological and structural features. All GPCRS share a common structural architype of seven hydrophobic transmembrane alpha-helices (TM1-7) linked by three alternating extracellular loops (EL1-3) and three alternating intracellular loops (IL1-3), followed by an extracellular amino terminus (NT) and an intracellular carboxyl terminus (CT). In terms of sequence conservation, the transmembrane domains remain the most structurally similar due to their key role in managing ligand binding, while the intracellular and extracellular domains vary in size and amino acid composition depending on the class of GPCRs. The intracellular domains (CT and ILs) regulate G protein binding and other downstream signaling and scaffolding proteins. The NT and ELs contain one or more N-glycosylation sites, which are essential for cell surface expression and conformation stabilization and may help to regulate GPCR signaling by orienting the loops away from the ligand binding pocket for unimpeded ligand binding access. A disulfide bridge forms between two cysteine residues in EL1 and EL2 to maintain proper folding conformation of the receptor (Wheatley et al., 2012). There are also two cysteine residues in the CT that get palmitoylated, allowing for the formation of a putative fourth intracellular loop (IL4) (Luttrell, 2008). However, further studies have shown in crystallization of the GPCR structure that the IL4 is part of the alpha-helical domains and is referred to as helix 8 or H8 region (Sensoy and Weinstein, 2015). (**Fig. 1**)

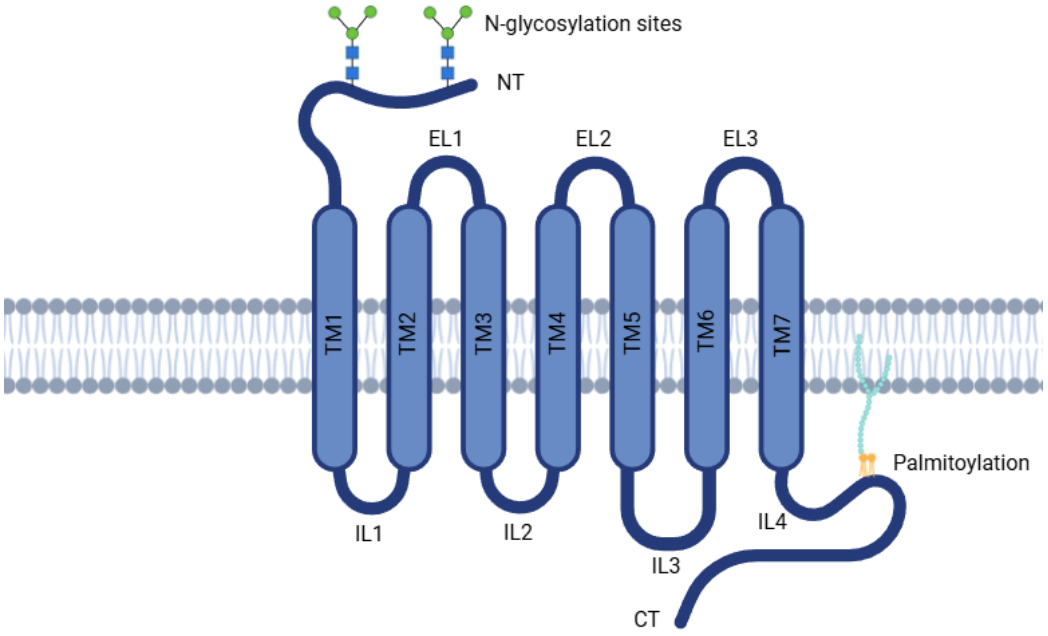

Figure 1. Schematic Diagram of GPCR Structure. A GPCR contains seven alpha-helix TM domains, forming the site of ligand binding. The TMs are connected by three ELs with an external NT segment containing N-glycosylation sites. There are also three ILs with an internal CT segment containing cysteine residues, serving as palmitoylation sites to form the IL4. The ILs and CT allow for interaction with the G-protein. Created with BioRender.com.

1.1.3. Classification of GPCRs

GPCRs have been historically classified using the A-F groups system which was first presented in 1994 by Attwood and Findlay, of which only four of the six GPCR groups were found in mammals. Regarding humans, GPCRs can be divided into five groups in what is known as the GRAFS system, corresponding to Glutamate (G), Rhodopsin (R), Adhesion (A), Frizzled/Taste2 (F) and Secretin (S) (Fredriksson et al., 2003; Schiöth and Fredriksson, 2005; Oldham and Hamm, 2008). Out of the five groups, the rhodopsin family is the largest and most studied group of GPCRs, consisting of 701 total receptors which makes up approximately 80% of all known GPCRs (Oldham and Hamm, 2008). As a result, the rhodopsin family can be further divided into four main groups: α (biogenic amine receptors like dopamine and serotonin receptors as well as opsin and melatonin receptors), β (peptide receptors like ghrelin, oxytocin and neurotensin receptors), γ (somatostatin, chemokine and opioid receptors), and δ (MAS-related receptors, glycoprotein receptors, purin receptors, and olfactory receptors) (Fredriksson et al., 2003).

Though the rhodopsin family has high sequence identity in its TM domains, its intracellular loops as well as the NT and CT exhibit structural diversity in both their length and amino acid residues. Crystallized structures show that the IL2 is the most conserved of the loop regions (20 ± 2 amino-acids), while the IL3 is the most disordered and divergent (41 ± 43 amino-acids). Both the NT and CT exhibit sequence diversity as well, with the NT containing 62 ± 98 amino-acids and the CT containing 53 ± 36 amino-acids (Moreira, 2014). Studies show that both the IL2 and IL3 are important for G-protein coupling, with specific residues demonstrating a role in the interaction of specific types of G-protein alpha subunits. As well, specific amino acid sequences in the TM regions play an important role in the functioning of the rhodopsin family, with about 20 highly conserved amino acids in the cytoplasmic side being important for receptor stability upon activation as well as proper protein folding. Specifically, an aspartate-arginine-tyrosine (DRY) motif at the cytoplasmic border of TM3 is essential for protein stabilization as well as G-protein activation and specificity (Moreira, 2014; Calebiro et al., 2021). Residues E/D3x49, R3x50, and E6x30 form an ionic interaction in the absence of an agonist, known as the “ionic lock”, keeping the receptor in an inactive conformation until an agonist can bind to break this lock (Calebiro et al., 2021).

1.1.4. G-proteins and GPCR Signaling

Crystallization and biophysical studies have demonstrated the large number of conformational changes occurring in the residues of the TM domains during ligand binding and GPCR activation, of which some have been described above. Altogether, these rearrangements result in a small rotation and upward movement of the TM3, movement of three TM domains towards the receptor centre and a larger rotation and outward movement of the intracellular region of TM6. These movements create an opening within the intracellular surface, allowing for heterotrimeric G-proteins and other signaling molecules to bind (Moreira, 2014; Calebiro et al., 2021) (**Fig. 2**). These G-proteins are essential for activating the classical signal transduction pathway of GPCRs and act as a mediator for the activation of downstream effector proteins, allowing for a wide variety of cellular responses to occur. The heterotrimeric G-protein is comprised of three subunits: Gα, Gβ and Gγ. As the β and γ units are strongly bound to each other, they are commonly regarded as one functional unit as they can only be dissociated through protein denaturation (Oldham and Hamm, 2008). Crystallized structures have been generated of each G-protein subunit, with more focus on the Gα subunit due to its predominant role in regulating GPCR activation. The Gα subunit ranges from 39-52 kDa and is composed of two domains: an a-helical domain, composed of a long helical guanosine diphosphate (GDP)/guanine triphosphate (GTP)-binding site enclosed by five structurally divergent helices, and a Ras-like GTPase domain (Luttrell, 2008; Moreira, 2014; Syrovatkina et al., 2017). The GDP/GTP binding site is flanked by two regions known as Switch I and Switch II, which are important for mediating GTP hydrolysis and permit changes in Gα conformation depending on the bound nucleotide. Switch I participates in the catalysis of GTP hydrolysis, with Switch II forming the binding pocket for the γ-phosphate of GTP (Bohm et al., 1997; Syrovatkina et al., 2017). The GTPase domain acts as a guanine exchange factor by phosphorylating GDP to form GTP and additionally serves as the binding site for the Gβγ dimer as well as the GPCR and other effector proteins (Bohm et al., 1997; Oldham and Hamm, 2008).

Based on the functional properties of the Gα protein, heterotrimeric G-proteins have been conventionally classified into four families: Gs/olf, Gi/o, Gq/11, and G12/13. Gs is expressed in most cell types and predominantly couples to stimulatory receptors, while Golf is expressed in olfactory sensory neurons as well as medium spiny neurons of the basal ganglia (Syrovatkina et al., 2017). Gi/o is the largest and most diverse family of G-proteins and couples to inhibitory GPCRs. Gs and Gi/o G-protein families exert their signaling effects through the activation and inhibition, respectively, of adenylyl cyclase (AC). The binding of a ligand to the TM domain of the GPCR shifts the receptor from an inactive to an active state and triggers a conformational change, allowing the conversion of GDP to GTP and dissociation of the Gα subunit from the βγ dimer. Gs catalyzes the conversion of adenosine triphosphate (ATP) into cyclic adenosine monophosphate (cAMP) through the activation of AC, a crucial second messenger molecule for regulating several biological processes. cAMP can subsequently activate cAMP-dependent protein kinase A (PKA), which can then go on to regulate different effector proteins through phosphorylation. In contrast, Gi inhibits the production of cAMP due to the inhibition of AC, leading to inhibition of PKA. In addition to PKA, the GTP-bound Gα subunit as well as the Gβγ complex can interact with different downstream effector proteins. Ion channels can be regulated by individual G-protein subunits, with the inhibition of N-type calcium channels regulated by Gαo and the stimulation of L-type calcium channels regulated by Gαs. Gβγ subunits were first implicated as a functional G-protein signaling entity when it was discovered that Gβγ can activate inward-rectifying K+ channels in cardiomyocytes, regulating the impact of vagal stimulation on cardiac activity (Logothetis et al., 1987). Gβγ subunits can also interact with certain kinases (G protein-coupled receptor kinases or GRKs) involved in receptor desensitization, regulating their activity by allowing for translocation to the plasma membrane to gain access to free receptors (Stoffel et al., 1997; Jones-Tabah et al., 2021).

The activation of Gq proteins can go on to activate phospholipase C (PLC), which can then catalyze the hydrolysis of the phospholipid phosphatidylinositol biphosphate (PIP2) into diacylglycerol (DAG) and inositol triphosphate (IP3). IP3 stimulates receptors located along the endoplasmic reticulum (ER) to release calcium, leading to the activation of protein kinase C (PKC). To restore the heterotrimeric G-protein complex, the GTPase domain of Gα hydrolyzes the GTP back into GDP and reunite the subunits of the heterotrimeric G-protein. This process is typically slow in comparison to other aspects of G-protein coupling. However, the rate can be substantially accelerated through the allosteric binding of GTPase-activating proteins (GAPs), also known as Regulators of G-protein Signaling (RGS) to Gα (Ross and Wilkie, 2000; Sprang et al., 2007).

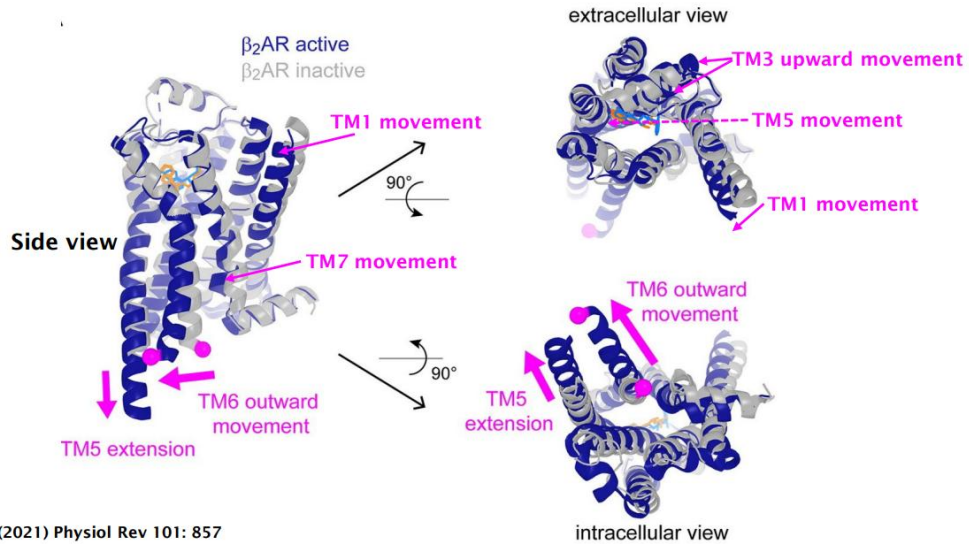

Figure modified from Calebiro et al (2021) Physiol Rev 101: 857

Figure 2. Conformational Changes Occurring in the GPCR During Ligand Binding. Activation of the GPCR results in several rotations and movements of the TM regions to allow for the binding of heterotrimeric G-proteins and other downstream signaling molecules. This includes movement of three TM domains towards the receptor centre, a small rotation and upward movement of TM3 and a larger rotation and outward movement of the intracellular region of TM6. Taken from (Calebiro et al., 2021).

1.1.5. Ternary Complex Model

The ternary complex model (TCM) was first proposed in 1980 by De Lean, Stadel and Lefkowitz to explain the cooperative relationship between the receptor, agonist and G-protein, focusing on the β-adrenergic receptor using a quantitative model. The TCM states that the receptor exists in a single convertible state. In the absence of G-protein coupling, the GPCR has equal affinity for both the inactive and active receptor state and can bind agonists with varying affinities. The coupling of G-proteins to the receptor then shifts this equilibrium towards the active state and stabilizes high-affinity agonist binding. Uncoupling shifts the equilibrium towards the inactive state and agonists display a lower binding affinity. The binding of antagonists remains unaffected regardless of the state of G-protein coupling (Luttrell, 2008). Overall, this theory was highly influential as it was one of the first to link agonist binding affinity with G-protein coupling in GPCRs; however, this model does not account for constitutive activity, where some GPCRs have been shown to signal even in the absence of agonist, as well as the role that partial or inverse agonists play in the state of the receptor. This led to the introduction of a new model known as the extended TCM, which states that there are multiple conformation states that the receptor can exist in: the inactive “R” state where agonists bind with low affinity, and the active “R*” state where agonists bind with high affinity and receptors can signal through even without agonist (Samama et al., 1993; Lefkowitz et al., 1993). It demonstrates that G-proteins enhance agonist binding and stabilizes the receptor in the R* state, while inverse agonists promote a shift in the equilibrium towards the R state and decrease G-protein coupling, keeping the receptor in an inactive conformation and suppressing constitutive activity. Partial agonists and antagonists stabilize both R and R*, keeping the receptor at equilibrium so it has equal affinity for both states.

1.1.6. Regulation of GPCR Signaling

Dampening of the GPCR signal, also known as desensitization, is essential for regulation of GPCR responsiveness and maintenance of cell surface receptor levels. This regulation can be described as either homologous or heterologous depending on the mechanism and affected GPCRs. Desensitization involves a series of sequential steps including phosphorylation by kinases on the GPCR intracellular domains,

internalization of the GPCR from the membrane through endocytosis, and either recycling of the GPCR back to the membrane for reuse or downregulation of GPCRs through degradation. Both forms of desensitization involve the phosphorylation of serine and threonine kinases on the GPCR IL3 and CT (**Fig. 3**). In heterologous desensitization, this phosphorylation is achieved by second messenger-activated protein kinases like PKA and PKC as described above, which can phosphorylate other GPCRs regardless of activation state or agonist occupancy, leading to uncoupling of the G-protein from the GPCR (Luttrell, 2008). It was previously believed that phosphorylation by PKA or PKC was the primary mechanism of GPCR desensitization. However, later studies revealing the phosphorylation and desensitization of the β2-adrenergic receptor (β2-AR) in lymphoma cells lacking PKA, as well as the ability of kinase to only phosphorylate agonist-occupied receptors, demonstrated that there may exist an additional mechanism for desensitization (Kelly et al., 2007).

In homologous desensitization, GPCRs undergo phosphorylation rapidly after agonist binding by specialized GPCR kinases (GRKs). To date, there are six known GRKs; GRK1, 2, 3, 4, 5, and 6, and they can be classified based on their membrane substrate specificity (Stoffel et al., 1997). GRKs are widely expressed through the CNS and periphery, showcasing their important role in regulating a wide set of physiological functions through the modulation of GPCR responsiveness. GRK2 and GRK3 were the first to be identified and purified based on their ability to phosphorylate the β-AR, one of the first receptors to be identified and one of the most extensively studied for its desensitization process. GRK phosphorylation has no impact on G-protein coupling; rather, it serves as a catalyst to increase the affinity of the GPCR for arrestin protein binding to the IL3 and CT domains, thereby preventing further GPCR-G-protein coupling (Ferguson et al., 1999; Luttrell, 2008). Removal of these serine and threonine residues on the cytosolic domains can either weaken or outright eradicate the interaction with arrestin, depending on the receptor. It has been shown that phosphorylation of the β2-AR by GRK2 increases the affinity of the receptor for β-arrestin 1 up to 10-30-fold (Luttrell, 2008).

There are four known arrestin proteins in vertebrates, with the first two expressed solely in the retina to regulate photoreceptor function. The remaining two, arrestin-3 (also known as β-arrestin-1) and arrestin-4 (β-arrestin-2) are found to regulate almost all other GPCR types (Luttrell, 2008). Not only are arrestin molecules essential for the desensitization process but they may also be a necessary component of endocytosis and resensitization. Overexpression of either wildtype β-arrestin 1 or 2 restored receptor sequestration, also known as endocytosis or internalization, of both the truncated and phosphorylation site-deficient β2-AR, whereby the C-terminal tail was truncated to remove all putative β-adrenergic receptor kinase 1 (βARK1 or GRK2) phosphorylation sites or tyrosine residue 326 was mutated to an alanine to block βARK1-mediated phosphorylation and sequestration (Ferguson et al., 1996). This shows that while GRK phosphorylation is an important intermediary step for regulating internalization of the receptor, it is not a required mechanism for inducing receptor internalization in the case of β-arrestin overexpression; rather, the phosphorylation simply increases the affinity for β-arrestin to bind to the receptor.

Clathrin-mediated endocytosis is the main endocytic pathway occurring during desensitization and involves the coating of the plasma membrane vesicle with clathrin and at least 40 other known types of adaptor proteins, including AP-2 and dynamin, to form clathrin-coated pits, facilitating fission of the vesicle from the membrane (Smith and Smith, 2022). Unlike the visual arrestins, β-arrestin contains binding motifs on its C-terminal tail for clathrin and the β2-adaptin subunit of the AP-2 complex, showcasing its ability to form complexes with these proteins to facilitate the targeting of GPCRs to the clathrin-coated pits for internalization (Goodman et al., 1996; Laporte et al., 1999). GPCRs can be grouped based on their affinity for each β-arrestin isoform. Class A receptors, which include β2-AR, μ-opioid and the D1 dopamine receptor (D1R), bind β-arrestin-2 with higher affinity than β-arrestin-1, whereas Class B, which includes angiotensin AT1a and neurotensin 1 receptors, bind each isoform with equal affinity (Oakley et al., 1999). While β-arrestins play a crucial role in inhibiting the GPCR signal, they can also transduce their own signal by connecting GPCRs to various other signaling pathways to

prolong GPCR signaling even in the absence of G-protein activity. One of the most well-studied β-arrestin-dependent signaling pathway involves activation of the mitogen-activated protein kinases (MAPK) cascade. While bound to the receptor, β-arrestin acts as a scaffold to recruit the binding of kinases Raf-1, MEK, and ERK, leading to the activation of ERK and subsequent uptake in the endosomal vesicles (Luttrell et al., 2001; Luttrell, 2008). While normal G-protein-dependent ERK activation occurs within minutes and results in translocation of ERK to the nucleus, β-arrestin-dependent ERK activation is much slower and retains ERK in the endosome and other cytoplasmic locations, affecting the cellular response through reduced phosphorylation of nuclear substrates (Eishingdrelo et al., 2015). This shows that ERK has a wide range of cellular functions that can be vastly regulated by GPCRs depending on the intended response.

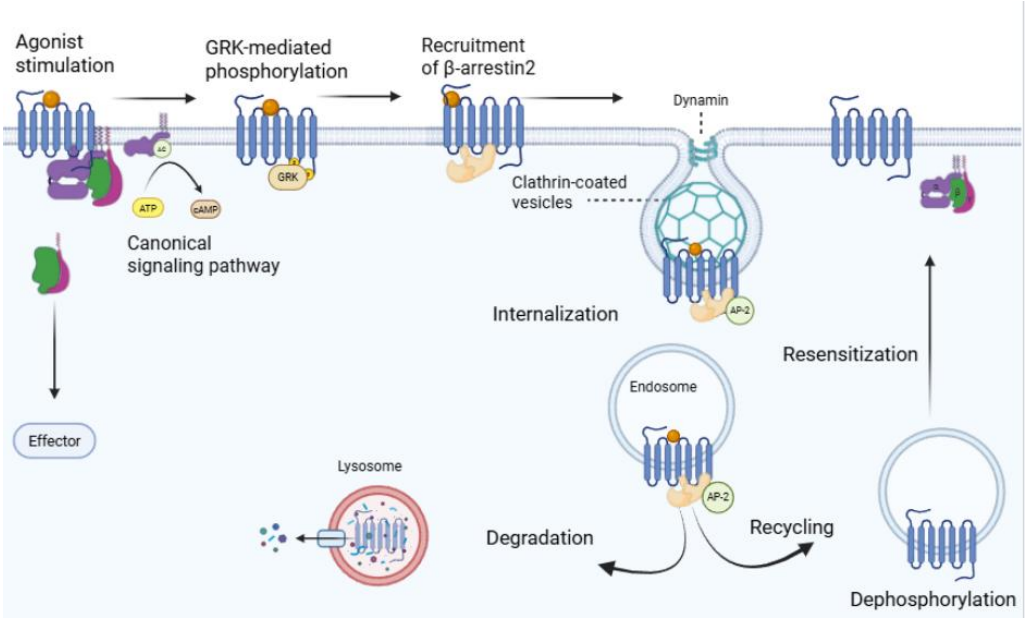

Figure 3. Schematic Diagram of GPCR Desensitization and Trafficking. Moments after ligand binding, the receptor is phosphorylated by GRKs on the CT and ILs, causing rapid disruption and uncoupling of the GPCR from its G protein. This phosphorylation promotes the binding of β-arrestin to the phosphorylated receptor to target the receptor for dynamin-dependent endocytosis through clathrin-coated vesicles. Internalized GPCRS are dephosphorylated and either sorted into lysosomes to be degraded or recycled back to the cell surface. Created with BioRender.com.

1.1.7. Positive Regulation of GPCRs

Beyond GRKs and arrestin proteins, GPCRs can also be positively regulated through their interactions with various other signaling and trafficking proteins, which can be organized into multi-protein "signalsomes" depending on the cellular response. These protein-protein interactions include heterodimerization and homodimerization, where two distinct receptors interact or two of the same receptors interact with each other, respectively. Most GPCRs exist as multimers, as they assemble in this way during synthesis, and dimerization is sometimes essential for trafficking to the plasma membrane (Luttrell, 2008). Dimerization can also modulate GPCR functioning, with heterodimerization between the AT_1A angiotensin receptor and B2 bradykinin receptor enhancing G-protein activation and altering agonist efficacy (Luttrell, 2008). GPCRs can also interact with Receptor Activity Modifying Proteins (RAMPs) and Post-Synaptic Density of 95 kDa (PSD95)-Disc large-Zona occludens (PDZ) Domain-Containing proteins, the latter forming a complex with a PDZ domain-binding motif on the C-terminal of several GPCRs. Both RAMPs and PDZ Domain-Containing Proteins have important roles in modulating receptor function, particularly by regulating receptor trafficking and localization (Luttrell, 2008).

1.2. The Dopamine System

1.2.1. Overview

The tyrosine-derived catecholamine 3,4-dihydroxyphenethylamine, more commonly known as dopamine (DA), is an essential neurotransmitter in the mammalian brain and is essential for the regulation of numerous central nervous system (CNS) functions including locomotion, cognition, mood, learning, reward and pleasure. DA also plays a role in the periphery, regulating functions like olfaction, hormone secretion, cardiovascular functioning and gastrointestinal motility (Missale et al., 1998; Beaulieu and Gainetdinov, 2011; Klein et al., 2019). DA exerts its effects through neural projections, of which its innervations are the most prominent in the brain. Four major dopaminergic pathways exist in the brain: the nigrostriatal, mesolimbic, mesocortical and tuberoinfundibular systems. Many of these pathways exert their effects by projecting through the DA-rich regions of the midbrain, known as the ventral tegmental area (VTA) and the substantia nigra pars compacta (SNc), with the tuberoinfundibular pathway signaling

through the arcuate nucleus and the periventricular nucleus of the hypothalamus towards the pituitary gland to regulate the production of prolactin. The nigrostriatal pathway transmits dopamine from the zona compacta of the SN towards the caudate nucleus and putamen of the dorsal striatum to control voluntary movement and associative learning. Both the mesolimbic and mesocortical pathways begin in the VTA, with the mesolimbic pathway terminating in the nucleus accumbens located in the ventral striatum while the mesocortical pathway terminates in the prefrontal cortex. These pathways regulate reward and motivation as well as executive functioning, respectively (Missale et al., 1998; Klein et al., 2019) (**Fig. 4**). Most of the DA synthesis in the body originates from tyrosine, where it is converted to L-3,4-dihydroxyphenylalanine (Levodopa/L-DOPA) by the rate-limiting enzyme tyrosine hydroxylase. Levodopa can then cross the blood brain barrier into neurons to be converted into DA by L-amino acid decarboxylase (DOPA decarboxylase) and subsequent reactions can convert DA to norepinephrine and then epinephrine (Klein et al., 2019) (**Fig. 5**). Given that DA transmission is so crucial to normal physiology, it is understandable why then dysfunctional dopamine neurotransmission is implicated in many disorders, some of the most well-known being Parkinson's Disease (PD), Levodopa-Induced Dyskinesia (LID), schizophrenia, Huntington's Disease and drug addiction.

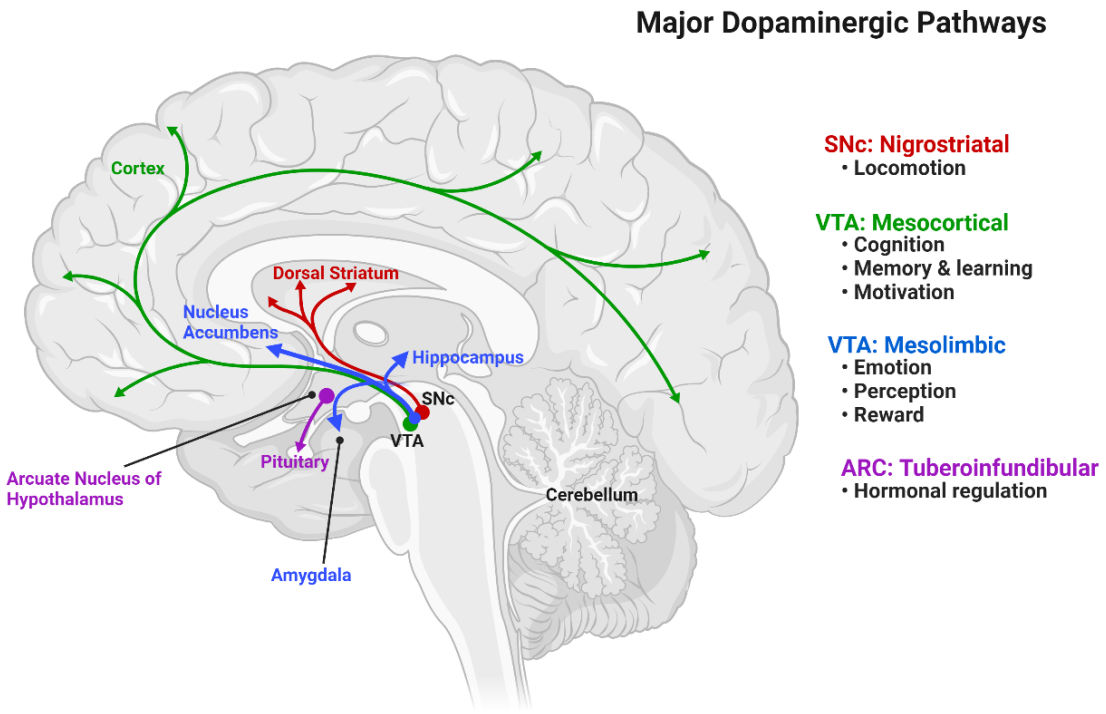

Figure 4. The Major Dopaminergic Pathways in the Brain. There are four main dopaminergic neuronal pathways. The nigrostriatal pathway (highlighted in red) projects from the substantia nigra para compacta (SNc) to the dorsal striatum and is responsible for regulating locomotion. The mesocortical pathway (highlighted in green) projects from the ventral tegmental area (VTA) to the cerebral cortex and regulates cognition, memory, learning and motivation. The mesolimbic pathway (highlighted in blue) projects from the VTA to the ventral striatum/nucleus accumbens (NAc), hippocampus and amygdala, and regulates emotion, perception and feelings of reward. Finally, the tuberoinfundibular pathway (highlighted in purple) projects from the arcuate nucleus of the hippocampus to the pituitary gland and is responsible for the regulation of hormone production. Created with BioRender.com.

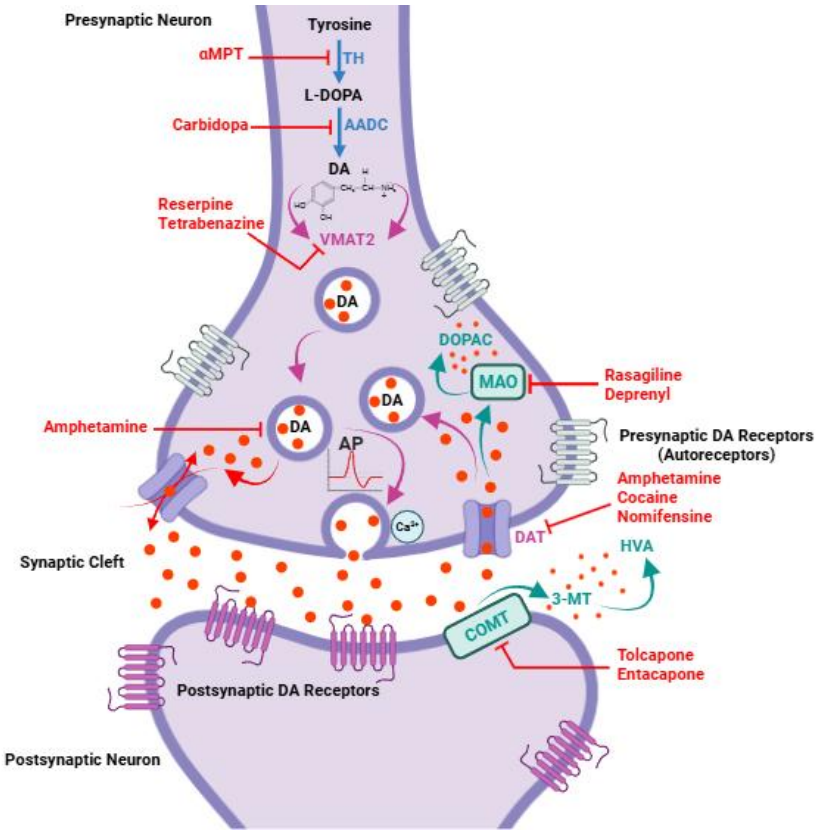

Figure 5. Schematic Diagram of Neuronal Dopamine Synthesis. Dopamine (DA) is synthesized from tyrosine in the presynaptic neuron. Tyrosine hydroxylase (TH) converts tyrosine to L-DOPA during the rate-limiting step. Decarboxylation by aromatic L-amino acid decarboxylase (AADC) converts L-DOPA to DA. DA can then be packaged into storage vesicles by vesicular monoamine transporter 2 (VMAT2) to be released into the synaptic cleft upon generation of an action potential and increase of Ca^{2+} influx in the synaptic terminal. Upon release, DA can either bind to dopaminergic autoreceptors on the presynaptic terminal, or it can activate postsynaptic DA receptors to activate various downstream signaling pathways. Excess DA in the synaptic cleft is either reuptaken by the dopamine transporter (DAT) or metabolized by monoamine oxidase (MAO) and catechol-O-methyltransferase (COMT). Highlighted in red are known drugs that inhibit DA synthesis, release, reuptake and degeneration. Created with BioRender.com.

1.2.2. Dopamine Receptor (DAR) Classification

DA exerts its physiological effects in the CNS and periphery through binding to GPCRs, of which there are five main subtypes (D1R, D2R, D3R, D4R, D5R) that are divided into two classes based on their structural, biochemical and pharmacological properties. The ability of DA to differentially modulate signaling activity through its interaction with a wide set of GPCRs is why DA cannot be simply categorized as either an excitatory or inhibitory neurotransmitter. The D1R and D5R constitute the D1-class, while the D2R, D3R and D4R constitute the D2-class. The D1-class couples to the $G\alpha_{s/olf}$ family of G proteins, thereby activating AC to increase the production of cAMP and stimulate PKA, whereas the D2-class couples to the $G\alpha_{i/o}$ family of G proteins to inhibit AC (Beaulieu et al., 2015; Klein et al., 2019). D2-class receptors are found both pre-synaptically on dopaminergic neurons as well as post-synaptically on dopamine-receptive cells, while D1-class receptors are more frequently observed post-synaptically and rarely localize on presynaptic terminals (Missale et al., 1998; Beaulieu and Gainetdinov, 2011; Klein et al., 2019). As well, the D1-class and D2-class differ in their genetic structure, with D1R and D5R each existing as a single isoform due to the lack of intron sequences in their coding regions, a common characteristic in most GPCR structures. In contrast, several introns are present within the D2-class receptors, with six introns found in the D2R gene, five in D3R and three in D4R, generating different variants of each receptor through alternative splicing (Dearry et al., 1990; Missale et al., 1998). Interestingly, only the D2R generates more than one functional splice variant, referred to as D2S (D2R-short) and D2L (D2R-long), with the long variant differing by an additional 29 amino acids in the IL3. These variants are generated from alternative splicing of an 87 base-pair exon between introns 4 and 5 and have been shown to exhibit distinct physiological, biochemical and pharmacological properties between each other, with D2S being predominantly expressed pre-synaptically and functioning as an auto-receptor whereas D2L is mostly found in postsynaptic terminals (Missale et al., 1998; Beaulieu and Gainetdinov, 2011). Most of the proteins encoded from the D3R variants have been shown to be nonfunctional. For the D4R, several polymorphic variants containing a 48 base-pair repeat sequence in

the IL3 have been discovered, with other repeat sequences up to 11 base-pairs being identified (Missale et al., 1998; Klein et al., 2019).

1.2.3. DAR Structure

Like most other GPCRs, the structure of DARs consists of the alpha-helical 7TM regions along with an extracellular NT linked with EL1-3 and intracellular CT linked with IL1-3. DA receptors display the highest degree of sequence homology within their TM domains. Members of the same class have considerable amino acid sequence conservation, with 80% identity between the TM domains of D1R and D5R, 75% identity between D2R and D3R, and 53% identity between D2R and D4R (Missale et al., 1998; Beaulieu and Gainetdinov, 2011). Overall, the D1R and D5R exhibit about 50% homology in their amino acid residues but over 80% within their TM regions (Tiberi et al., 1991). Structurally, dopamine receptors exhibit the most divergence in their cytoplasmic domains, with the CT being about seven times longer for the D1-class than the D2-class. Both DAR classes contain a cysteine (Cys) residue in the CT, which is thought to be important for anchoring the CT to the membrane as well as enhancing the affinity for cytoplasmic proteins to associate with the membrane. While this cysteine residue is located near the beginning of the D1-class CT, it is present near the end of the CT for the D2-class. Two cysteine residues on the proximal end of the D1R CT act as palmitoylation sites, found at residues Cys347 and Cys351, and are the only sites of palmitoylation on the receptor, as removal of both sites completely abolished palmitoylation. This post-translational modification is known to enhance the binding of cytosolic proteins with the receptor (Jin et al., 1999). The anchoring of the CT to the membrane from Cys palmitoylation has been proposed to form the H8 region, as previously discussed above, and this domain has been demonstrated to confer subtype-specific ligand binding and activation properties as well as regulating β-arrestin-mediated desensitization without directly affecting G-protein coupling selectivity (Tumova et al., 2004; Yang et al., 2019). D1-class receptors exhibit a much shorter IL3 than the D2-class, with a long IL3 being an important characteristic in inhibitory GPCRs for the coupling of Gi proteins to inhibit AC. Akin to all other GPCRs, DARs possess two cysteine residues to stabilize the receptor structure by forming an intramolecular disulphide bridge. Regarding the D1-class, the IL3 and CT remain similar in size but

exhibit sequence divergence, whereas the IL1 and IL2 are both highly conserved in the D1R and D5R (Missale et al., 1998).

Many studies using site-specific mutagenesis have observed the IL3 and CT as major determinants in regulating G-protein coupling and AC activation (Tiberi et al., 1991; Tiberi and Caron, 1994). Therefore, the sequence diversity between the D1-class IL3 and CT may explain the observed distinct functional properties of the D1-class as it relates to DA potency and binding affinity, constitutive activation, AC activation, GRK-mediated phosphorylation and desensitization, and receptor levels (Jensen et al., 1995; Charpentier et al., 1996; Jackson et al., 2000; Lamey et al., 2002; Tumova et al., 2003). The carboxyl terminal domain of the IL3 (IL3-C) has been demonstrated to modulate the equilibrium between the inactive and active conformations of several GPCRs. This activity is regulated by two distinct amino acid residues in the IL3-C of the D1-class, as swapping of these residues between the D1R and D5R resulted in each receptor exhibiting constitutive properties alike to that of the other subtype (Charpentier et al., 1996).

1.2.4. DAR Expression

DA receptors are broadly expressed throughout the CNS as well as periphery regions like the heart, retina and kidneys, with the D1R being the most widely expressed receptor out of all other subtypes. The level of each receptor in the brain is variable depending on the region, with D1R having high expression in the nucleus accumbens, caudate putamen, SN pars reticulata (SNr) and the amygdala with lower expression in the hippocampus, cerebellum and hypothalamus. The D5R exists in significantly lower amounts than the D1R, being expressed in the prefrontal cortex, premotor cortex, the dentate gyrus of the hippocampus and the striatal cholinergic interneurons (Jones-Tabah et al., 2022). After the D1R, the D2R is the 2nd most widely expressed receptor and is found in regions like the nucleus accumbens, striatum, VTA and olfactory tubercule. Though they exist in many of the same brain regions, colocalization between D1R and D2R is rare. The D3R and D4R are expressed at much lower levels than the other subtypes, with the D4R having the lowest expression in the brain. The D4R is mostly localized to the retina, with lower

expression levels in the frontal cortex, amygdala, hippocampus and hypothalamus. The expression of the D3R is more localized to the limbic areas such as the olfactory tubercle and the nucleus accumbens; however, it is still detectable in very low levels in the SNc, striatum, VTA and various cortical areas (Missale et al., 1998; Beaulieu and Gainetdinov, 2011; Klein et al., 2019).

1.2.5. DAR Canonical Signaling Pathway

As previously described, D1-class receptors couple to Gαs/olf proteins to activate AC, increase production of cAMP and activate PKA, whereas D2-class receptors exert the opposite effect by coupling to Gαi/o to inhibit AC. PKA is an important regulator of several different genes and downstream signaling pathways, and has many targets including glutamate and GABA receptors, ion channels, cAMP response element-binding protein (CREB), and dopamine and cAMP-regulated phosphoprotein 32 (DARRP-32), a multifunctional protein predominantly expressed in medium spiny neurons (MSNs) that can act as a feedback loop to regulate PKA activity depending on its post-translational modifications. Activated PKA can go on to phosphorylate DARRP-32 on its Threonine 34 (Thr34) residue, promoting its inhibitory activity on protein phosphatase 1 (PP1), an enzyme responsible for histone dephosphorylation. On the other hand, the inhibition of PKA activity during stimulation of D2-class receptors reduces DARPP-32 phosphorylation at Thr34, preserving PP1 activity and histone dephosphorylation. Dephosphorylation of DARPP-32 can also be promoted through casein kinase 1 (CK1), which phosphorylates DARPP-32 at Serine 137 to downregulate PKA-mediated phosphorylation at Thr34. The activation of calmodulin-dependent protein phosphatase 2B (PP2B/calcineurin) through increased calcium concentrations from D2-class receptor activation can dephosphorylate Thr34. DARPP-32 can also be regulated through phosphorylation on its other residues. For example, cyclin-dependent kinase 5 (CDK5) can phosphorylate DARPP-32 at Threonine 75 (Thr75), thereby blocking the inhibition of PP1. Casein kinase 2 (CK2) can phosphorylate DARPP-32 at Serine 97/102 to enhance PKA-mediated DARPP-32 phosphorylation (Beaulieu et al., 2015; Klein et al., 2019). Therefore, D1-class stimulation enhances PKA-mediated signaling by rendering its potential gene targets more accessible for transcription and expression through the activation of DARPP-32.

1.2.6. DAR Non-Canonical Signaling Pathway

Aside from the regulation of AC activity and cAMP production through coupling to Gs/olf or Gi/o, there is evidence suggesting that the D1R can couple to Gαq proteins, modulating the activity of PLC; however, the physiological conditions regulating this manner of signaling remain poorly understood. PLC catalyzes the production of IP3 and DAG, increasing intracellular calcium levels and activating PKC, respectively. Intracellular calcium production can also activate PKC variants such as the calcium/calmodulin-dependent PK II (CAMKII) and the protein phosphatase calcineurin/protein phosphatase 2B (PP2B). This has been suggested to occur primarily through the formation of D1R-D2R heterodimers, which are co-expressed in small populations of MSNs in the nucleus accumbens as well as certain regions of the basal ganglia. However, the contribution of the D2-class in regulating PLC-mediated signaling is unclear, as some studies have demonstrated the regulation of PLC by D1-class receptors in vivo without activation of D2-class receptors, as well as a lack of Gαq/Gα11 coupling to D1R-D2R heteromers (Beaulieu et al., 2015; Frederick et al., 2015). There have been several mechanisms proposed to explain the Gαq signaling seen in vivo. One possible explanation is that PLC activation and calcium mobilization may be Gβγ-dependent, as prior studies have shown sequestration of Gβγ to the membrane ablated the calcium response in response to D1R and D2R activation (Chun et al., 2013; Jones-Tabah et al., 2021). As well, the type of agonist bound may be an important factor in the mobilization of calcium, as several D1R agonists from the benzazepine family appear to differentially effect calcium mobilization, with 6-chloro-2,3,4,5-tetrahydro-1-(3-methylphenyl)-3-(2-propenyl)-1H-3-benzazepine-7,8-diol (SKF83822) selectively activating D1R-mediated cAMP production with no effects on calcium movement, whereas 6-chloro-2,3,4,5-tetrahydro-3-methyl-1-(3-methylphenyl)-1H-3-benzazepine-7,8-diol (SKF83959) selectively activates calcium release with no effect on cAMP production (Jin et al., 2003; Chun et al., 2013). However, the results of these studies are controversial as a study by D'Aoust and Tiberi found that SKF83959 mediates AC activation in HEK293 cells expressing low levels of D1R and D5R (D'Aoust and Tiberi, 2010) (**Fig. 6**).

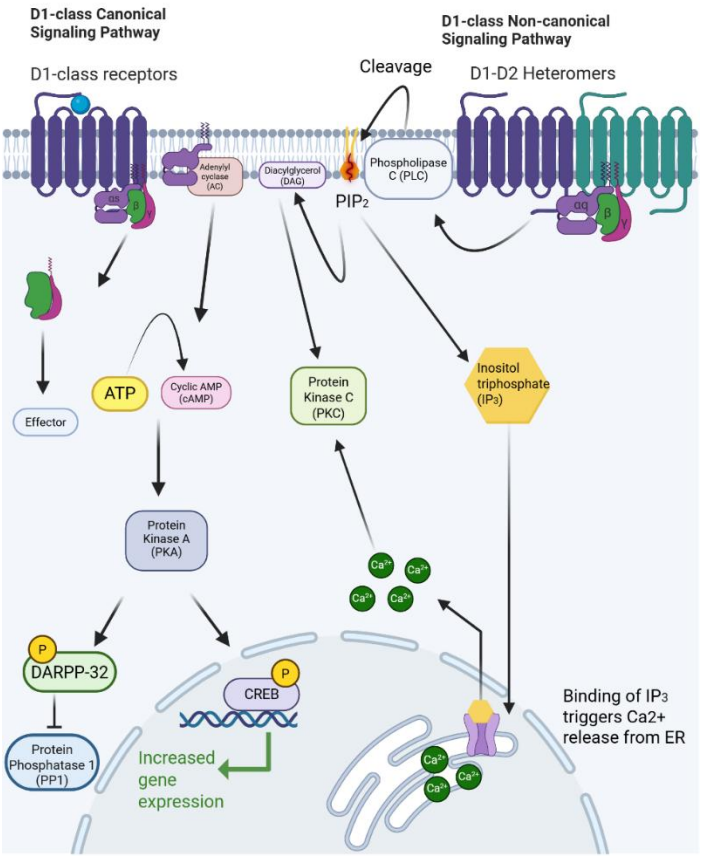

Figure 6. Schematic Diagram of the D1-Class Canonical and Non-Canonical Signaling Pathway. The D1-class of receptors primarily signal through the Gαs/olf coupled pathway AC to increase intracellular cAMP. This action subsequently stimulates PKA to activate the inhibitory function of DARPP-32 on PP1, as well as phosphorylates CREB to transcribe genes. The non-canonical pathway, primarily acting through D1R-D2R heterodimers signals through Gαq to stimulate PLC. PLC catalyzes the hydrolysis of PIP2 to produce DAG and IP3. IP3 production leads to a release of intracellular calcium from the ER. This production of calcium, along with DAG, can activate PKC. Created with BioRender.com.

1.2.7. Regulation of DARs

Like other GPCRs, DARs undergo agonist-mediated desensitization to regulate their physiological responsiveness. As previously described, serine and threonine residues on the IL3 and CT are phosphorylated by second messenger-dependent PKA or PKC as well as GRKs to induce endosomal internalization and sorting of the DAR to be degraded or recycled back to the membrane (Tiberi et al., 1996; Mason et al., 2002). There are seven known members of GRKs, and it has been demonstrated that each DAR subtype can be regulated by different subsets of GRKs. The D1R can act as a substrate for GRK2, GRK3 and GRK5, with GRK3 substantially enhancing the desensitization of D1R relative to GRK2. Interestingly, cells expressing GRK5 displayed an additional 40% reduction in maximal AC activation of D1R relative to cells expressing GRK2 and GRK3 (Tiberi et al., 1996; Sedaghat and Tiberi, 2011). Studies have shown that the CT is the predominant D1R domain for GRK phosphorylation as well as the IL3 to a lesser extent, with GRK-mediated phosphorylation of the CT thought to act as a primer to facilitate subsequent IL3 phosphorylation. It has been thought that the IL3 and CT are in close association with each other under basal conditions; however, phosphorylation of the CT and IL3 alters conformation of the IL3 to allow binding of arrestin molecules, inducing receptor internalization (Kim et al., 2004). Site-directed mutagenesis of serine and threonine residues in the IL3 and CT of D1R have revealed that agonist-induced phosphorylation is mediated by individual residues, as isolated substitution of Thr 360 and its adjacent residue Glu 359 to alanine completely abolished D1R phosphorylation and desensitization. Although there is no definitive consensus on the exact CT residues phosphorylated by each GRK, studies have shown that GRK2 preferentially phosphorylates serine and threonine residues flanked by acidic amino acid residues towards the CT side, whereas GRK5 typically acts on serine residues flanked by basic amino acid residues towards the NT side (Lamey et al., 2002). Studies with *in-vitro* cellular systems have shown that overexpression of GRK2 enhances phosphorylation of the D1R, D2R and D3R, showcasing a predominant role for GRK2 in mediating DAR desensitization (Gainetdinov et al., 2004). However, as deletion of the GRK2 gene in mice results in embryonic lethality (Jaber et al., 1996), it is impossible to know the exact role of this kinase in DAR regulation. Altogether, it can be

postulated that the degree of desensitization and regulation of DAR signaling is critically dependent on the manner of GRK recruitment and its phosphorylation pattern.

1.2.8. Direct and Indirect DAR Signaling Pathways

As previously discussed, the striatum is the primary input structure regulating motor function in the dopaminergic system and is a major component of the basal ganglia, the major neuronal network for motor control comprised of the external globus pallidus (GPe), internal globus pallidus (GPi), the subthalamic nucleus (STN) and the SN (Smith et al., 1998; Thibault et al., 2013; Gerfen, 2023). The regulation of movement by the basal ganglia is complex and involves the processing and transmission of information from the motor cortex through two separate and parallel pathways, known as the indirect and direct pathways. These pathways are formed from the axons of GABAergic MSNs, the predominant cell type of the striatum, which send and receive excitatory afferent signals from thalamic and cortical glutamatergic fibers as well as dopaminergic neurons from the SNc at their dense dendritic projections (Thibault et al., 2013). MSNs in the direct pathway make inhibitory connections with the GPi and the substantia nigra pars reticulata (SNr), which in turn decreases the degree of inhibitory output towards the thalamus. The disinhibited thalamus can then send excitatory signals back to the motor cortex to facilitate the initiation and execution of motor activity. In contrast, MSNs in the indirect pathway make inhibitory connections with the GPe, reducing the inhibition of the STN. Instead of directly signaling to the thalamus, the disinhibited STN excites the GPi and SNr, increasing inhibition of the thalamus. Thalamic activity to the motor cortex is subsequently decreased and motor activity is suppressed (Thibault et al., 2013; Smith et al., 1998). MSNs in the direct pathway have been found to express very high amounts of D1R with very little presence of D2R, whereas MSNs in the indirect pathway express high levels of D2R with minimal D1R expression.

1.2.9. Dysfunctional DA Signaling and Treatments

Understanding the role that DARs play in regulating motor function through these pathways is important, especially when looking at how this signaling becomes dysregulated in diseases affecting the dopaminergic system. It was first established in the early 1960's through the pioneering work of Arvid Carlsson and Oleh Hornykiewicz that Parkinson's Disease (PD) results from dopamine neuron degeneration in the striatum. This degeneration creates an imbalance in the activity of the direct and indirect pathways, causing a relative overactivity of the indirect pathway. The loss of dopamine neurons in the SN leads to dopamine deficiency in the basal ganglia, resulting in increased thalamic output to the motor cortex through the indirect pathway whereas the output is decreased in the direct pathway. This mechanism is thought to be the primary cause of the slow bradykinetic movements, muscle rigidity and tremors that are frequently experienced by patients with PD. In contrast, Huntington's Disease (HD), a neurodegenerative disorder with elevated dopamine levels and involuntary hyperkinetic motor symptoms as hallmark symptoms in early stages of the disease, is associated with an imbalance in favour of the direct pathway (Smith et al., 1998; Klein et al., 2019; Gerfen, 2023). While L-Dopa is still the most effective and commonly used treatment to boost endogenous dopamine synthesis in PD patients, it only provides therapeutic benefits in lessening the symptoms of PD and does not impact the neurodegeneration of dopamine neurons. Therefore, PD continues to progress even with continuous L-Dopa treatment, resulting in reduced clinical effectiveness over time.

One obstacle with the use of L-Dopa to treat PD is the development of Levodopa-Induced Dyskinesia (LID), which frequently occurs in PD patients after long-term use of L-Dopa. This disorder exhibits similar symptoms to that of PD, with patients experiencing slow involuntary movements and muscle contractions, and presents as an additional challenge in being able to find appropriate pharmacological interventions to treat PD. Fortunately, new D1R agonists are being developed that show promise in replacing L-Dopa. These agonists act to shift striatal activity towards the direct pathway and alleviate motor impairment, with these treatments being largely successful at treating symptoms in animal model of PD. These agonists can be categorized into four main classes: Benzazeprine agonists,

Tetrahydroisoquinoline agonists, Isochromans, and Non-catecholamine agonists (Jones-Tabah et al., 2021; Klein et al., 2019). Though these drugs appear beneficial in treating PD symptoms, they remain limited in their clinical effectiveness for a variety of reasons, such as the presence of adverse effects, rapid tolerance buildup, short half-life and the lack of D1-class selectivity. Though the exact causes of LID are yet to be fully understood, it is thought that the hypersensitization of the D1-class is a significant contributing factor. Due to their perceived structural similarities and high degree of sequence homology, it has not been possible so far to pharmacologically differentiate between the D1R and D5R, with agonist affinities being almost identical between the two receptors (Missale et al., 1998). Other effective therapeutic treatments have included lesioning of the GPi as well as deep brain stimulation of the STN to reduce excitatory output to the GPi, thereby improving motor cortical activity (**Fig. 7**).

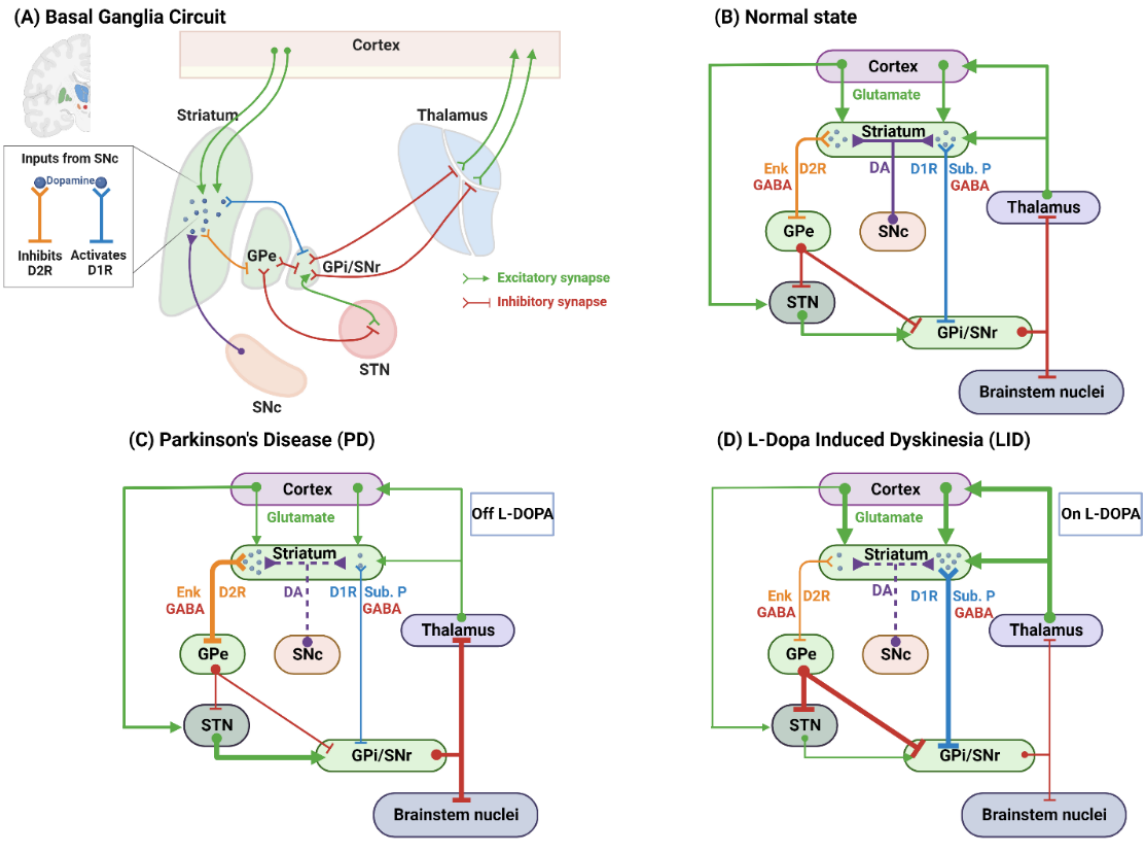

Figure 7. Schematic Diagram of the Direct and Indirect Circuits of the Basal Ganglia and Thalamus in Normal and Diseased States. (A) The basal ganglia consist of the striatum, the internal and external segments of the globus pallidus (GPi and GPe, respectively), the substantia nigra pars compacta (SNc), the substantia nigra pars reticulata (SNr) and the substantia nigra (STN). Together, these structures are linked to form an intricate network of excitatory and inhibitory connections, depicted in the green and red lines, respectively. (B) The striatum receives excitatory glutamatergic signals from the cortex. The striatum can then send inhibitory GABAergic signals through the direct pathway (depicted in blue), projecting to the GPi/SNr, and the indirect pathway (depicted in orange), projecting to the GPe. The GPe can then send inhibitory output signals to the GPi/SNr and the STN, the latter of which can excite the GPi/SNr. Inhibition of the GPi/SNr modulates thalamic and brainstem activity to promote or suppress locomotion. (C) The degeneration of dopaminergic neurons in the striatum during Parkinson's Disease (PD) results in decreased inhibitory output to the GPi/SNr through both pathways, causing an increase in inhibitory output to the thalamus and brainstem nuclei, leading to symptoms of dyskinesia. (D) Treatment

of PD with Levodopa can result in overactivation of striatal neurons, leading to increased inhibition of the GPi/SNr through both pathways. This decreases inhibitory output to the brainstem nuclei and thalamus. Created with BioRender.com.

1.2.10. DAR Pharmacological Properties

As previously discussed, efforts to pharmacology differentiate between the D1-class receptors have fallen short (Missale et al., 1998). However, studies have revealed that there are differences in the pharmacological properties between the D1R and D5R. Specifically, the D5R exhibits greater affinity for agonists, greater constitutive activity and lower affinity for antagonists than the D1R. Dopamine appears to have a 10-fold greater affinity for the D5R than the D1R, whereas antagonists like butaclamol and spiperone exhibit a 6-fold greater affinity for the D1R. Studies show that the D5R exhibits higher basal AC activity than the D1R; however, upon agonist stimulation, the maximal activation of AC was higher for D1R than D5R (Tiberi et al., 1991; Tiberi and Caron, 1994). It has been demonstrated that these distinct properties are attributed to the divergent amino acid residues of the D1-class, as previously mentioned above, specifically within the IL3 and CT as well as the IL4 to a lesser extent.

1.2.11. DAR-Interacting Proteins (DRIPs)

Studies have demonstrated that DARs are regulated throughout their lifecycles by a series of cytoskeletal, adaptor and trafficking proteins known as dopamine-receptor interaction proteins (DRIPs). Many of these DRIPs have been identified using a yeast two-hybrid system (Y2H), in which specific regions of the DAR (usually the CT or IL3) are used to “pull out” potential interacting partners from a human brain cDNA library. This method has revealed that the D1-class and D2-class interact with different sets of DRIPs, likely due to the distinct sequence homology in their cytoplasmic structures, which highlights the important role that these proteins play in regulating the biochemical and physiological functions of each DAR (Bergson et al., 2003). Gaining a better understanding of how these proteins act to modulate DAR activity can help to develop novel treatments for disorders compromising the dopaminergic system, as well as improve their efficacy and safety, through an enhanced understanding of the molecular

mechanisms that are implicated in dysfunctional dopamine signaling. These proteins include cytoskeletal proteins like neurofilament-M (NF-M) and postsynaptic density-95 (PSD-95) as well as adaptor proteins and chaperones like DRiP78, calnexin and calveolin-1 (Wang et al., 2008). NF-M was found to interact with the IL3 of D1R in vivo and regulates trafficking of the receptor, with co-expression of D1R with NF-M in HEK293 cells resulting in over 50% reduction in the Bmax of the receptor as well as reducing D1R-mediated cAMP production. Studies using confocal microscopy showed that NF-M reduced D1R expression at the cell surface while promoting its accumulation in the cytosol. Interestingly, the co-expressed D1R with NF-M that were still present at the cell surface were resistant to agonist-mediated desensitization, demonstrating a role for NF-M in regulating D1R receptor expression and trafficking. Colocalization was found to occur in the pyramidal cells and interneurons of the frontal cortex as well as the striatum, with over 50% of MSNs expressing these proteins together (Kim et al., 2002).

Another protein found to interact with and regulate the activity of the D1R is PSD-95, a scaffolding protein from the membrane-associated guanylyl kinase (MAGUK) family that has been previously shown to regulate the internalization and synaptic transmission of N-methyl-D-aspartate (NMDA) receptors (Kim and Sheng, 2004; Zhang et al., 2007). PSD-95 interacts with the CT of D1R both in HEK293 cells as well as in vivo, within the dendritic spines of mice. Similarly to NF-M, PSD-95 was demonstrated to inhibit D1R-mediated cAMP production as well as reduce cell surface expression of D1R while increasing its expression in the cytosol. Interestingly, PSD-95 does not modulate the agonist binding properties of D1R, showcasing that PSD-95 may only regulate the endocytosis of D1R under constitutive activity. The regulation of D1R by PSD-95 may be dependent on the activity of the endocytic GTPase dynamin, as co-expression of a dominant negative mutant form of dynamin with PSD-95 and D1R completely abolished D1R endocytosis under constitutive activity (Zhang et al., 2007). A study by Li et al showed that PSD-95 can interact with a Gγ subunit, highlighting a potential mechanism for PSD-95 in its ability to regulate D1R activity by possibly modulating G-protein coupling (Li et al., 2006). Unpublished studies in the Tiberi lab have also shown that PSD-95 can interact with the IL3 of D5R in HEK293 cells

as well as in vivo, colocalizing in neuronal dendrites in the hippocampus and cortex, and similarly to its interaction with the D1R, does not affect the binding properties of D5R. However, PSD-95 increases D5R-mediated cAMP production and ERK1/2 activation as well as inhibits agonist-mediated internalization of the receptor through a dynamin- and βArr2-dependent pathway (Bassam Albraidy, Ph.D. Thesis, 2023).

Interestingly, another MAGUK protein has recently been identified as a D1R-interacting protein. SAP102 forms a complex with the IL3 of the D1R and modulates D1R activity oppositely to PSD-95, increasing D1R-mediated cAMP production and ERK1/2 activation. SAP102 also promotes an increase in the agonist-mediated phosphorylation of D1R as residues Thr354 and Ser372/373, but surprisingly, reduces D1R internalization in the presence of an agonist. As it has been previously described in earlier sections that phosphorylation by GRKs increases affinity for βArr2 to bind to the receptor and facilitate receptor desensitization and subsequent internalization, SAP102-D1R complex formation may impede access for GRKs to phosphorylate other cytoplasmic residues that are essential for mediating βArr2 binding, resulting in reduced D1R internalization. This may also explain the increased phosphorylation of Thr354 and Ser372/373, as the GRKs may be overcompensating for the reduced access to these other cytoplasmic residues (Bassam Albraidy, Ph.D. Thesis, 2023)

Furthermore, studies have suggested that the endoplasmic reticulum (ER) chaperone protein DRiP78 interacts with the motif FxxxFxxxF found on the proximal CT portion of the D1R, with its overexpression obstructing its transport out of the ER and reducing its glycosylation and ligand binding. This is thought to occur through blockage of a cargo-selection signal through binding and masking of an ER-export signal, the FxxxFxxxF motif in this case. Endogenous levels of DRiP78 appear to be required for efficient D1R transport outside of the ER., with competing peptides that interfere with DRiP78 reducing this export. This demonstrates a role for DRiP78 in regulating the export of D1R based on its cellular levels (Bermak et al., 2001). Another ER chaperone protein, calnexin, interacts with both D1 and D2-class receptors to regulate the expression of cell surface proteins. Calnexin is important for protein folding and

quality control and additionally acts as a chaperone for newly synthesized glycoproteins. The inhibition of glycosylation, as well as overexpression of calnexin, is shown to partially blocks its complex formation with D1R (Wang et al., 2008). D1R can also localize in caveolae-containing lipid raft microdomains, which was shown in studies using COS-7 cells to be regulated through a complex formation with calveolin-1 at a distinct caveolae-binding motif in the TM7 of D1R (Kong et al., 2007). Prior studies have shown that caveolae have a well-defined role in mediating the activity of several signal transduction pathways in GPCRs (Yamamoto et al., 1998; Allen et al., 2007). This motif regulated the agonist-induced internalization of D1R into caveolin-1-enriched sucrose fractions specifically through a slower PKA-independent pathway, showcasing an important role for caveolae in mediating D1R internalization (Kong et al., 2007).

Finally, the Tiberi lab recently identified the Promyelocytic Leukemia Zinc Finger (PLZF) as a novel interactor with the D1-class receptors and unpublished studies in the lab have shown that PLZF exhibits subtype-specific regulation of D1-class activity. Notably, PLZF increases D1R-mediated cAMP production and ERK1/2 activation while hindering that of D5R. PLZF also decreases the internalization of D1R but increases D5R internalization. The underlying processes controlling these PLZF-mediated changes in D1-class activity remain to be fully understood.

1.3. Promyelocytic Leukemia Zinc Finger (PLZF)

1.3.1. Discovery of PLZF

The PLZF protein, also known by its genetic codes ZFP145 (Zinc Finger Protein 145) or ZBTB16 (Zinc finger and bric à brac, tramtrack, and broad Domain-Containing Protein 16) was first discovered in a patient with acute promyelocytic leukemia (APL), a rare subtype of acute myeloid leukemia resulting from the accumulation of malignant myeloid cells due to blocked differentiation at the intermediate promyelocytic stage. Over 95% of patients diagnosed with APL present with a t(15; 17) (q22;q21) reciprocal chromosomal translocation, resulting in a chimeric gene formed by a fusion between the promyelocytic leukemia (PML) and the retinoic acid receptor alpha (RARα) genes. Patients with this

form of APL can be successfully treated with the administration of all-trans retinoic acid (ATRA) to restore proper differentiation of immature promyelocytes into mature granulocytes. APL has been associated with four known chromosomal translocations, all involving chimeric genes formed from a fusion with the RARα gene and abnormal RAR signaling. In the case of APL involving PLZF, patients present with a 46,xy,t(11;17) (q23;21) translocation without any rearrangement of chromosome 15. Further molecular analysis showed that the RARα was rearranged and fused with PLZF to form two new chimeric genes: PLZF-RARα and RARα-PLZF. The PLZF-RARα fusion protein can then bind to retinoic acid response elements (RAREs) to interfere with normal RARα functioning via a double negative effect. Patients with this form of APL are poorly, if at all responsive to ATRA treatment or conventional chemotherapy (Chen et al., 1993; Li et al., 1997; Shaknovich et al., 1998).

1.3.2. PLZF Structure

The PLZF protein is encoded by the ZBTB16 gene and is found on chromosome 11q23 alongside a series of related genes belonging to the Krüppel-like zinc finger family, a group of eukaryotic proteins containing stabilizing zinc ions and have regulatory roles in DNA transcription and RNA packaging. The human ZBTB16 gene has three functional splice variants composed of seven exons that all exhibit shared homology between exons 3 and 6. The first transcript is 2,477 bp while the second transcript is 2,249 bp in length, both encoding a 673 amino acid long protein. The third transcript is 1,728 bp long and encodes a 550 aa protein. The structure of PLZF is made up of an N-terminal bric à brac, tramtrack, and broad-complex domain, also known as the poxvirus and zinc finger domain (BTB/POZ), a centre RD2 domain and a C-terminal Krüppel-like C2H2 zinc finger domain (Suliman et al., 2012). The BTB/POZ domain is made up of four α-helical segments connected by β-sheet turns. This domain is highly conserved in mammals and is essential for DNA looping, homodimerization and protein-protein interactions, including complex formation with nuclear co-repressors to assert its transcriptional repressive activity. It is 120 amino acids long and has been shown to bear responsibility for the dominant negative properties of the PLZF-RARα fusion seen in PLZF-mediated APL (Zollman et al., 1994; Li et al., 1997; Ahmad et al.,

1998). While the Repression Domain 2 (RD2) domain of PLZF has been less characterized than its other domains, it has been demonstrated in numerous studies that post-transcriptional modifications at this domain modify the transcriptional activity of PLZF. For example, SUMOylation at lysine 242 of PLZF via small ubiquitin-related modifier 1 (SUMO-1) is shown to regulate the ability of PLZF to transcriptionally repress the activity of its target genes (Kang et al., 2003). The nine C2H2 zinc fingers found at the C-terminal domain of PLZF facilitate sequence-specific DNA binding to the regulatory promotor regions of its target genes to carry out its transcriptional control (Li et al., 1997; Sha et al., 2024) (**Fig. 8**).

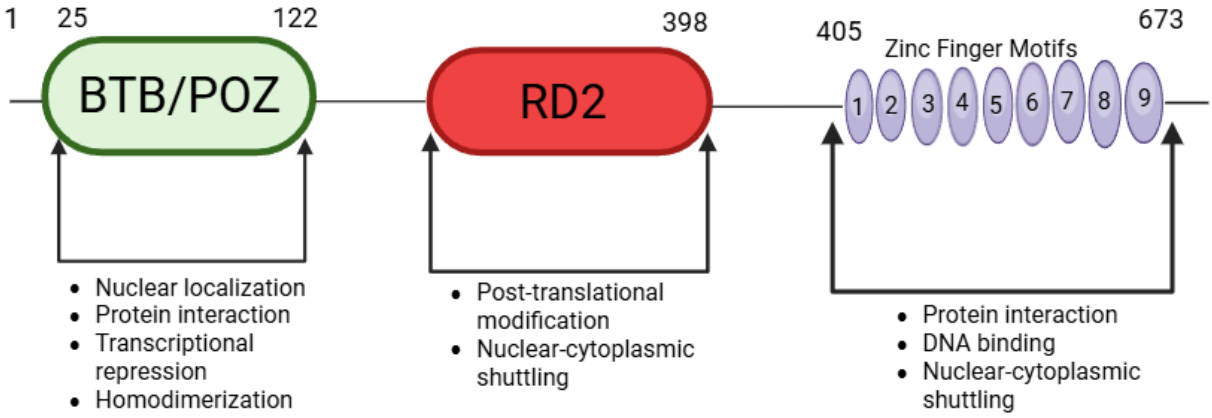

Figure 8. Schematic Diagram of Full-Length PLZF Protein Structure. There are three functional domains within the primary transcript of PLZF. They consist of the NT BTB/POZ domain, the centre RD2 domain, and the CT zinc finger domain, with the important functions of each domain listed below. Created with BioRender.com.

1.3.3. PLZF Functions

1.3.3.1. PLZF and Embryonic Limb Development

PLZF is a master transcriptional regulator and acts through the formation of multi-protein complexes on the promotors of its target genes. These complexes include nuclear corepressors SMRT, Sin-3, and N-CoR, which can recruit class I and II histone deacetylase complexes through its BTB/POZ domain to locally reduce chromatin acetylation, thereby restricting genetic access to transcriptional machinery (Barna et al., 2002; Liu et al., 2016). While PLZF is more commonly known as a transcriptional repressor, it can induce gene expression depending on the molecular context (Kolesnichenko and Vogt, 2011). PLZF plays a wide role in regulating numerous physiological processes including stem cell maintenance and renewal, immune function and embryonic skeletal development. PLZF is directly involved in regulating embryonic formation of the limbs and axial skeleton through its upstream transcriptional repression of the Hox gene family. Hox genes are essential for specifying the correct placement and formation of body parts along the anterior-posterior (AP) axis of the developing embryo. PLZF acts as a growth inhibitor and pro-apoptotic factor in the limb bud as well as alters the spatial expression of the HoxD gene complex, causing homeotic transformations of anterior into posterior structures. ZFP145 inactivation in mice leads to drastic changes in limb skeletal patterning along the AP axis, including fusion of the tibia and fibula as well as interdigital webbing in the hindlimbs and forelimbs (Barna et al., 2000; Barna et al., 2002). The Sonic hedgehog (Shh) gene is also involved in these changes, with Hox5 interacting with PLZF to restrict its expression in the forelimb bud (Xu et al., 2013). PLZF regulates the transcription of Hox genes through close interaction with polycomb family proteins, controlling their ability to bind to cis elements along the Hox gene locus (Barna et al., 2002). Polycomb proteins act as transcriptional repressors of the Hox family as well as other genes involved in spatial patterning through histone modifications (Golbabapour et al., 2013).

1.3.3.2. PLZF and the Cell Cycle

Another function of PLZF relates to its negative regulatory control on the cell cycle. PLZF expression significantly suppresses cell growth and causes cell aggregation in the G0/G1 phase, likely achieved through its inhibition of the cyclin A2 gene (Shaknovich et al., 1998). Interestingly, the RARα-PLZF fusion protein activates the transcription of the cyclin A2 promotor, showcasing a potential role for cyclin A2 in mediating the aggressive phenotype of PLZF-mediated APL (Yeyati et al., 1999). PLZF overexpression was also shown to induce apoptosis and inhibit myeloid differentiation, further demonstrating its role as a pro-apoptotic factor (Shaknovich et al., 1998; Bernardo et al., 2007). PLZF has also been shown to be important in maintaining stem cell homeostasis, particularly in the context of spermatogenesis, by regulating both the maintenance and renewal of stem cells. PLZF is predominantly expressed in undifferentiated spermatogonial progenitor cells (SPCs) and is closely associated with the SPC differentiation-promoting genes Kit, Stra8, Sohlh2 and Dmrt1, repressing their transcriptional activity to preserve the stem cell population (Song et al., 2020; Ghasemi et al., 2024). Mice lacking the ZFP145 gene showed a progressive loss of spermatogonia with age, with increased apoptosis and subsequent loss of tubule structure without any obvious defects in the supporting Sertoli cells (Costoya et al., 2004). Other studies have shown that homozygous mutations in PLZF result in a limited number of normal spermatozoa in young mice and progressive loss of the germ cell line after birth (Buaas et al., 2004). It has been demonstrated that PLZF inhibits the activity of mammalian TOR complex 1 (mTORC1), a signaling complex that is important for maintaining stem cell homeostasis through phosphorylation of various elements of the transcriptional machinery (Ma and Blenis, 2009). The lack of mTORC1 activation in PLZF-knockout SPCs inhibits its response to the glial cell - derived neurotrophic factor (GDNF), an essential growth factor for stem cell self-renewal, via negative feedback to its receptor. PLZF negatively influences mTORC1 activity by inducing expression of the mTORC1 inhibitor Redd1, showcasing the importance of the mTORC1-PLZF functional relationship in preserving the SPC pool and highlighting the dual nature role of PLZF as both a transcriptional repressor and activator (Hobbs et al., 2010; Kolesnichenko and Vogt, 2011).

1.3.3.3. Protective Effects of PLZF

As a transcriptional activator, PLZF can also enhance the interferon immune response by inducing the activity of specific interferon-stimulated genes. Wildtype mouse embryonic fibroblasts (MEFs) exhibited far greater interferon-mediated protection against infection from induced infection of the Semliki Forest Virus than in ZBTB16-knockout MEFs. Induction of the antiviral gene Oas1g was markedly impaired in these knockout mice, causing them to be more susceptible to viral infection than their wildtype counterparts (Xu et al., 2009). PLZF expression also mediates conditioned protection of the cochlea from acoustic trauma, whereby a pre-exposure to a moderate-level sound can protect the inner ear from hearing loss caused by subsequent and more intense sounds. Following a period of restraint stress, whereby mice are subjected to a 12-hour restraint in a ventilated tube followed by 2 hours of acoustic noise exposure, PLZF mRNA becomes upregulated in the mouse cochlea, specifically within the spiral ganglion, organ of Corti and the stria vascularis, as well as within the brain. Mice that were deficient for PLZF did not experience conditioned cochlear protection despite maintaining similar hearing levels as their wild-type counterparts (Peppi et al., 2011).

1.3.3.4. PLZF and Autophagy

Studies have shown that PLZF can regulate the autophagy pathway in cells. Autophagy is an essential intracellular mechanism used to control the accumulation of misfolded proteins through the targeting of autophagosomes and later to lysosomes for protein degradation via the proteasome and recycling of the degraded components. Dysfunctions in the autophagy process can cause buildups of these misfolded proteins and is the cause of many human neurodegenerative disorders like Alzheimer’s Disease (AD), HD and PD. One way that proteins are targeted for degradation is through the ubiquitin system by attaching polyubiquitin chains onto the lysine residues of these protein targets. This system typically involves three enzymes: E1, which mediates the ATP-dependent ubiquitin activation; E2, which conjugates the active ubiquitin molecule and with the help of the E3 ligase, catalyzes its transfer to the target protein (Furukawa et al., 2003; Geyer et al., 2003). Ring domain E3s are one of the most well-studied classes of E3s and form a complex with members of the cullin (Cul) family to mediate binding specificity to its target

substrate. Studies have shown that BTB/POZ proteins act as substrate-specific adaptor proteins with Cul3-based ubiquitin ligases, with the domain being essential for the interaction and ubiquitin-mediated degradation of Btb1p, a yeast protein closely related to the human growth suppression protein BPOZ2 (Geyer et al., 2003). Additionally, PLZF has been demonstrated to form a complex with Cul3 and can transport the protein to the nucleus, inducing changes in ubiquitination through association with a nuclear chromatin-modifying complex. This function was found to be essential for the differentiation of several B and T lymphocyte effector programs and may also be a contributing factor to the oncogenic role of PLZF in leukemia and other cancers (Mathew et al., 2012). The role of PLZF as a Cul3 adaptor protein has primarily been shown to regulate autophagy. One of the most important proteins involved in autophagy is Atg14L, also known as Beclin 1-associated autophagy-related key regulator (Barkor), a mammalian protein necessary for autophagosome formation (Sun et al., 2008; Matsunaga et al., 2009; Diao et al., 2015). A study by Zhang et al has demonstrated that the ubiquitination and degradation of this protein is controlled by the Zbtb16-Cullin3-Roc1 E3 ubiquitin ligase complex and occurs through a direct protein interaction between the centre RD2 domain of PLZF and the C-terminal BATS domain of ATG14 (Zhang et al., 2015). The modulation of ATG14 activity through this pathway is regulated through a wide range of GPCR ligands and agonists, with GPCR activation suppressing the autophagic destruction of misfolded proteins (Abd-Elrahman et al., 2019). Serum starvation was also found to degrade Zbtb16 and subsequently increase levels of ATG14. Additionally, activation of the Glycogen Synthase Kinase 3-beta (GSK3β) has been shown to regulate the autophagic properties of PLZF through phosphorylation of the protein, mediating its degradation and leading to increased cellular levels of ATG14. The knockdown of multiple Gα proteins increased both ATG14L levels and autophagic flux, suggesting that autophagy is regulated through a subset of GPCR signaling mechanisms (Zhang et al., 2015). Pharmacological inhibition has shown to reduce the accumulation of these proteins through the promotion of autophagy. A study by Abd-Elrahman et al showed that the metabotropic glutamate receptor 5 (mGluR5) regulates the autophagic clearance of Aβ oligomers in AD through the ZBTB16 pathway. Interestingly, this was

through a sex-dependent pathway, with pharmacological inhibition reducing oligomer buildup in male mice whereas female mice experienced an exacerbated accumulation of oligomers (Abd-Elrahman et al., 2019). These treatments may even act as a treatment for neurodegenerative disorders involving a defective autophagy system (**Fig. 9**).

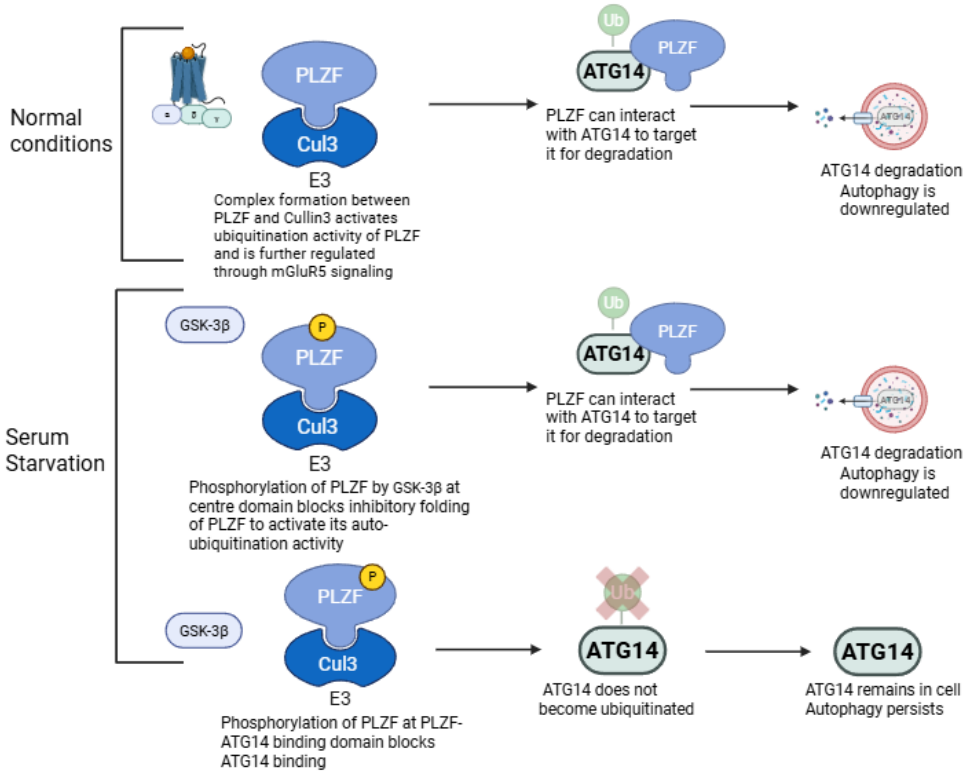

Figure 9. The Regulation of Autophagy by PLZF. PLZF regulates the autophagy process through its effect on the ATG14 protein. Through its association with the Cullin3-Roc1 E3 ubiquitin ligase complex, PLZF allows for the ubiquitination and degradation of ATG14, subsequently downregulating autophagy. This process is further regulated through mGluR5 signaling. Under serum starvation conditions, PLZF can be degraded, leading to a concomitant increase in ATG14 levels. Under these same conditions, the activation of GSK3β can regulate autophagy by phosphorylating PLZF at two different sites to either promote or inhibit the ubiquitination activity of PLZF. Created with BioRender.com.

1.3.4. PLZF Location

Extensive research has been conducted to better understand the functional dynamic role of PLZF by studying its localization within the cell. PLZF has been discerned to co-localize within nuclear speckles alongside the PML protein (Koken et al., 1997). Nuclear speckles are dynamic subnuclear domains which contain large concentrations of small nuclear ribonucleoproteins (snRNPs) and other splicing-related proteins essential for pre-mRNA processing and are thought to be important regions for mRNA transcription and protein phosphorylation (Handwerger and Gall, 2006). Some of these speckles are essential for transcription and it has been demonstrated that PLZF loses its transcriptional regulatory activity as it is shuttled out of the nuclear speckles. For example, a study was published looking at the role of the regulation of epidermal growth factor receptor (EGFR) through GPCR signaling. Activation of this receptor is mediated by its ligand heparin-binding EGF-like growth factor (HB-EGF), which gets cleaved from its membrane-bound form by the phorbol ester and PKC activator 12-*O*-tetradecanoylphorbol-13-acetate (TPA) to release a soluble form of HB-EGF, which is essential for EGFR transactivation by GPCR signaling (Prenzel et al., 1999). The carboxyl-terminal remnant of the cleaved HB-EGF (HB-EGF-C) can be shuttled into the nucleus and interact with the zinc finger domain of PLZF, triggering its nuclear export. This export was found to reverse the transcriptional repression of cyclin A as well as the delayed cellular growth and accumulation of cells in the G0/G1 phase in HT1080 cells (Nanba et al., 2003). It is possible that the transcriptional regulation by PLZF in the nuclear speckles is regulated by Epsin, a cytosolic protein that mediates clathrin-mediated endocytosis through its direct interactions with clathrin, AP-2 and Eps15. Epsin 1 was identified as an interactor with PLZF between residues 262-673 at the epsin NH_2-terminal homology (ENTH) domain of epsin 1 and upon co-transfection of both proteins, a nuclear pool of epsin was detected. CHO cells incubated with leptomycin B, an antifungal antibiotic that can block the Crm1-dependent nuclear export pathway of several proteins, caused accumulation of Epsin 1 in the nucleus, but not in control cells. Therefore, despite its prominent role in regulating endocytosis in the cell periphery, epsin 1 may be found in the nucleus under certain conditions and it may regulate the

transcriptional activity of PLZF through its ability to shuttle the protein to and from the nuclear speckles. PLZF may also play a versatile role in regulating proteins outside of the nucleus.

1.3.5. PLZF Interactions with Other Proteins

1.3.5.1. PLZF and the RARα

As previously discussed, PLZF can form a complex with RARα in t(11;17) APL through its zinc finger domain (Chen et al., 1993). RARs act as transcription factors through RAR/RXR heterodimers and the binding of ATRA to RAR activates its transcriptional regulatory activity of target RARE-containing genes through a series of conformational changes, allowing for chromatin remodelling and increased binding of RNA polymerase to promoters. Studies have demonstrated that the interaction with PLZF interferes with the transcriptional activity of RARα in HeLa cells and is ligand-independent, meaning that PLZF does not interfere with the ligand binding activity of RARα. PLZF impedes the dimerization of RARα with RXRα, demonstrating that the symptoms of t(11;17) APL likely do not occur because of PLZF interfering with RARα-ligand interaction but rather it prevents the transcriptional activity from blockage of the heterodimerization of RARα-RXRα (Martin et al., 2003).

1.3.5.2. PLZF and the AT2R

PLZF also forms a complex with the C-terminal domain of angiotensin II type 2 receptor (AT2R), a GPCR that plays important roles in the development of cardiovascular diseases such as hypertension and cardiac hypertrophy. The stimulation of AT2R by its peptide, Ang II, induced co-localization of AT2R and PLZF at the plasma membrane of CHO-K1 cells and subsequent translocation of PLZF to the nucleus and AT2R to the perinuclear region between 1-3 hours after stimulation. Ang II failed to induce nuclear translocation when cells were transfected with AT2R or PLZF only, showcasing that ligand-induced nuclear import of PLZF is specifically regulated through its co-localization with AT2R. This translocation may also be dependent on epsin 1, as it was observed that epsin 1 became associated with PLZF in the cytosol prior to Ang II stimulation and that stimulation induced nuclear translocation of both proteins together (Senbonmatsu et al., 2003). Interestingly, β-arrestin was not necessary for this translocation

despite it being an important component for mediating the internalization of angiotensin II type 1A receptor (AT1AR) (Ferguson et al., 2001).

It was detected through immunoblotting that stimulation of AT2R by Ang II induced phosphorylation of PLZF at its Tyr669 residue and mutation of this specific phosphorylation site blocked the nuclear translocation of PLZF, as well as administration of the tyrosine kinase-specific inhibitor genistein. Upon translocation to the nucleus, PLZF can activate the p85α PI3K gene through a complex formation between its zinc finger domain and the upstream flanking region of p85α PI3K, stimulating protein synthesis in cardiomyocytes (Senbonmatsu et al., 2003). p85α PI3K is an important regulatory subunit of several PI3K isoforms, which are significant for generating lipids during receptor-mediated signaling processes (Vanhaesebroeck et al., 1997). The increased expression of p85α PI3K was dependent on both AT2R and PLZF and its enhanced expression may fuel the growth factor-mediated cardiac hypertrophy response (Senbonmatsu et al., 2003). PLZF is highly expressed in the heart (Cook et al., 1995) and prior studies have demonstrated a lack of cardiac hypertrophy in mice lacking AT2R, demonstrating that cardiac hypertrophy may be in part stimulated by the AT2R-PLZF-P85a PI3K pathway. This is also in line with findings that PLZF-deficient mice do not experience left ventricular hypertrophy which is expected with chronic Ang II infusion (Wang et al., 2007). As a GPCR, AT2R couples to Giα2 and Giα3 (Zhang and Pratt, 1996). Pretreatment of cells with the Gi/o inhibitor PTX not only inhibited the concurrent translocation of AT2R and PLZF following Ang II stimulation but additionally prevented expression of the p85a PI3K gene, indicating that Gi plays a role in the interaction with AT2R and subsequent nuclear translocation of PLZF (Senbonmatsu et al., 2003).

1.3.5.3. PLZF and the Prorenin Receptor

PLZF also forms a complex with the (pro)renin receptor (RER), a single transmembrane receptor with important implications in mediating the effects of renin on blood pressure control (Nguyen et al., 2002; Schefe et al., 2008). Previously, no direct protein interactors had been identified for RER. A novel RER signaling pathway was discovered in 2006 within human kidney cells and rat cardiomyoblasts when a

Y2H screen and coimmunoprecipitation experiments identified the zinc finger domain of PLZF as a direct interactor with the receptor. Similarly to AT2R and Ang II, RER regulates the nuclear translocation of PLZF upon renin stimulation and subsequently induces transcription of p85a PI3K in the nucleus (Schefe et al., 2006; Schefe et al., 2008). Interestingly, interaction with PLZF represses transcription of the RER itself likely through a PLZF cis-element identified in the RER promotor through site-directed mutagenesis, with renin stimulation inducing a 6-fold recruitment of PLZF to the RER promotor (Schefe et al., 2006).

1.3.5.4. PLZF and the Go protein

Another PLZF-interacting partner pulled out by the Y2H screen is the alpha subunit of the Go protein, a member of the inhibitory G-protein family and the most abundant heterotrimeric G-protein in the brain.Y2H screens were performed for the alpha subunit as its downstream effects had not been clearly identified at the time. As well, its role in regulating standard GPCR signaling processes such as AC and cAMP production remained unclear. PLZF was confirmed to interact with the active form of Goα both under *in vitro* and *in vivo* conditions. Immunoprecipitation studies also concluded that the alpha subunit of Gi interacts with PLZF. Interestingly, its interaction appears to enhance the transcriptional repressive activity of PLZF, with repression of luciferase gene transcription being completely abolished upon treatment with PTX (Won et al., 2008). As previously discussed, PLZF represses progression of the cell cycle through its repressed transcription of the cyclin A2 gene (Yeyati et al., 1999). Co-transfection of HEK293T cells with both PLZF and Gαo inhibited cyclin A2 levels by 54% compared to 27.2% reduction in cells transfected with PLZF alone, suggesting that Gαo enhances PLZF transcriptional repressive and contributes to its role in suppressing cell growth (Won et al., 2008). The enhancement of PLZF-regulated growth suppression through Gαo is mediated by activation of the Gi/o-coupled cannabinoid receptor in HL60 cells, which can endogenously activate Gi/o proteins in these human APL cell lines (Childers, 2006; Won et al., 2008).

1.3.5.5. PLZF and the D1-class

Finally, unpublished studies in the Tiberi lab have identified PLZF as being a novel interactor of the D1-class of dopamine receptor. PLZF was first identified through a Y2H screen using the IL3 of D5R and the CT of D1R, and its complex formation was validated through co-immunoprecipitation studies. It was demonstrated that dopamine stimulation enhanced PLZF complex formation with both the D1R and D5R while administration of cis-flupentixol, a D1-class inverse agonist, hindered complex formation, suggesting that PLZF exhibits a higher affinity for the active R* conformation of the D1-class. Studies were performed to assess the effect of D1-class functional properties on PLZF interaction, such as GloSensor cAMP assays, ERK1/2 activation assays and ELISA to study the effects of internalization and recycling properties of the receptor. Interestingly, it was discovered that PLZF confers differing effects of the functional activity between D1R and D5R. For example, co-transfection of HEK293 cells with both PLZF and D1R increased the production of cAMP levels relative to cells transfected with D1R alone. Contrarily, cells co-transfected with both PLZF and D5R observed decreased cAMP production relative to cells transfected with D5R alone. Similarly, co-transfection of D1R and PLZF increased ERK1/2 activation relative to D1R alone, whereas it decreased ERK1/2 activation for cells co-transfected with D5R and PLZF relative to D5R alone. Results from ELISA assays showed that cells co-expressing both D1R and PLZF experienced a decline in D1R internalization, whereas cell expressing D5R and PLZF showed an increase in D5R internalization. Receptor recycling properties are also increased for cells with both D1R and PLZF, whereas it is decreased for cells with D5R and PLZF. These differences in functional properties exerted by PLZF on the D1-class may be the result of PLZF interacting with different cytoplasmic regions on each receptor, as demonstrated by the results of the Y2H screen. As previously discussed, the D1-class exhibit sequence divergence in their cytoplasmic domains, particularly in the IL3 and CT, which correspond to differences in DAR functional activity such as agonist binding affinity, signalling pathways and receptor internalization, which are shown to be regulated through receptor interaction with DRIPs as previously discussed. It remains to be known as to the exact molecular

mechanisms that underlie these functional changes with regards to the interaction between PLZF and the D1-class.

1.3.6. PLZF in the CNS

1.3.6.1. PLZF and Brain Development

The PLZF protein has broad regulatory functions throughout the CNS. A study by Cook et al published in 1995 was one of the first studies to investigate how PLZF influences CNS development and functioning. At the time, it had recently been discovered that PLZF was involved in a novel retinoid signaling pathway implicated in the pathogenesis of APL (Chen et al., 1993). Additionally, other members of the C2H2 zinc-finger gene family had been identified in regulating hindbrain segmentation such as the mammalian Krox-20 gene, a zinc finger transcription factor required for rhombomere development in the segmented embryonic hindbrain (Giudicelli et al., 2001; Dezmazières et al., 2009). The hindbrain is a crucial structure of the vertebrate brain for regulating vital physiological functions such as breathing and heart rate. This structure is divided into 7-8 metameric units known as rhombomeres during early vertebrate embryogenesis, occurring at approximately 8.5 to 10.5 days post-coitum (Cook et al., 1995; Dezmazières et al., 2009). This process, in addition to the development of other cortical structures, is a complicated and tightly regulated process involving the proliferation, differentiation, cell fate determination and migration of neural stem cells (NSCs). Ensuring a proper balance between the self-renewal of NSCs and their differentiation into adult neurons through neurogenesis is crucial to ensure there exists enough neurons to suffice for proper brain development. Defects in this balance have been implicated in numerous types of brain malformations (Lin et al., 2019). In the paper published by Cook et al., mouse and chicken homologous were cloned and studied to identify potential genes of interest that may be implicated in embryonic hindbrain formation, as shown by their changes in spatial and temporal expression. PLZF was found to display a highly dynamic and spatially restricted expressed pattern within the hindbrain. PLZF mRNA is initially expressed in high levels throughout the brain but starting from 8.5 days post-coitum, PLZF becomes restricted to specific domains of the hindbrain, midbrain and parts of the forebrain, with

its highest expression in the rhombencephalon, suggesting that PLZF is involved in regulating vertebrate hindbrain segmentation (Cook et al., 1995).

Along with the hindbrain, other published papers suggest that PLZF may regulate development in other neural regions during embryogenesis. PLZF is shown to exhibit dynamic temporal patterns of expression during development, with PLZF expression detected in Pax6+ cells as early as embryonic day 7.5 in the anterior neuroepithelium and eventually spreads to the neuroectoderm until day 10 (Avantaggiato et al., 1995). Other studies with Pax6+ cells have found expression of PLZF in the prosencephalon at day 9.5 and 10.5, highlighting an important role for PLZF in regulating the early stages of neurogenesis. PLZF expression appeared to decrease after day 12.5, with a dramatic decrease in the telencephalon at day 11.5 (Lin et al., 2019) (**Fig. 10**). In that same paper by Lin et al, mice were generated with a single nucleotide change in the first coding exon of the PLZF gene, resulting in a severely truncated and non-functional protein. The brains of those PLZF-deficient mice showed substantial declines in cerebral cortex size in addition to the number of deep-layer cortical neurons. The loss of PLZF resulted in smaller average dorsal cortical areas and hemisphere lengths in comparison to wild-type mice with functional PLZF proteins. Specifically, these deficient mice exhibited brain volume decreases restricted to the cortex and hippocampus areas only, as well as a prominent reduction in the neocortical thickness of layer 6 and a significant decrease in neurons expressing Tbr1, a positive marker for deep-layer cortical neurons (Lin et al., 2019; Usui et al., 2021) (**Fig. 11**). Interestingly, markers for layer 5 and layers 2/3 displayed no noticeable changes between wild-type and PLZF-deficient mice, demonstrating that PLZF regulates early-stage neurogenesis in a domain-specific manner, with its loss altering the formation of deep layer neural structures (Lin et al., 2019).

The loss of PLZF also appears to have an impact on brain function and behaviours, possibly due to the exhibited changes in cortical structures. PLZF-deficient mice showed a loss of recognition memory when compared with wildtype mice, as those deficient mice displayed no change in preference during novel object recognition tests (Lin et al., 2019; Usui et al., 2021). Other studies found that ZBTB16 knockout

results in social impairments and repetitive grooming as well as object-burying behaviours with no apparent differences in locomotion activity, behaviours that are all characteristic of autism spectrum disorder (ASD) (Usui et al., 2021). As social impairments are also a key symptom of schizophrenia, Usui et al wanted to investigate if PLZF has a role in mediating symptoms of schizophrenia. Prior studies using a pathway-based bioinformatics approach have indicated ZBTB16 as a potential candidate gene for influencing the onset of schizophrenia, with many single-nucleotide polymorphisms being identified within the gene (Sun et al., 2010; Meda et al., 2014). It has been reported in numerous studies that impulsive risk-taking is a key characteristic of schizophrenia (Cheng et al., 2012; Reddy et al., 2014), so an open-field test was conducted in mice to evaluate the impact of ZBTB16 knockout on their risk-taking behaviour. These mice spent significantly increased time and distance in the centre of the arena compared to wild-type mice with no changes in the number of arena entries, demonstrating an elevation in risk-taking behaviour in these mice and showcasing a new role for PLZF in regulating schizophrenia symptoms (Usui et al., 2021). The impact of PLZF gene knockout on molecular morphology and cellular composition was also evaluated, as it has been repeatedly shown that the activation of microglia is implicated in the formation and maintenance of synapse numbers in addition to the development of neurological disorders like ASD and schizophrenia (Fan et al., 2023). ZBTB16-deficient mice displayed a significant increase in both dendritic spine and microglial numbers compared to wildtype, signifying that PLZF may potentially regulate brain behaviours through structural changes in the cortex as well as individual neuronal components.

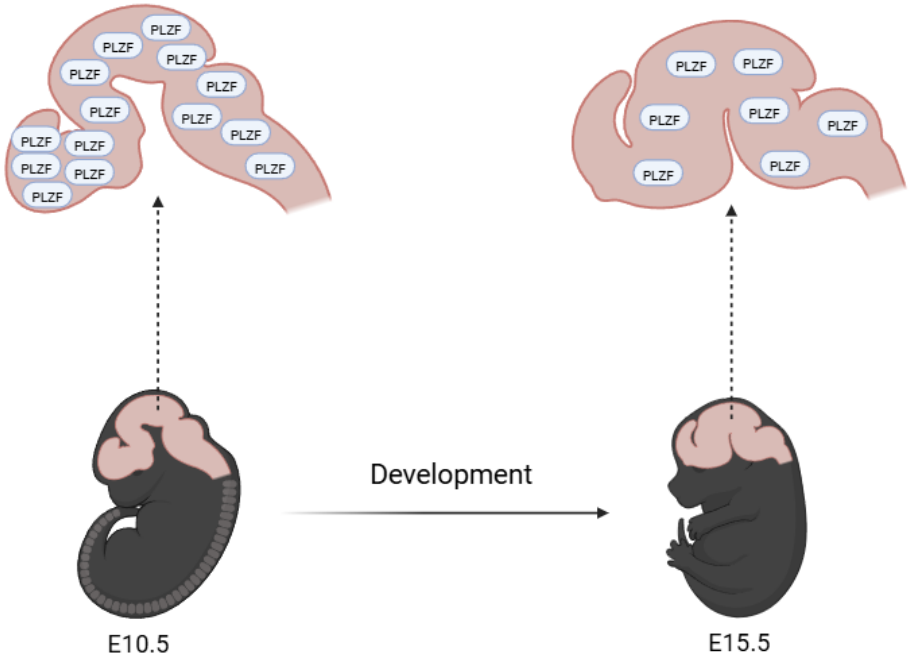

Figure 10. Schematic Diagram of the Regulation of Early Mouse Neurogenesis by PLZF. PLZF is shown to be expressed as early as E7.5 in the anterior neuroepithelium of the mouse embryo and spreads to the entire neuroectoderm around E10-E10.5. This broad expression is located particularly in the prosencephalon (forebrain) and was found to decrease after E12.5, with a dramatic decline in the telencephalon after E11.5.

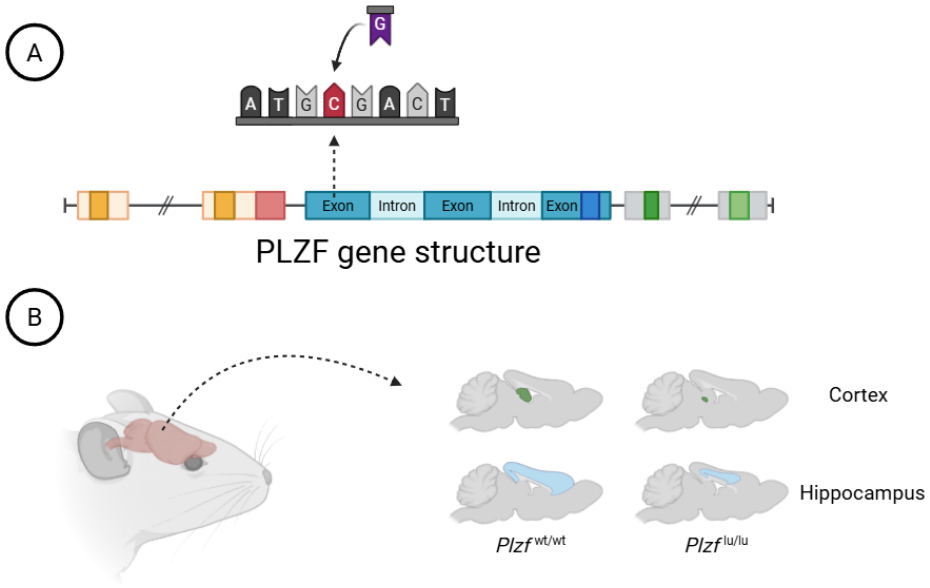

Figure 11. Schematic Diagram of the Regulation of Mouse Cortical Structure Size by PLZF. (A) PLZF-deficient mice ($PLZF^{lu/lu}$) spontaneously arose due to a single nucleotide change in the first coding exon of the PLZF gene, resulting in a truncated protein. (B) Mice with this deficiency experienced significant reductions in their dorsal cortical surface area and hemisphere length compared to wildtype mice ($PLZF^{wt/wt}$), particularly within the cortex and hippocampus.

1.3.6.2. PLZF and Neurological Disorders

Changes in PLZF expression levels have also been related to brain disorders like Alzheimer's Disease (AD) and Huntington's Disease (HD). A study by Huguet et al explored the impact of genes regulating dopaminergic cell fate on the manifestation of HD symptoms, as dopaminergic hyperactivity in the SNc and VTA is a major mediator of HD symptoms. It is thought that mutations in the Htt gene, which codes for the huntingtin protein, may be the cause of this dopamine hyperactivity rather than striatal neurodegeneration as other studies have hypothesized. These mutations may alter the fate of transcription factors such as PLZF which control dopaminergic cell fate (Huguet et al., 2019). Using transgenic rat models of HD (tgHD), changes in expression patterns were evaluated for a select number of transcription factors that have been previously shown to play a role in regulating neuronal cell fate, one of which was the ZBTB gene. Through this study, it was discovered that ZBTB16 was significantly upregulated in both the SNc and VTA regions of the tgHD rats compared to wildtype. ZBTB16 expression was positively correlated with the expression of Msx1, an important gene for determining early cell fate of midbrain dopaminergic neurons (Andersson et al., 2006; Huguet et al., 2019). Interestingly, only the expression of ZBTB16 was found to be significantly enhanced in the dorsal raphe nucleus (DRN) compared to all other genes in the study. Altogether, this suggests that PLZF plays an important role in coordinating changes in early dopaminergic cell fate that are characteristic of HD pathogenesis (Huguet et al., 2019). The ZBTB16-mediated mechanism of autophagy has also been shown to mediate HD pathology in huntingtin-knockin zQ715 mice through mGluR5 signaling. A 12-week treatment of 2-chloro-4-((2,5-dimethyl-1-(4-(trifluoromethoxy)phenyl)-1H-imidazol-4-yl)ethynyl)pyridine (CTEP), a negative allosteric modulator of mGluR5, resulted in a reduced size and number of huntingtin aggregates in these mice in addition to reduced neuronal apoptosis in brain tissue. These effects were correlated with reduced ZBTB16 activation, likely due to inhibitory phosphorylation from the activation of GSK3β, which was associated with increased expression of the autophagy protein ATG14 (Abd-Elrahman et al., 2018). The ZBTB16-mediated mechanism of autophagy has also been implicated in other neurodegenerative disorders, with studies demonstrating its contribution to the pathogenesis of AD, a neurodegenerative disorder

characterized by the neurotoxic accumulation of beta amyloid plaques in the brain, leading to neuronal loss and progressive cognitive decline. CTEP administration was found to reduce the accumulation of Aβ oligomers and rescue cognitive function. This inhibition was associated with a GSK3β-dependent degradation of ZBTB16 and a subsequent stabilization of ATG14 (Abd-Elrahman et al., 2020). The role of PLZF in mediating AD and HD pathology may also be regulated through optineurin, a multifunctional protein that forms a complex with members of the Group I metabotropic glutamate receptor family and regulates their downstream signaling pathways, most notably through attenuation of PLCβ and IP3 formation in mGluR1. Optineurin deletion not only enhances Ca2+ mobilization following mGluR5 activation but enhances both GSK3β activity and ZBTB16 breakdown while abolishing mGluR5-mediated inactivation of the GSK3β/ZBTB16 pathway (Ibrahim et al., 2021). Altogether, this demonstrates an important role for PLZF in the regulation of downstream GPCR signaling and highlights its potential as a therapeutic target in the treatment of neurological disorders.

1.3.6.3. PLZF and Stroke

As previously discussed, PLZF forms a complex with both the AT2R and the RER. Stroke is a widespread and debilitating medical emergency affecting millions of individuals worldwide, and the renin-angiotensin system (RAS) is heavily implicated. Prior studies using animal models have shown that blockage of the AT1R through pretreatment with the medication cardesartan can have protective effects on the brain by improving neurological outcomes post-stroke (Krikov et al., 2008). Additionally, these effects are partially and indirectly mediated by the AT2R (Li et al., 2012). Therefore, studies were conducted to determine if PLZF plays a role in these protective outcomes. Human neuronal KELLY cells with endogenous PLZF expression were incubated with glutamate for 24 hours to induce neurotoxicity and mimic neuronal injury. Glutamate-induced cytotoxicity triggers the release of calcium ions into the cell to promote oxidative stress, leading to cell damage and death (Murphy et al., 1989; Fang et al., 2014). After this incubation period, it was shown that 65% of cells survived and this survival rate increased to 80% when PLZF was overexpressed, demonstrating that PLZF mediates neuroprotection in neuronal

injuries. This overexpression also caused a substantial upregulation of the production of AT2R transcripts in addition to a reduction in cyclin A2 transcription, showcasing that these effects may be facilitated through the antiproliferative effects of PLZF-mediated stem cell renewal and this may be further mediated through its complex formation with the AT2R, a receptor known for its neuroprotective and antiproliferative effects in stroke. This is further validated by the ubiquitous expression pattern of PLZF and both the AT2R and RER throughout the brain, including the cortex and striatum (Seidel et al., 2010). Seidel et al tested these effects in-vivo using the middle cerebral artery occlusion (MCAO) model, a well-established and widely used model to mimic stroke in-vivo through blockage of the middle cerebral artery to induce local brain ischemia (Shahjouei et al., 2016). Interestingly, transcription of cyclin A2 was significantly upregulated on the injured ipsilateral hemisphere while PLZF and AT2R levels were downregulated at both measured time points, showcasing the negative effects of stroke on PLZF expression and further validating the neuroprotective effects of PLZF on stroke recovery (Seidel et al., 2010).

1.3.6.4. PLZF and Neural Progenitor Cells

As previously described, the development of the CNS is spatially and temporally regulated through the differentiation of multipotent NSCs and progenitor cells (NPCs) into neurons and glial cells, while ensuring enough progenitors exist to generate other later-born cell types such as glia (Gaber et al., 2013). NPCs are overtly represented in the developing spinal cord and are sustained by several types of mitogenic growth factors, including the Fibroblast Growth Factors (FGFs). FGFs are expressed throughout neural tissues and acts through their respective tyrosine kinases (FGFRs), whereby ligand binding to these receptors leads to the activation of multiple different downstream signaling pathways such as ERK1/2, STAT3 and PLC to inhibit neuronal differentiation and promote cell division (Guillemot and Zimmer., 2011). As undifferentiated NPCs begin their transition into cells like astrocytes and oligodendrocytes, their maintenance becomes heavily dependent on FGF signaling (Kang and Song, 2010; Furusho et al., 2011). Therefore, there is immense interest in understanding how FGFR and mitogenic factor signaling is fine-tuned to regulate NPC development. PLZF was identified as a factor

potentially involved in NPC maintenance in the spinal cord, as its upregulation was detected in mice deficient of Olig2, a gene important for the development of oligodendrocytes and astrocytes and thought to play a role in repressing the transcription of genes involved in NPC self-renewal (Mukouyama et al., 2006; Skaggs et al., 2011). PLZF was also shown to suppress early stages of neurogenesis in zebrafish but its mechanism of action in later developmental changes remained unknown at the time. Gaber et al showed that PLZF becomes broadly expressed within NPCs in the neural tube between embryonic stages 2.5 and 3, however, this expression later becomes restricted to a central domain associated with glial progenitors. PLZF expression in this zone becomes undetectable during the period of astrocyte progenitor migration into grey matter for differentiation. PLZF promotes the maintenance of these progenitor cells and reduces their differentiation into neurons through its transcriptional repressor functions, with its expression increasing the expression of NPC marker gene SOX2 by 26% and reducing differentiated neuron marker gene NEUN by 39% relative to controls. Incorporation of two short hairpin RNAs to knock down PLZF expression substantially affected NPC maintenance, reducing the expression of several genes associated with NPC maintenance and increasing differentiation of interneurons expressing high levels of PLZF. PLZF knockdown decreased FGFR3 expression while its ectopic expression expanded FGFR3 expression. Similarly, misexpression of FGFR3 reduced SOX2-expressing cells by 25%, showcasing that the effects of PLZF in regulating NPC maintenance are mediated through a heightened response to FGFR signaling. Overall, this demonstrates the importance of PLZF in regulating NPC maintenance and gliogenesis through FGFR3 expression and STAT3 activity as well as restricting neuronal differentiation.

2. Objectives and Hypothesis

As previously mentioned, dopamine receptor signaling is regulated by the binding of cytoskeletal, adaptor, and signaling DRIPs. These DRIPs have been shown to play a role in nearly all aspects of the receptor life cycle, and more research is needed as to their role in governing dopamine receptor functioning. Given the immense involvement of dopamine receptors in regulating human physiology, as well as the fact that dysfunctions in their signaling has been implicated in a wide range of CNS disorders, a growing subset of pharmacological research has been devoted to gaining a deeper understanding of the DRIPs and their role in receptor functioning. The identification of DRIPs may be used to improve our understanding of these debilitating diseases and facilitate further development of novel therapeutics. A useful method for identifying protein interactions is the Y2H screen. This screening method has revealed a completely different subset of DRIPs between the D1 and D2 classes of dopamine receptors (Bergson et al., 2003), highlighting the substantial variation in interacting partners with each dopamine receptor class. Many of the disorders described above are implicated by defective D1-class signaling, however, due to the high degree of homology between the subtypes, developing clinically useful ligands that are selective for each receptor has proven to be immensely difficult, rendering the D1-class as pharmacologically indistinguishable (Jones-Tabah et al., 2022). Regardless, evidence shows the IL3 and CT of the D1 and D5 receptors exhibit key structural and functional differences, respectively, in their amino acid compositions, as well as in ligand binding and G-protein coupling properties (Missale et al., 1998; Tumova et al., 2003). As previously mentioned, previous unpublished studies in the Tiberi lab identified PLZF as a D1-class interactor with the IL3 of D5R and the CT of D1R. Additionally, PLZF was found to convey differential regulation within the signaling and trafficking properties of the D1-class. PLZF increases cAMP production and ERK1/2 activation in the D1R, while decreasing both in the D5R. As well, PLZF hinders D1R internalization but increases D5R internalization. As the D1R and D5R each possess unique serine and threonine phosphorylation sites (Moritz et al., 2023), differences in PLZF-D1-class binding location may interfere with agonist-mediated phosphorylation to confer these subtype-specific trafficking properties. However, as the D1R is the most abundant receptor in the CNS and is

largely implicated in disorders compromising the dopaminergic system (Missale et al., 1998; Beaulieu and Gainetdinov, 2011), the focus of this thesis is to better understand the molecular mechanisms underlying the regulation of D1R activity by PLZF.

Therefore, I hypothesize that PLZF modulates the dopamine-mediated phosphorylation of D1R through its recruitment to the D1R CT. I propose these objectives to test my hypothesis:

- Measure the extent of D1R phosphorylation when various lengths of the D1R CT are removed in the absence of PLZF
- Measure the extent of D1R phosphorylation in the presence of PLZF with full-length D1R as well as with various truncated CT forms of the D1R
- Characterize the CT regions of D1R interacting with PLZF

3. Materials and Methods

3.1. Materials

Eagle's minimal essential medium (EMEM), incubation buffer (EMEM without phenol red), and phosphate buffered saline (PBS) are from Wisent Bioproducts (Saint-Jean-Baptiste, QC, Canada). Trypsin-ethylenediaminetetraacetic acid (trypsin-EDTA), fetal bovine serum (FBS) and gentamicin (50 mg/mL) are from ThermoFisher Scientific (Burlington, ON, Canada). (2-hydroxyethyl)-1-piperazineethanesulfonic acid (HEPES) buffer is from ThermoFisher Scientific (Burlington, ON, Canada). Bio-Safe II biodegradable scintillation cocktail is from Research Products International (Mount Prospect, IL, USA). [N-Methyl-^{3}H]-SCH23390 is from Revvity (Mississauga, ON, Canada). Bio-Rad protein assay dye reagent concentrate and DC Protein Assay Reagents A, B and S are from Bio-Rad Laboratories (Mississauga, ON, Canada). Ascorbic acid (AA), dopamine hydrochloride (DA), cis-flupenthixol, soybean trypsin inhibitor, leupeptin, pepstatin A, benzamidine, phenylmethylsulfonyl fluoride (PMSF), Bovine serum albumin (BSA), rabbit monoclonal anti-Flag antibody and anti-FLAG M2 affinity gel are from Sigma-Aldrich (Oakville, ON, Canada). Rabbit monoclonal anti-PLZF antibody is from Cell Signaling Technology (Danvers, MA, USA). Mouse monoclonal anti-alpha tubulin antibody is from Millipore Sigma (Oakville, ON, Canada). Rabbit polyclonal anti-phosphorylated Thr354 and rabbit polyclonal anti-phosphorylated Ser372/Ser373 are from 7TM Antibodies (Jena, Germany). Horseradish peroxidase (HRP)-conjugated rabbit polyclonal anti-GST antibody is from Bethyl Laboratories (Montgomery, TX, USA). ECL HRP-conjugated donkey polyclonal anti-rabbit whole antibody, ECL HRP-conjugated sheep polyclonal anti-mouse F(ab')$_2$ fragment antibody, and Amersham ECL Prime Western Blotting Detection Reagents A and B are from Cytiva (Mississauga, ON, Canada).

3.2. Methods

3.2.1. Cell Culture and Transfection

HEK293 cells were cultured from passages 40-52 in complete EMEM supplemented with 10% (v/v) heat-inactivated FBS and 40 μg/ml gentamicin. These cells were grown within a 37°C incubator containing a 5% CO_2 atmosphere. Cells were seeded in 100-mm culture dishes at approximately 2.2 million cells per dish and cells were transiently transfected with human D1R, a mutant form of human D1R (ΔN-IL3, ΔC-

IL3, Cys347-STOP, Cys351-STOP, Val388-STOP, Ser417-STOP and Ser431-STOP) and HA-tagged PLZF. Cells were transfected either with empty pCMV5 vector, D1R, mutant D1R, HA-PLZF alone or a combination of D1R with PLZF or mutant D1R with PLZF. Empty pCMV5 vector was transfected when appropriate to ensure that the total amount of DNA transfected was 5 ug per 100-mm dish, as prior studies in our lab demonstrate that 5 μg of DNA per dish gives maximal expression (Plouffe et al., 2010). Cells transfected with 5 μg of empty pCMV5 vector or pCMV5 with HA-PLZF and untagged D1R were used as negative control conditions. Between 18-24 hours after transfection, cells were washed once with 5 ml of PBS, detached from plate using 0.5 ml of Trypsin-EDTA, resuspended in 6 ml of complete EMEM and reseeded in new 100-mm dishes (12 ml/dish) for radioligand binding assays and immunoprecipitation studies. Cells were subsequently grown for an additional 48 hours until the day of the experiment.

3.2.2. Radioligand Binding Assay

Radioligand binding assays were performed to assess the expression level of wildtype and mutant D1R in transfected HEK293 cells by obtaining the total number of receptor binding sites (B_{max}). Cells seeded in 100-mm dishes were washed with 5 mL of cold PBS and then lysed in a total volume of 10mL of cold lysis buffer (comprised of 10 mM Tris-HCl, pH 7.4; and 5 mM EDTA, pH 8.0) by scrapping cells in dishes. Lysed cell mixtures were transferred into centrifuge tubes and centrifuged at 40,000 gat 4°C for 20 minutes to pellet cellular membranes. After centrifugation, the resulting membrane pellet was resuspended in 2 mL cold lysis buffer and homogenized at 15000 r.p.m. for 15 seconds using a Kinematica Brinkmann Polytron 3000. After homogenization, 8 mL of cold lysis buffer was added to each tube for a total volume of 10mL membrane homogenate, then centrifuged again at 40,000 g for 20 minutes at 4°C. The final membrane pellet was homogenized at 15000 r.p.m. for 15 seconds in 600-800 ul resuspension buffer (comprised of 62.5 mM Tris-HCl, pH 7.4; and 1.25 mM EDTA, pH 8.0). 100ul of membrane homogenate was then added to test tubes containing 300ul of binding buffer (62.5 mM Tris-HCl, pH 7.4; 1.25 mM EDTA, pH 8.0; 200 mM NaCl; 8.33 mM KCl; 6.7 mM $MgCl_2$; and 2.5mM $CaCl_2$), 50 ul of radioactive [N-Methyl-3H]-SCH23390 (82-83.9 Ci/mmol) and 50 ul of either cis-flupentixol or water. In total, the final reaction mixture contained 50 mM Tris-HCl, pH 7.4; 1mM EDTA; 120 mM

NaCl; 5 mM KCl; 4mM MgCl2; 1.5 mM CaCl2; and a saturating concentration of approximately 7-9 nM of [N-Methyl-3H]-SCH23390, either in the absence or presence of 10 uM *cis*-flupenthixol. The tubes with and without cis-flupentixol allow for determination of non-specific and total binding, respectively, of [N-Methyl-3H]-SCH23390 to membranes. Membranes were incubated within this mixture for 90 minutes at room temperature and binding reactions were terminated by rapid filtration onto glass fiber filters using a Brandel M-48 Semi-Automated Harvesting System. Filters were then washed three times with cold washing buffer (comprised of 50 mM Tris-HCl, pH 7.4; and 100 mM NaCl) and added to scintillations vials containing 3 mL of Bio-Safe biodegradable scintillation fluid. Bound *N*-methyl-3H]-SCH23390 radioactivity was measured using a Beckman LS 6500 liquid scintillation counter. The Bradford protein assay was performed to calculate the total membrane protein concentration in each reaction mixture, using the Bio-Rad protein assay dye reagent in conjunction with the remaining homogenized membrane. Membrane protein values were standardized against BSA. B_{max} was calculated in pmol/mg of membrane protein using total membrane protein concentration calculated from the Bradford along with bound *N*-methyl-3H]-SCH23390 radioactivity in DPM calculated from the scintillation counter.

3.2.3. Co-immunoprecipitation

Complete EMEM was aspirated from 100-mm dishes containing HEK293 cells and cells were subsequently incubated in incubation buffer (EMEM without phenol red; 20 mM HEPES; 10ug/ml gentamicin) containing either DA (10 µM final, dissolved in ascorbic acid (AA)) or AA as a vehicle (0.1 mM final) for 15 mins in a 37°C incubator containing a 5% CO_2 environment. After incubation, cells were placed on ice, media was aspirated, and cells were washed with 5 mL of cold PBS. Cells were lysed by scrapping with 1mL of cold radioimmunoprecipitation assay buffer (RIPA) (10mM Tris-HCl, pH 8.0, 1mM EDTA, 1% Triton X-100, 0.1% Sodium Deoxycholate, 0.1% SDS, 140mM NaCl buffer) containing 0.1% protease inhibitors (Aprotinin, Benzamidine, Leupeptin, Pepstatin A, PMSF, Trypsin Inhibitor) and lysates were collected in microcentrifuge tubes. Cell lysates were solubilized by rotating end-over-end for 1 hour at 4°C and then centrifuged at 13000 g for 15 min to remove insoluble cell material. The Bio-Rad DC assay was used to measure lysate protein concentrations using BSA as a protein standard. Based on

the DC assay calculations, 20 ug of protein were taken as input samples with 1:1 ratio of 4× SDS-PAGE Laemmli buffer. Anti-Flag M2 affinity gel was washed twice with 1mL of Tris-buffered saline (TBS) to remove impurities. 1 mg of solubilized protein lysate according to the measured protein concentration was then incubated with 50 ul of the Anti-Flag matrix for 2 hours by end-over-end rotating at 4°C. After rotation, anti-Flag matrix was washed 5 times with 1 mL RIPA+ buffer to remove non-specific binding, followed by elution of samples with 65ul of 4× SDS-PAGE Laemmli buffer overnight at room temperature. After elution, samples were stored at -20°C until used in Western Blot.

3.2.4. GST-Protein Purification and Pulldown Assay

GST-fusion proteins for the IL3 and CT of D1R were constructed through PCR amplification of these domains using the D1R in pCMV5 vector as a template, digested and ligated into the pGEX4T-1 vector linearized with the corresponding enzymes (5'-BamHI and 3'-XhoI). The pGEX-4T1 constructs were cloned into OverExpress C41 competent cells and E. Coli bacterial GST-tagged fusion proteins were produced as indicated by the manufacturer. Proteins were purified on Glutathione-Sepharose 4B bead matrix. Before pulldown, purified recombinant proteins were analyzed by Coomassie Brilliant Blue R-250 staining as well as SDS-PAGE and Western Blotting using an anti-GST antibody (**Fig. 12**). On the day of the pulldown assay, HEK293 cells overexpressing HA-PLZF in 100mm dishes were aspirated, washed twice with 5 mL of cold PBS and lysed in approximately 1mL of cold RIPA+ buffer with 0.1% protease inhibitors. All subsequent steps are identical to that of the immunoprecipitation protocol described in "(Co)immunoprecipitation" section. 1mg of solubilized protein lysate was incubated by end-over-end rotation at 4°C for 2 hours with 25 µl of purified GST-fusion proteins (or 25 µl GST for control conditions) and 25µl of Glutathione Sepharose 4B in microcentrifuge tubes. After incubation, GST-proteins and Glutathione Sepharose 4B matrix were washed 5 times with 1 mL cold RIPA+ buffer. Samples were eluted overnight with 65ul Laemmli buffer. 20 µg of protein were taken as input samples based on the DC protein assay calculations with a 1:1 ratio of 4× Laemmli buffer. After elution, samples were stored at -20 °C until used in Western Blot.

3.2.5. Western Blot

Western Blot samples from each experiment were collected and loaded into 10% (v/v) polyacrylamide gels for SDS-PAGE, then subsequently transferred onto PVDF membranes using the Bio-Rad Trans-Blot SD Semi-Dry Transfer Cell at 12V for 10 minutes. SDS-PAGE gels were run to separate proteins and to detect PLZF (~75 kDa), phosphorylated Thr354 and phosphorylated Ser372/373 (~80 kDa); alpha-tubulin (50 kDa) and GST fusion proteins (37-45 kDa). After transfer, membranes were incubated in Blotto blocking buffer (comprised of 50 mM Tris-HCl, pH 8.0; 80 mM NaCl; 2 mM CaCl2; 5% [w/v] non-fat dry milk; 0.2% [v/v] NP-40; and 0.02% [w/v] NaN3) on a rocking platform shaker for 1 hour at room temperature. Membranes were then washed three times with TBS containing Tween-20 (20 mM Tris-HCl, pH 7.4; 137 mM NaCl; and 0.2% (v/v) Tween 20) for 5 minutes. Afterwards, membranes were incubated with either rabbit monoclonal anti-PLZF to analyze levels of PLZF interaction, rabbit polyclonal anti-phosphorylated Thr354 to detect phosphorylation of the D1R cytoplasmic tail residue Thr354, rabbit polyclonal anti-phosphorylation Ser372/373 to detect phosphorylation of the D1R cytoplasmic tail residues Ser372 and Ser373, monoclonal rabbit anti-Flag to detect receptor levels, polyclonal HRP-conjugated anti-GST to detect GST fusion protein levels, and monoclonal mouse anti-alpha tubulin to assess total cellular input levels. Anti-phosphorylated antibodies were left to incubate overnight on a rocking platform shaker at 4°C to ensure maximal detection due to antibody instability, whereas all other antibodies were incubated at room temperature for 1 hour on a rocking platform shaker. Following primary antibody incubation, membranes were washed three times for five minutes with TBS-T, incubated for 1 hour with the appropriate secondary HRP-conjugated antibodies (ECL anti-mouse IgG for alpha-tubulin detection or anti-rabbit IgG for all other primary antibodies excluding GST). Membranes were subsequently washed three times with TBS-T for five minutes and bands corresponding to the applicable protein were visualized using a dilution of Amersham ECL Prime A&B. Images were acquired using the DNR Bio-Imaging Systems MicroChemi 2.0 gel imaging system. To remove bound antibodies and detect different proteins of interest on the same membrane, membranes were incubated with stripping buffer (comprised of 500 mM glacial acetic acid; 100 mM β-mercaptoethanol; and 0.5 % [w/v] SDS).

Membranes were then washed three times for five minutes with TBS-T on a rocking platform shaker, incubated for one hour at room temperature with Blotto on a rocking platform shaker and the appropriate antibody was incubated either overnight at 4°C or at room temperature for one hour on a rocking platform shaker. The densitometric analysis of protein bands was performed using ImageJ software.

3.2.6. Statistical Analysis

GraphPad Prism (version 10.6.1) was used for all statistical analyses and curve fitting. All data is expressed as mean ± SEM. Immunoreactive bands for coimmunoprecipitation and phosphorylation studies were quantified using ImageJ software as described in the figure legends. One-way ANOVA were performed using GraphPad Prism as noted in the figure legends, with $p \leq 0.05$ used as a threshold for statistical significance.

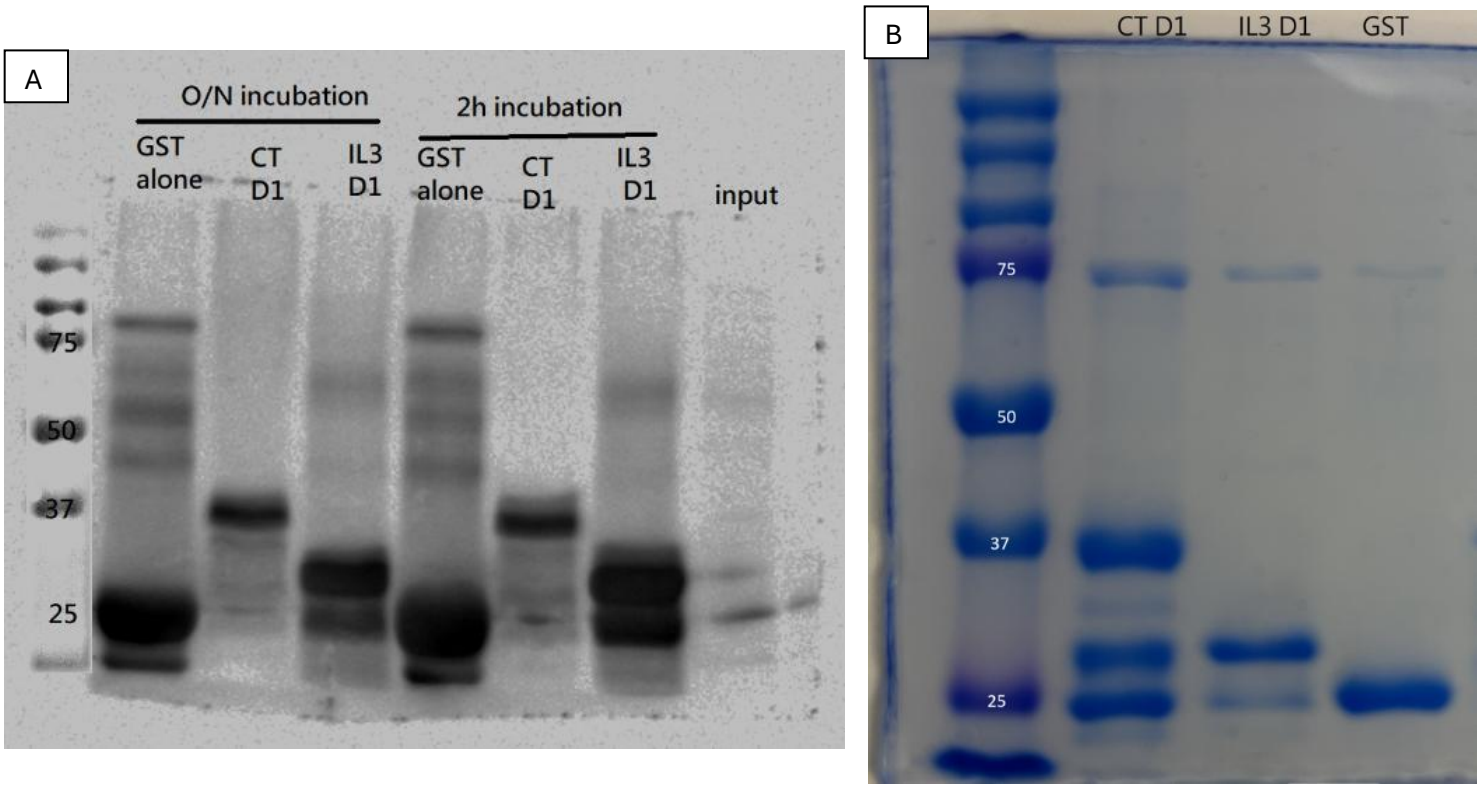

Figure 12. Analysis of Purified GST-Fusion Proteins. Purified GST proteins fused with either the IL3 of D1R, IL3 of D5R or CT D1R were analyzed through (A) SDS-PAGE and Western Blotting using an anti-GST antibody, as well as (B) Coomassie Brilliant Blue R-250 staining.

4. Results

In this section, I will begin by discussing the results from my studies on the impact of three D1R CT regions (Val388-Leu416; Ser417-Val430; Ser431-Thr446) located downstream of phosphorylation of residues Thr354 and Ser372/Ser373. Then, I will examine the role of PLZF on the phosphorylation of Thr354 and Ser372/Ser373. Since PLZF was initially identified as an interactor with the CT of D1R, I will determine if deletion of distal CT domains interfere with the PLZF-mediated regulation of D1R Thr354 and Ser372/373 phosphorylation. Finally, I will conclude this section by assessing the results I obtained from mapping the interaction domains of PLZF, as its interaction site on the D1R may be a contributing factor to its role in mediating the phosphorylation of Thr354 and Ser372/Ser373 on the D1R.

4.1. Assessing the role of the D1R cytoplasmic tail residues in dopamine-mediated phosphorylation of Thr354 and Ser372/Ser373

4.1.1. Truncation of the D1R distal cytoplasmic tail impacts phosphorylation of upstream residues

It is well-known that phosphorylation of activated GPCRs by GRKs is a critical regulatory step in mediating the downstream effects of receptor desensitization (Tiberi et al., 1996; Sedaghat and Tiberi, 2011; Jean-Charles et al., 2017). This effect is explained by the phospho-barcode hypothesis, which states that a unique phosphorylation pattern within the cytoplasmic domains of the receptor acts as a “barcode” to dictate specific downstream cellular responses (Jean-Charles et al., 2017; Kaya et al., 2020). Also, the elimination of various D1R CT regions has been shown to impact the GRK2 and GRK3regulation of DA-mediated phosphorylation (Jackson et al., 2002; Kim et al., 2004; Sedaghat and Tiberi, 2011). However, it remains unknown as to how the truncation of specific CT regions impacts the phosphorylation of certain residues. Studies show that the D1R contains 32 different serine and threonine residues, although it remains to be known if all residues are phosphorylated (Tiberi et al., 1996; Moritz et al., 2023). To analyze this, HEK293 cells were transfected with either wildtype Flag-tagged D1R or various Flag-tagged truncated forms of the D1R (fVal388, fSer417, fSer431), with the number corresponding to the most distal amino acid number after the site of truncation (**Fig. 13**). Truncations were generated by inserting

STOP codons between various residues along the CT. The purposes of these truncated receptors were to illustrate the effect that different groups of CT residues impart on the degree of D1R phosphorylation at residues Thr354 and Ser372/Ser373. Importantly, these truncated mutants did not display any significant differences in agonist and antagonist affinities relative to wild type D1R. Likewise, all truncated human D1R receptors retain similar agonist-independent and dependent Gs coupling properties relative to the wild type D1R (data not shown), with the exception of fCys351 that display a higher DA-induced maximal activation of adenylyl cyclase (Jackson et al., 2001).

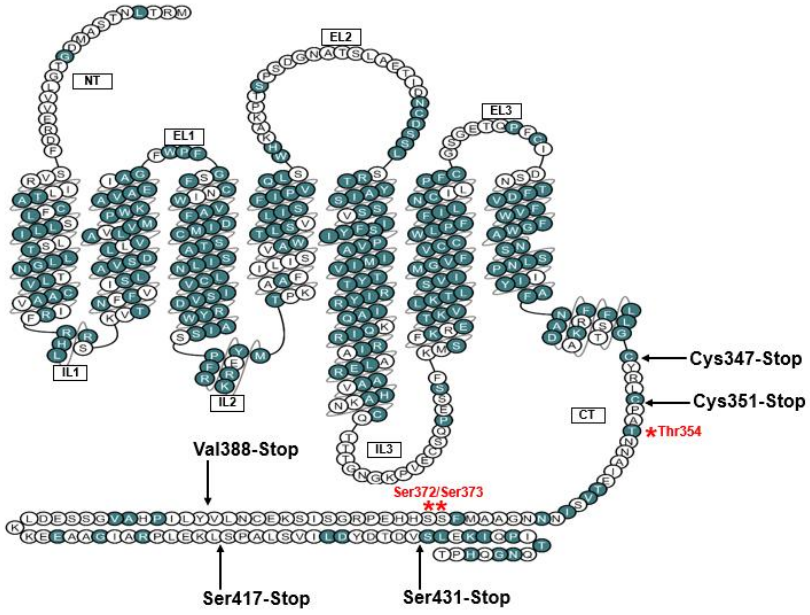

Figure 13. Schematic Diagram of Phosphorylation Residues Thr354 and Ser372/Ser373 on the D1R. Highlighted in blue are the D1R amino acid residues that are homologous to the D5R, while divergent D1R residues are highlighted in white. Flag-tagged truncated receptors downstream of the phosphorylation sites (fVal388-STOP, fSer417-STOP and fSer431-STOP) were used to study the impact of the D1R CT residues on PLZF-mediated regulation of D1R phosphorylation, with the arrows pointing to the specific sites of truncation along the D1R CT. Truncated receptors upstream of the phosphorylation sites (fCys347-STOP and fCys351-STOP) were used to test the efficacy of the phosphorylation antibodies used in these experiments (pThr354 and pSer372/Ser373). Generated with gpcrdb.com.

IP experiments were performed in transfected HEK293 cells under DA stimulation. In all experiments, anti-FLAG M2 agarose matrix beads were used to immunoprecipitate the Flag-tagged receptors and phosphorylation was analyzed through Western blot by probing with anti-phosphorylated Thr354 (pThr354) and anti-phosphorylated Ser372/Ser373 (pSer372/Ser373), corresponding to three CT residues phosphorylated by GRKs on the D1R. A proof-of-principle experiment was first performed using HEK293 cells transfected with Flag-tagged forms of D1R truncated at residues Cys347 and Cys351 to confirm the efficacy of both antibodies, with both mutant receptors having been truncated above the sites of phosphorylation. The results from these experiments show that phosphorylation of Thr354 and Ser372/373 does not occur in HEK293 cells transfected with fCys347 and fCys351 mutants (**Figs. 14, 15**), demonstrating that these antibodies are precisely recognizing their specific phosphorylation sites.

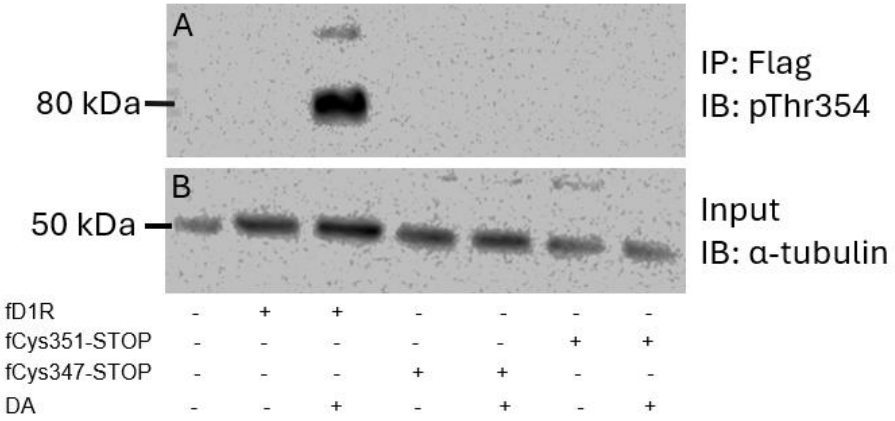

Figure 14. pThr354 Antibody Recognizes Specific Phosphorylation Site. Proof-of-principle experiment of co-immunoprecipitation and immunoblotting of HEK293 cells transfected with Flag-tagged D1R (fD1R) and mutant forms of fD1R truncated at residues Cys347 (fCys347-STOP) and Cys351 (fCys351-STOP) then subjected to 15 minutes of stimulation with vehicle (AA) or 10 μM DA. Negative controls were transfected with empty pCMV5 vector. Immunoprecipitated receptors were unable to be detected by anti-Flag antibody due to loss of protein from membrane stripping as well as technical issues with membrane transferring, but radioligand binding assays were performed to confirm presence of receptors. IPs were boiled during preparation of Western blot samples, resulting in a possible protein aggregation and the presence of extra bands (>80 KDa) during phosphorylation detection. (A) Receptors were immunoprecipitated using anti-Flag conjugated beads and probed with anti-phosphorylated Thr354 (pThr354) to confirm accurate detection of Thr354 phosphorylation. (B) Inputs were probed with anti-alpha tubulin antibody. Bmax values are 1.01 (fD1R), 4.75 (fCys347-STOP), and 1.07 (fCys351-STOP). N = 1.

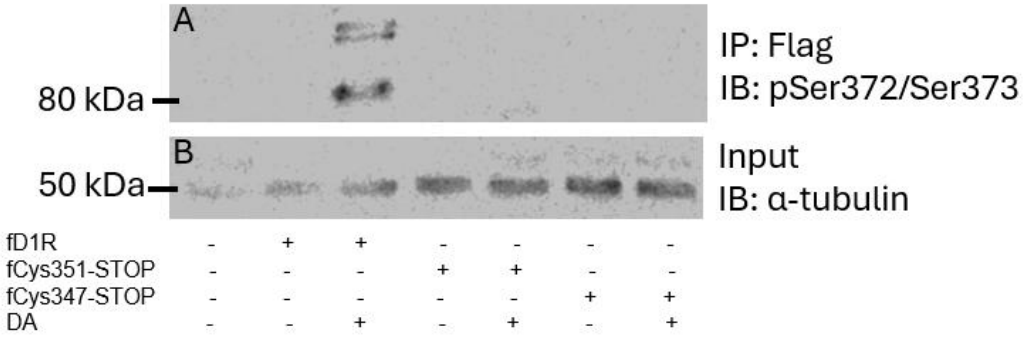

Figure 15. pSer372/Ser373 Antibody Recognizes Specific Phosphorylation Site. Proof-of-principle experiment of co-immunoprecipitation and immunoblotting of HEK293 cells transfected with Flag-tagged D1R (fD1R) and mutant forms of fD1R truncated at residues Cys347 (fCys347-STOP) and Cys351 (fCys351-STOP) then subjected to 15 minutes of stimulation with vehicle (AA) or 10 μM DA. Negative controls were transfected with empty pCMV5 vector. Immunoprecipitated receptors were unable to be detected by anti-Flag antibody due to a potential loss of protein from membrane stripping as well as technical issues with membrane transferring, but radioligand binding assays were performed to confirm presence of receptors. IPs were boiled during preparation of Western blot samples, resulting in a possible protein aggregation and the presence of extra bands (>80 KDa) during phosphorylation detection. (A) Receptors were immunoprecipitated using anti-Flag conjugated beads and probed with anti-phosphorylated Ser372/373 (pSer372/Ser373) to confirm accurate detection of Ser372/373 phosphorylation. (B) Inputs were probed with anti-alpha tubulin antibody. Bmax values are 3.84 (fD1R), 5.59 (fCys347-STOP), and 2.98 (fCys351-STOP). N = 1.

Following the validation of the pThr354 and pSer372/Ser373 antibodies, I assessed the role of the three downstream CT regions in the regulation of these D1R phosphorylation sites. Results show that phosphorylation of these residues becomes hindered with increasing truncation of the D1R CT, with the Val388 mutant showing little to no phosphorylation at either of these sites (Fig. 16, 17). Overall, this

demonstrates that the distal D1R CT domains are important for DA-induced phosphorylation of the upstream residues Thr354 and Ser372/Ser373.

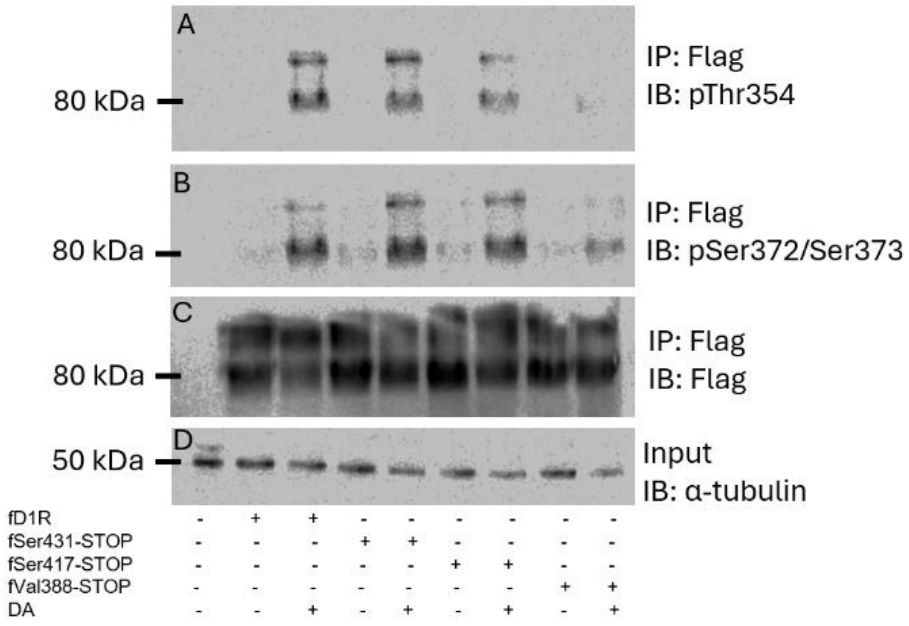

Figure 16. **Removal of Distal D1R CT Domains Reduces Phosphorylation of Thr354 and Ser372/Ser373 in a Successive Manner.** Representative experiment of co-immunoprecipitation and immunoblotting of HEK293 cells transfected with Flag-tagged D1R (fD1R) or mutant forms of fD1R truncated at residue Ser431 (fSer431-STOP), Ser417 (fSer417-STOP) or Val388 (fVal388-STOP), then subject to 15 minutes of stimulation with vehicle (AA) or 10 μM DA. Negative controls were transfected with empty pCMV5 vector. (A) Receptors were immunoprecipitated using anti-Flag conjugated beads and probed with anti-phosphorylated Thr354 (pThr354). Membrane filter was stripped and re-probed for (B) anti-phosphorylated Ser372/Ser373 (pSer372/Ser373) and again for (C) anti-Flag. IPs were boiled during preparation of Western blot samples, resulting in a potential protein aggregation and the presence of extra bands (>80 kDa) during phosphorylation detection. (D) Inputs were probed with anti-alpha tubulin antibody. Bmax values (mean ± SEM) are 3.45±0.49 (fD1R), 3.85±0.76 (fVal388-STOP), 3.81±0.77 (fSer417-STOP) and 4.35±0.70 (fSer43-STOP). N = 4.

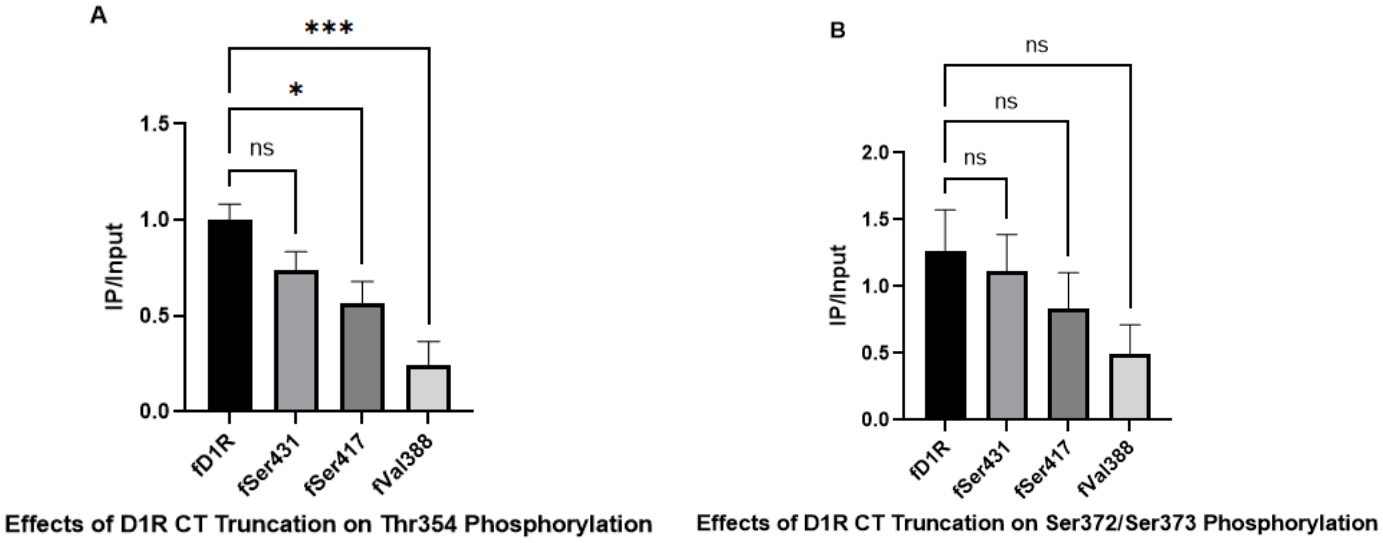

Figure 17. Quantification of the Removal of Distal D1R CT Domains on Phosphorylation of Thr354 and Ser372/Ser373. Densitometric analysis using ImageJ software for the immunoprecipitation of fD1R and mutant forms of fD1R truncated at residues Val388, Ser417 and Ser431 under stimulation of HEK293 cells using 10 μM DA for 15 mins. Blots were quantified with ImageJ and analyzed with GraphPad Prism to evaluate effects of cytoplasmic tail truncations on the phosphorylation of residues (A) Thr354 and (B) Ser372/Ser373. Bmax values (mean±SEM) are 3.45±0.49 (fD1R), 3.85±0.76 (fVal388), 3.81±0.77 (fSer417) and 4.35±0.70 (fSer431). Statistical analysis was performed using column analysis and one-way ANOVA. N = 4.

4.2. The role of PLZF in the dopamine-induced D1R phosphorylation process

4.2.1. PLZF hinders dopamine-mediated phosphorylation of D1R on CT Thr354 and Ser372/Ser373 residues with its regulation mediated by specific domains of the CT

Prior work in the Tiberi lab has shown that PLZF reduces the internalization of the D1 receptor (Josephine Zein, M.Sc. Thesis, 2022). As previously described, phosphorylation is a key mechanism in the desensitization process, decreasing the affinity of the GPCR for its cognate G-protein and increasing affinity for β-arrestin to bind to the IL3 and CT, facilitating endocytosis of the receptor (Kim et al., 2004). Therefore, PLZF may alter D1R internalization through inhibition of phosphorylation. As well, it was previously identified through a Y2H screen that PLZF interacts with the CT of D1R. Therefore, the regulation of phosphorylation by PLZF may be mediated by its interaction with the CT. To analyze this, HEK293 cells were transfected with either wildtype fD1R or various Flag-tagged truncated forms of the D1R (fVal388, fSer417, fSer431) in the presence or absence of HA-tagged PLZF. As in Part 1, these truncated receptors were employed to showcase the effect that different groups of CT residues impart on D1R phosphorylation, except in this case, they are now additionally co-expressed with PLZF. IP experiments were performed in transfected HEK293 cells under DA stimulation. Anti-FLAG M2 agarose matrix beads were used to immunoprecipitate the Flag-tagged receptors and phosphorylation was analyzed through Western blot by probing with pThr354 and pSer372/Ser373. The results demonstrate that co-expression of PLZF reduces phosphorylation at residues Thr354 and Ser372/Ser373 on the D1R CT. This regulation of phosphorylation by PLZF is either enhanced or diminished depending on the CT domain of truncation. For example, phosphorylation of these sites is further reduced when PLZF is co-expressed with the mutant receptor fSer431 (**Fig. 18, 19)**, whereby the D1R is truncated at residue Ser431 to remove its downstream residues. Considering that PLZF reduces D1R phosphorylation (Fig. 16-19), my results suggest that these residues downstream of Ser431 are likely not involved in the regulation of D1R phosphorylation by PLZF and thus may not be involved in its interaction.

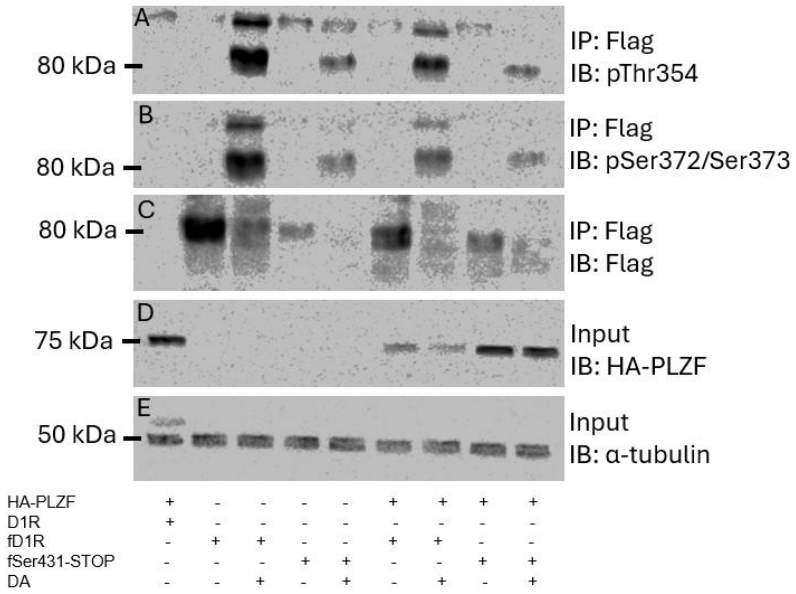

Figure 18. PLZF Reduces Phosphorylation of Thr354 and Ser372/Ser373 on D1R, which is Further Reduced with Truncation of the D1R CT at Ser431. Representative experiment of co-immunoprecipitation and immunoblotting of HEK293 cells transfected with Flag-tagged D1R (fD1R) or mutant forms of fD1R truncated at residue Ser431 (fSer431-STOP) in the presence or absence of HA-PLZF, then subjected to 15 minutes of stimulation with vehicle (AA) or 10 μM DA. Negative controls were transfected with PLZF and untagged D1R. (A) Receptors were immunoprecipitated using anti-Flag conjugated beads and probed with anti-phosphorylated Thr354 (pThr354). Membrane filter was stripped and re-probed for (B) anti-phosphorylated Ser372/Ser373 (pSer372/Ser373) and again for (C) anti-Flag. Not all immunoprecipitated receptors were able to be detected by anti-Flag antibody due to a potential loss of protein from membrane stripping as well as technical issues with membrane transferring, but radioligand binding assays were performed to confirm presence of receptors. IPs were boiled during preparation of Western blot samples, resulting in a possible protein aggregation and the presence of extra bands (>80 KDa) during phosphorylation detection. (D) Inputs were probed with anti-PLZF and (E) anti-alpha tubulin antibody. Bmax values (mean±SEM) are 7.30±1.51 (D1R+PLZF), 7.68±0.92 (fD1R), 5.78±1.74 (fD1R+PLZF), 7.23±1.92 (fSer431), and 4.64±1.03 (fSer431+PLZF). Statistical analysis was performed using column analysis and one-way ANOVA. N = 4

Figure 19. Quantification of PLZF-Mediated Reduction of Thr354 and Ser372/Ser373 Phosphorylation of Wildtype D1R and D1R Truncated at Ser431. Densitometric analysis using ImageJ software for the immunoprecipitation of fD1R, fD1R with HA-PLZF, a mutant form of fD1R truncated at residues Ser431 (fSer431), and the Ser431 mutant with PLZF (fSer431+PLZF), all transfected into HEK293 cells that were stimulated with either AA or 10 μM DA for 15 mins. Blots were quantified with ImageJ and analyzed with GraphPad Prism to examine effects of cytoplasmic tail truncations in the presence or absence of HA-PLZF on the phosphorylation of residue (A) Thr354 and (B) Ser372/Ser373. Bmax values (mean±SEM) are 7.30±1.51 (D1R+PLZF), 7.68±0.92 (fD1R), 5.78±1.74 (fD1R+PLZF), 7.23±1.92 (fSer431), and 4.64±1.03 (fSer431+PLZF). Statistical analysis was performed using column analysis and one-way ANOVA. N = 4

Next, to investigate if there were other CT domains involved in this regulation of D1R phosphorylation by PLZF, I employed mutant forms of the receptor where the D1R CT was truncated further upstream, specifically at residues Ser417 (fSer417) and Val388 (fVal388). Interestingly, removal of the CT at Ser417 (**Fig. 20, 21**) and Val388 (**Fig. 22, 23**) diminishes the reduction of Thr354 and Ser372/Ser373 phosphorylation imposed by PLZF. Therefore, these downstream residues may be important for the regulation of D1R phosphorylation, which may be mediated through a possible interaction with PLZF.

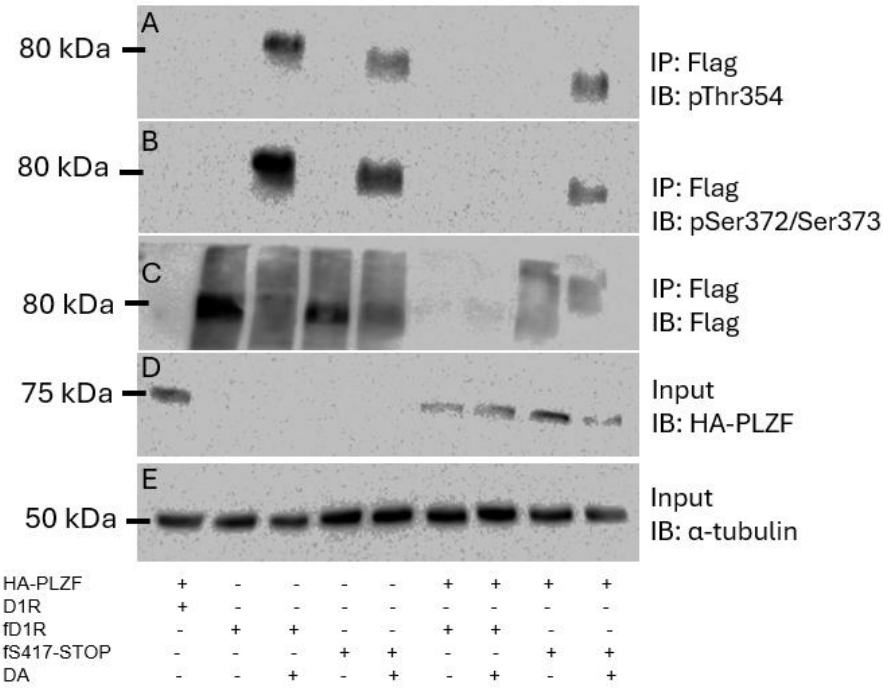

Figure 20. Removal of D1R CT at Residue Ser417 Diminishes the Regulation of Thr354 and Ser372/Ser373 Phosphorylation Imposed by PLZF. Representative experiment of co-immunoprecipitation and immunoblotting of HEK293 cells transfected with Flag-tagged D1R (fD1R) or mutant forms of fD1 truncated at residue Ser417 (fSer417-STOP), in the presence or absence of HA-PLZF, then subjected to 15 mins stimulation with vehicle (AA) or 10 μM DA. Negative controls were transfected with PLZF and untagged D1R. (A) Receptors were immunoprecipitated using anti-Flag conjugated beads and probed with anti-phosphorylated Thr354 (pThr354). Membrane filters were stripped and re-probed for (B) anti-phosphorylated Ser372/Ser373 (pSer372/Ser373) and again for (C) anti-Flag. Not all immunoprecipitated receptors were able to be detected by anti-Flag antibody due to a potential loss of protein from membrane stripping as well as technical issues with membrane transferring, but radioligand binding assays were performed to confirm presence of receptors. (D) Inputs were probed with anti-PLZF and (E) anti-alpha tubulin antibody. Bmax values (mean± SEM) are 0.73±0.24 (D1R+PLZF), 4.56±1.46 (fD1R), 4.00±2.73 (fD1R+PLZF), 11.09±3.67 (fSer417), and 4.64±2.23 (fSer417+PLZF). N = 3.

Figure 21. Quantification of PLZF-Mediated Reduction of Thr354 and Ser372/Ser373 Phosphorylation of Wildtype D1R and D1R Truncated at Ser417. Densitometric analysis using ImageJ software for the immunoprecipitation of FD1, fD1 with HA-PLZF, a mutant form of fD1 truncated at residues Ser417 and the Ser417 mutant with PLZF, all transfected into HEK293 cells that were stimulated with either AA or 10 μM DA for 15 mins. (A) Blots were quantified with ImageJ and analyzed with GraphPad Prism to evaluate effects of cytoplasmic tail truncations in the presence or absence of HA-PLZF on the phosphorylation of residue (A) Thr354 and (B) Ser372/Ser373. Bmax values (mean±SEM) are 0.73±0.24 (D1R+PLZF), 4.56±1.46 (fD1R), 4.00±2.73 (fD1R+PLZF), 11.09±3.67 (fSer417), and 4.64±2.23 (fSer417+PLZF). Statistical analysis was performed using column analysis and one-way ANOVA. N = 3

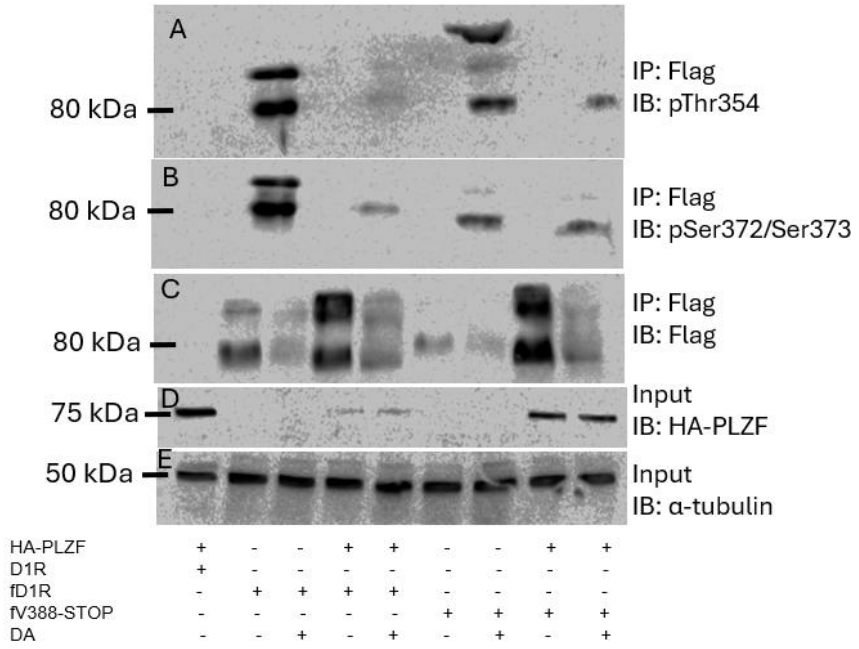

Figure 22. Removal of D1R CT at Residue Val388 Diminishes the Regulation of Thr354 and Ser372/Ser373 Phosphorylation Imposed by PLZF. Representative experiment of co-immunoprecipitation and immunoblotting of HEK293 cells transfected with Flag-tagged D1R (fD1R), mutant forms of fD1R truncated at residue Val388 (fVal388), in the presence or absence of HA-PLZF, then subjected to 15 mins stimulation with vehicle (AA) or 10 μM DA. Negative controls were transfected with PLZF and untagged D1R. (A) Receptors were immunoprecipitated using anti-Flag conjugated beads and probed with anti-phosphorylated Thr354 (pThr354). Membrane filters were stripped and re-probed for (B) anti-phosphorylated Ser372/Ser373 (pSer372/Ser373) and again for (C) anti-Flag. Not all immunoprecipitated receptors were able to be detected by anti-Flag antibody due to a potential loss of protein from membrane stripping as well as technical issues with membrane transferring, but radioligand binding assays were performed to confirm presence of receptors. IPs were boiled during preparation of Western blot samples, resulting in a possible protein aggregation and the presence of extra bands (>80 KDa) during phosphorylation detection. (D) Inputs were probed with anti-PLZF and (E) anti-alpha tubulin antibody. Bmax values (mean±SEM) are 7.60±5.52 (D1R+PLZF), 7.76±5.03 (fD1R), 8.34±4.18 (fD1R+PLZF), 6.06±5.26 (fVal388), and 8.77±4.42 (fVal388+PLZF). N = 3.

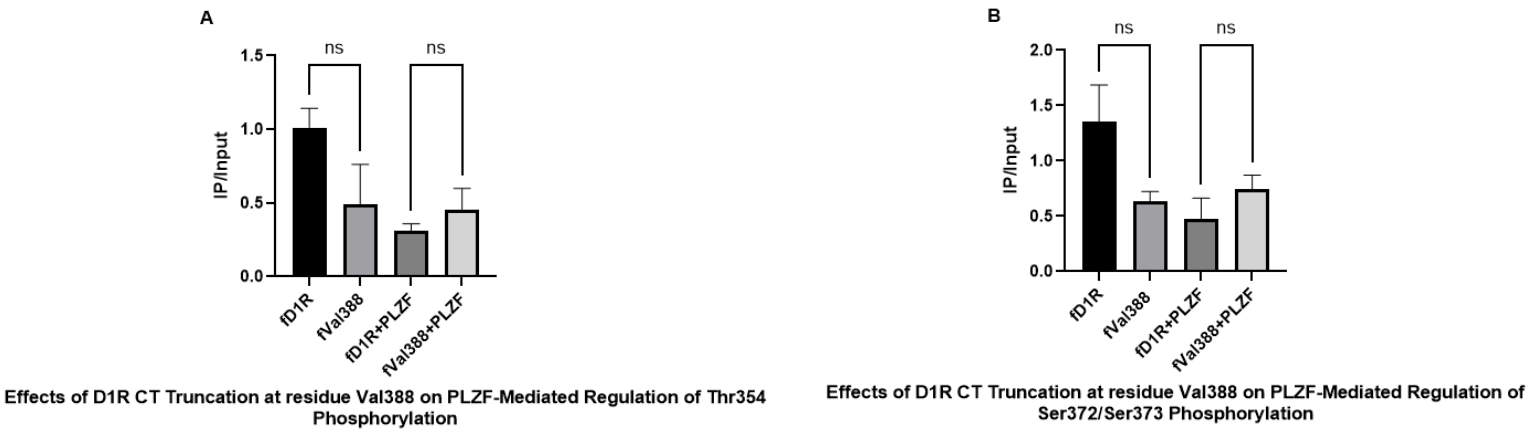

Figure 23. Quantification of PLZF-Mediated Reduction of Thr354 and Ser372/Ser373 Phosphorylation of Wildtype D1R and D1R Truncated at Val388. Densitometric analysis using ImageJ software for the immunoprecipitation of fD1R, fD1R with HA-PLZF, a mutant form of fD1R truncated at residues Val388 and the Val388 mutant with PLZF, all transfected into HEK293 cells that were stimulated with either AA or 10 μM DA for 15 mins. Blots were quantified using ImageJ to analyze effects of cytoplasmic tail truncations in the presence or absence of HA-PLZF on the phosphorylation of residue Thr354 and Ser372/Ser373. Bmax values (mean±SEM) are 7.60±5.52 (D1R+PLZF), 7.76±5.03 (fD1R), 8.34±4.18 (fD1R+PLZF), 6.06±5.26 (fVal388), and 8.77±4.42 (fVal388+PLZF). N = 3.

4.3. Mapping the interaction domains of PLZF on the D1-class

4.3.1. Removal of the D1R CT does not impact PLZF recruitment to the D1R

Prior studies have demonstrated that the CT constitutes a major site for protein-protein interactions on the D1R (Bermak et al., 2002; Kim et al., 2002). PLZF was identified to interact with the CT through Y2H studies and has been previously shown to form interactions with the D1R through preliminary coimmunoprecipitation studies (Josephine Zein, M. Sc. Thesis, 2022), however it remains to be known the precise site on the D1R CT that PLZF is recruited to. Identifying this site may help to understand the mechanistic basis behind the regulation of D1R phosphorylation by PLZF, as I previously showed that truncation of D1R CT domains hinders the effects of PLZF on reducing Thr354 and Ser372/Ser373 phosphorylation on the D1R. To identify the site of interaction for PLZF, HEK293 cells were transfected with HA-tagged PLZF and Flag-tagged D1R or its truncated CT counterparts (fCys347, fCys351, fVal388, fSer417, fSer431). The reasoning behind this was that if PLZF was no longer detectable during immunoprecipitation of the mutated receptor, this would indicate that the missing domain was the site of interaction for PLZF or at least was involved in its recruitment to the D1R. I first started by using the three most distal truncated receptors (Δ388, Δ417, Δ431), as it was previously demonstrated that the residues downstream of Val388 may be involved in the regulation of Thr354 and Ser372/Ser373 phosphorylation by PLZF. Interestingly, removal of these CT domains does not hinder PLZF recruitment; rather, it appears to heighten its complex formation with the D1R (**Fig. 24, Fig. 25)**, demonstrating that these residues are not involved in forming an interaction with PLZF.

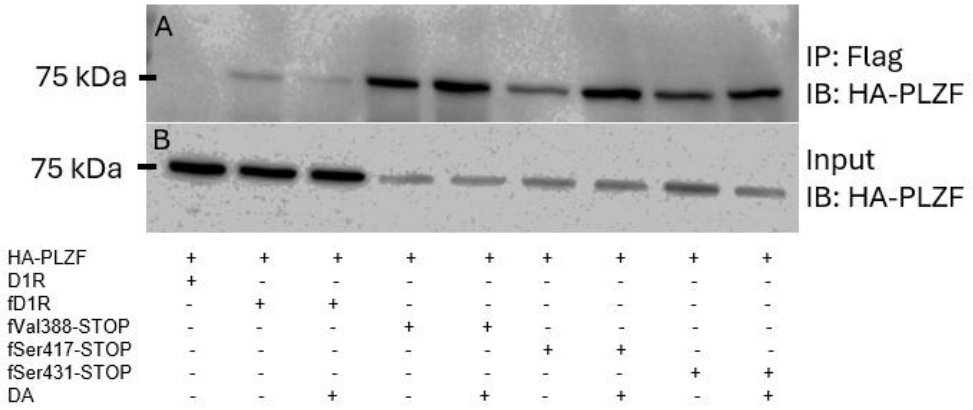

Figure 24. Removal of D1R CT at Residues Val388, Ser417 and Ser431 Does Not Inhibit PLZF Complex Formation. Representative experiment of co-immunoprecipitation and immunoblotting of HEK293 cells transfected with HA-PLZF and Flag-tagged D1R (fD1R) or mutant forms of fD1R truncated at residues Val388 (fVal388-STOP), Ser417 (fSer417-STOP) or Ser431 (fSer431-STOP), then subjected to 15 minutes of stimulation with vehicle (AA) or 10uM DA. Negative controls were transfected with PLZF and untagged D1R. (A) Receptors were immunoprecipitated using anti-Flag conjugated beads and probed with anti-PLZF. (B) Inputs were also probed with anti-PLZF. Immunoprecipitated receptors were unable to be detected by anti-Flag antibody due to a potential loss of protein from membrane stripping as well as technical issues with membrane transferring, but radioligand binding assays were performed to confirm presence of receptors. Bmax values (mean±SEM) are 0.21±0.14 (D1R+PLZF), 1.64±0.33 (fD1R+PLZF), 8.05±3.72 (fVal388+PLZF), 3.36±1.93 (fSer417+PLZF) and 5.00±3.51 (fSer431+PLZF). N = 3.

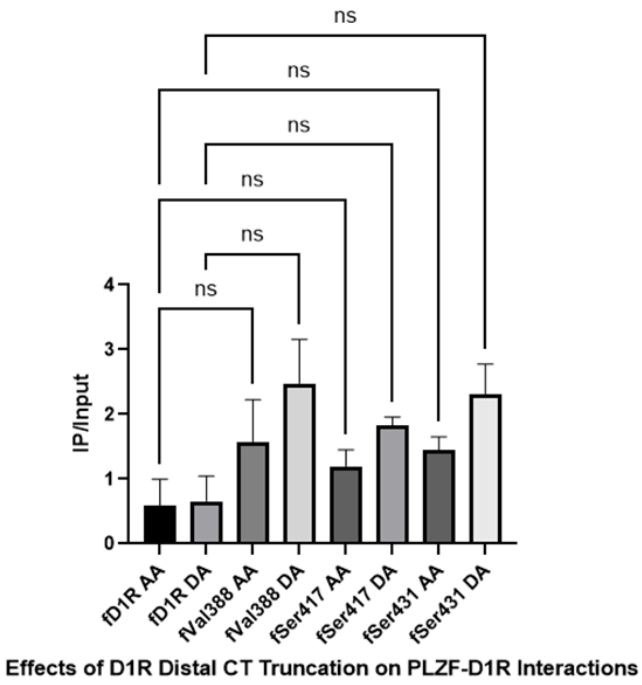

Figure 25. Quantification of the Effect of D1R CT Domain Removal at Val388, Ser417 and Ser431 on PLZF Complex Formation Under Basal and Dopamine-Stimulated Conditions. Densitometric analysis using ImageJ software for the co-immunoprecipitation of HA-PLZF with Flag-tagged D1R (fD1R) or mutant forms of fD1 with CT truncated at either residue Val388 (fVal388), Ser417 (fSer417) or Ser431 (fSer431), all transfected into HEK293 cells that were under stimulation with either AA or 10 μM DA for 15 minutes. Blots were quantified with ImageJ and analyzed with GraphPad Prism to analyze effects of removal of distal cytoplasmic domain residues on the interaction between receptor and PLZF. Bmax values (mean±SEM) are 0.21±0.14 (D1R+PLZF), 1.64±0.33 (fD1R+PLZF), 8.05±3.72 (fVal388+PLZF), 3.36±1.93 (fSer417+PLZF) and 5.00±3.51 (fSer431+PLZF). Statistical analysis was performed using column analysis and one-way ANOVA. N = 3

Based on those results, I postulated that PLZF must be interacting upstream of Val388, so I hypothesized that using a mutant receptor whose CT was truncated at a proximal site (fCys347 and fCys351) would inhibit PLZF recruitment to the CT. Upon performing co-IPs with these mutant receptors, I saw similar effects: complete removal of the CT (fCys347-STOP) as well as truncation at residue Cys351 (fCys351-STOP) does not impair PLZF recruitment to the D1R (**Fig. 26, Fig. 27**). Altogether, this highlights that PLZF does not form a complex with the D1R CT and there may be other domains, such as the helix 8 (H8) or the IL3 that are involved in this interaction.

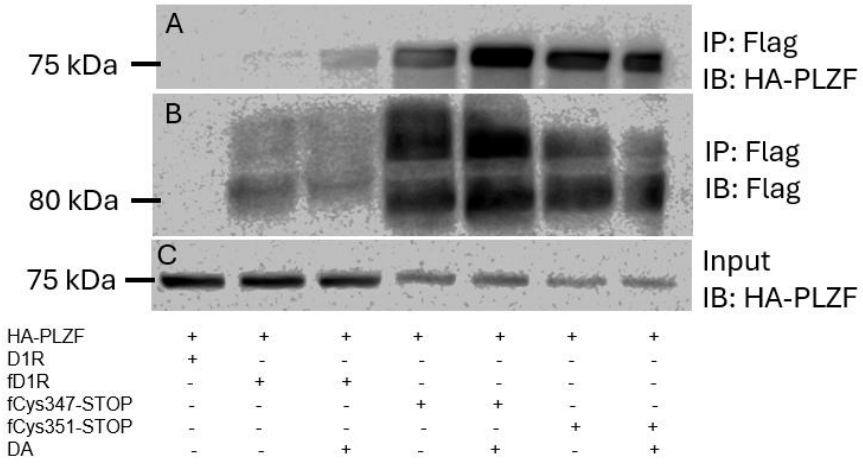

Figure 26. Removal of D1R CT at Residues Cys347 and Cys351 Does Not Inhibit PLZF Complex Formation. Representative experiment of co-immunoprecipitation and immunoblotting of HEK293 cells transfected with HA-PLZF and Flag-tagged D1R (fD1R) or mutant forms of fD1R truncated at residues Cys347 (fCys347-STOP) and Cys351 (fCys351-STOP), then subjected to 15 mins stimulation with vehicle (AA) or DA. Negative controls were transfected with PLZF and untagged D1R. Receptors were immunoprecipitated using anti-Flag conjugated beads and probed with (A) anti-PLZF. Membrane was stripped and re-probed for (B) anti-Flag. (C) Inputs were also probed with anti-PLZF. Bmax values (mean±SEM) are 0.1±0.03 (D1R+PLZF), 4.26±0.94 (fD1R+PLZF), 3.11±0.50 (fCys347+PLZF), and 1.35±0.20 (fCys351+PLZF). N = 6.

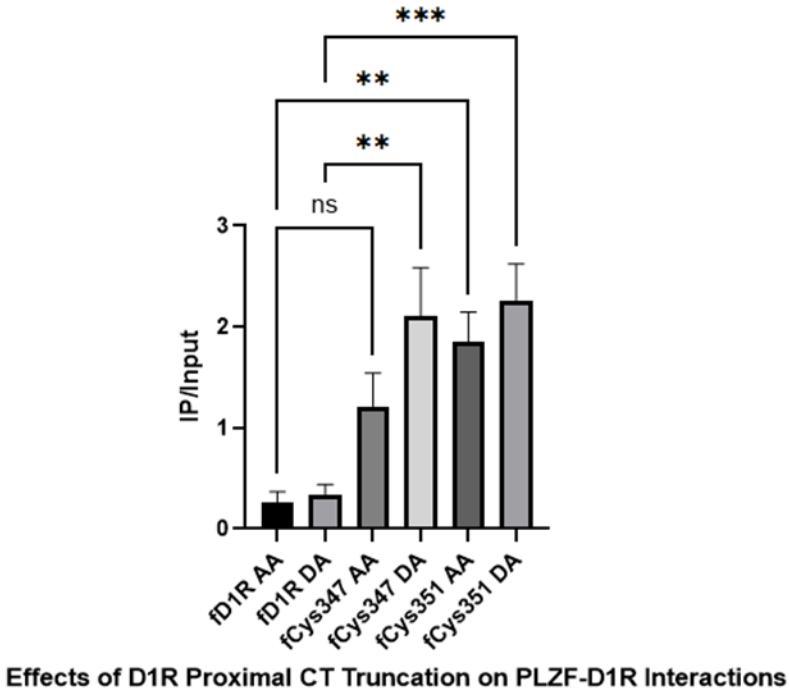

Figure 27. Quantification of the Effect of D1R CT Domain Removal at Cys347 and Cys351 on PLZF Complex Formation Under Basal and Dopamine-Stimulated Conditions. Densitometric analysis using ImageJ software for the co-immunoprecipitation of HA-PLZF with Flag-tagged D1R (fD1R) or mutant forms of fD1R with the CT truncated at either residue Cys347 (fCys347) or Cys351 (fCys351), all transfected in HEK293 cells under stimulation with either AA or 10 μM DA for 15 minutes. Blots were quantified with ImageJ and analyzed with GraphPad Prism to examine effects of removal of proximal cytoplasmic domain residues on the interaction between the D1R receptor and PLZF.) Bmax values (mean±SEM) are 0.1±0.03 (D1R+PLZF), 4.26±0.94 (fD1R+PLZF), 3.11±0.50 (fCys347+PLZF), and 1.35±0.20 (fCys351+PLZF). Statistical analysis was performed using column analysis and one-way ANOVA. N = 6.

4.3.2. PLZF interacts with the IL3 in addition to the CT

As previously described, Y2H screening performed in our lab pulled out PLZF as a potential interactor with the CT of D1R; however, based on our co-IP results, complete removal of the D1R CT still yields recruitment of PLZF. To confirm which D1R domains are interacting with PLZF, HEK293 cells were transfected with HA-tagged PLZF, and a pulldown assay was performed using recombinant GST proteins fused with either the IL3 or CT domain of the D1-class. Glutathione Sepharose beads were used to immunoprecipitate the GST-tagged fusion proteins and PLZF interaction was assessed through Western Blot by probing with anti-PLZF. The results show that PLZF forms an interaction with the CT of D1R, confirming the results from the Y2H screen. However, the results also identified an interaction between PLZF and the IL3 of D1R, albeit a weaker affinity than the CT of D1R (**Fig. 28**). Altogether, these findings imply that PLZF may form a complex with both the IL3 and CT domains of the D1R in vitro, with PLZF having a particularly stronger affinity for the CT.

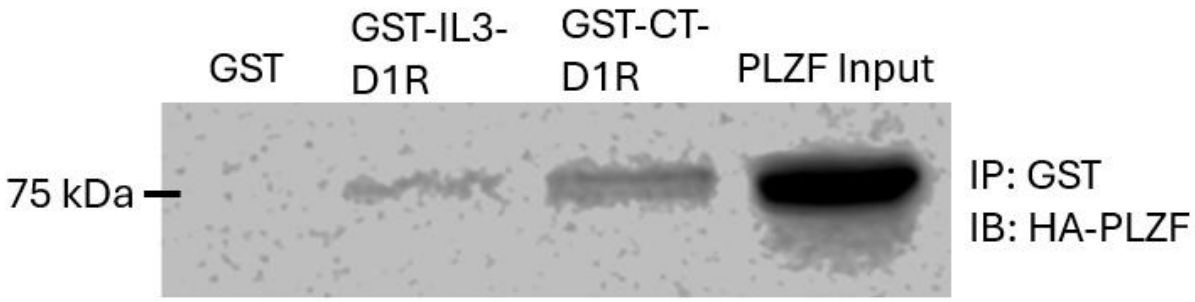

Figure 28. PLZF Interacts with IL3 and CT of D1R. Representative experiment of GST-tagged protein pulldown and immunoblotting of HEK293 cells transfected with HA-PLZF. HA-PLZF was pulled down using Glutathione Sepharose beads conjugated with GST-proteins fused with the IL3 and CT domain of D1R and probed with anti-PLZF antibody. Inputs were also probed using anti-PLZF antibody. N = 3

4.3.3. DA stimulation, in addition to specific IL3 segments, differentially modulates PLZF binding to D1R

To better understand the role of the IL3 domain in regulating PLZF recruitment to the D1R, HEK392 cells were transfected with receptors containing mutated forms of the IL3 (IL3-ΔN or IL3-ΔC), corresponding to proteolytic cleavage at specific sites of the IL3 to remove either its N-terminal or C-terminal end (**Fig. 29**).

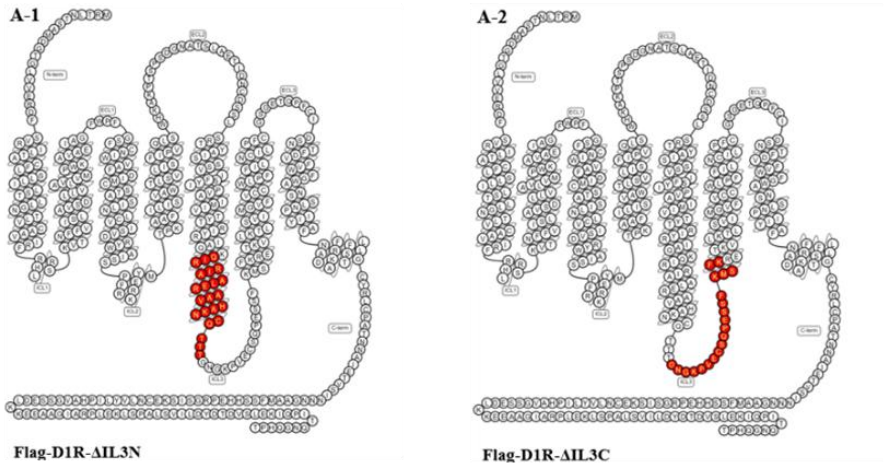

Figure 29. Sites of IL3 Domain Truncation for Mutated D1R Receptors Used in PLZF-D1R Interaction Domain Mapping. Residues highlighted in red corresponded to the residues that are truncated for each mutant IL3-D1R construct. A-1 corresponds to the residues of the N-terminus of IL3 that were truncated (Q224-T245), while A-2 corresponds to the residues truncated in the C-terminus of the IL3 (G246-K285).

IP experiments using these truncated IL3 mutants were performed in transfected HEK293 cells under 10 μM DA stimulation for 15 minutes, as it has been well-established that complex formation between GPCRs and their interacting proteins can be modulated through the presence of agonists and antagonists (Slater et al., 2016). Anti-FLAG M2 agarose matrix beads were used to immunoprecipitate the Flag-tagged receptors and PLZF interaction was assessed through Western Blot by probing with anti-PLZF. The results show that complex formation is increased with IL3-ΔN under basal conditions but is decreased during DA stimulation. Contrarily, IL3-ΔC decreases complex formation under basal conditions but becomes strongly increased under DA stimulation (**Fig. 30, 31**). Overall, these results suggest that PLZF complex formation is potentially multifaceted and variable, depending on multiple factors including receptor conformation and the presence of an agonist.

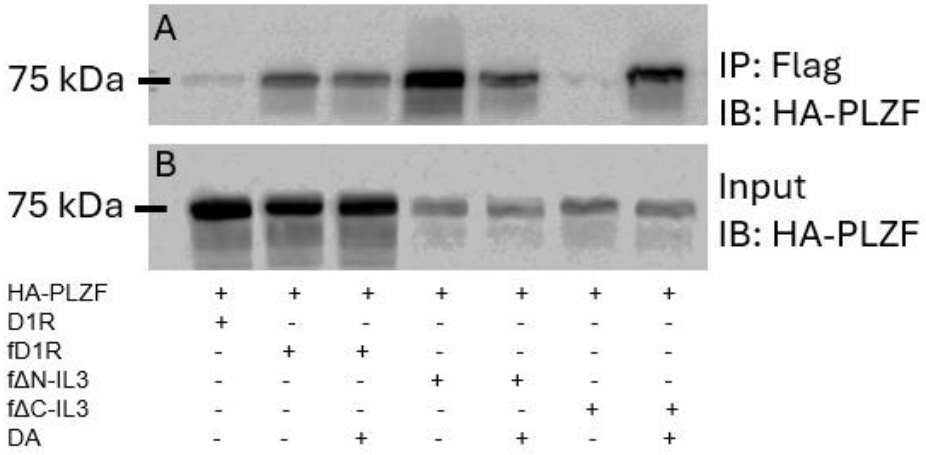

Figure 30. Removal of D1R IL3 Domains Oppositely Modulates PLZF Complex Formation Under Basal and Dopamine-Stimulated Conditions. Representative experiment of co-immunoprecipitation and immunoblotting of HEK293 cells transfected with HA-PLZF and Flag-tagged D1R (fD1R) or mutant forms of fD1R cleaved at the N terminus (fΔN-IL3) and C terminus (fΔC-IL3) of the IL3, then subjected to 15 minutes of stimulation with vehicle (AA) or 10 uM DA. Negative controls were transfected with PLZF and untagged D1R. (A) Receptors were immunoprecipitated using anti-Flag conjugated beads and probed with anti-PLZF. (B) Inputs were also probed with anti-PLZF. Immunoprecipitated receptors were unable to be detected by anti-Flag antibody due to a potential loss of protein from membrane stripping as well as technical issues with membrane transferring, but radioligand binding assays were performed to confirm presence of receptors. Bmax values are 2.02±0.25 (D1R+PLZF), 4.10±1.52 (fD1R+PLZF), 0.69±0.29 (fΔN-IL3+PLZF), and 5.10±1.0 (fΔC-IL3+PLZF). N = 3.

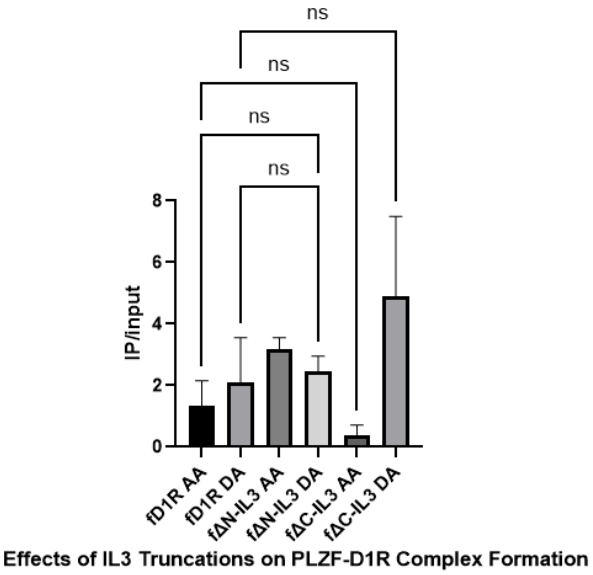

Figure 31. Quantification of the Effect of D1R IL3 Domain Removal on PLZF Complex Formation Under Basal and Dopamine-Stimulated Conditions. Densitometric analysis using ImageJ software for the co-immunoprecipitation of HA-PLZF with Flag-tagged D1R (fD1R) or mutant forms of fD1R with removal of either the N-terminus (fΔN-IL3) of the IL3 or C-terminus (fΔC-IL3) of the IL3, all transfected in HEK293 cells under stimulation with either AA or 10 μM DA for 15 minutes. (A) Blots were quantified with ImageJ and analyzed with GraphPad Prism to evaluate effects of IL3 truncations on the interaction between receptor and PLZF. (C) Quantifications were normalized for respective Bmax values. (B) Bmax values (mean±SEM) are 2.02±0.25 (D1R+PLZF), 4.10±1.52 (fD1R+PLZF), 0.69±0.29 (fΔN-IL3+PLZF), and 5.10±1.0 (fΔC-IL3+PLZF). Statistical analysis was performed using column analysis and one-way ANOVA. N = 3

5. Discussion

Studies have shown that dopamine receptors are regulated by the interactions of numerous cytoskeletal, adaptor and signaling proteins, referred to in the literature as DRIPs (Bergson et al., 2003). Given that DARs are some of the most abundant receptors in the CNS and dysfunctions in their biochemical functioning have been implicated in numerous neurological and psychological disorders, many efforts have been taken to further investigate the role of these proteins in regulating the signaling and trafficking pathways mediating individual DAR subtypes (Goldman-Rakic, 1998; Wang et al., 2008). Our lab conducted Y2H screens, whereby the protein products of a cDNA library are screened with a selected GPCR-derived domain, to delve into the full complement of possible DRIPs (Tanowitz & von Zastrow, 2004). Using this proteomic approach, we identified the Promyelocytic Leukemia Zinc Finger, which was found to interact with the IL3 of D5R and the CT of D1R. The D1R-PLZF interaction was confirmed through co-immunoprecipitation studies (Josephine Zein, 2022, Master's Thesis, University of Ottawa). Further assays were performed to better understand the impact of PLZF on the functional activity of the D1-class, where it was discovered that PLZF differentially modulates D1-class signaling and trafficking behaviour in a subtype-specific manner. Specifically, PLZF increases D1R-stimulated cAMP activity and ERK activation but decreases D5R-stimulated cAMP activity and ERK activation. PLZF also downregulates D1R internalization but facilitates the internalization of D5R. The results from these studies prompted further interest in understanding the underlying mechanisms surrounding these effects. Given the role of phosphorylation in mediating receptor internalization as well as prior unpublished results showing that β-arrestin recruitment to the D1R is decreased in the presence of PLZF, our lab wanted to investigate if PLZF has an influence on the phosphorylation status of the receptor as well as the overall role of the CT domains in mediating DA-induced phosphorylation. We also wanted to see if this effect is mediated through the location of PLZF interaction on the D1R given the number of Ser and Thr phosphorylation sites on the D1R (Tiberi et al., 1996; Sedaghat and Tiberi, 2011; Moritz et al., 2023). My M.Sc. thesis focuses solely on the role of PLZF in the D1R as the D1R is the most abundant DAR in the CNS and is more widely implicated in neurological disorders like PD (Missale et al., 1998; Beaulieu and Gainetdinov, 2011). Additionally, the long-term administration of Levodopa for treating PD is frequently

associated with the onset of LID, which is known to result from increased D1R-mediated transmission at the level of the direct pathway (Bezard et al., 2001; Aubert et al., 2005). Given the high structural homology between the D1R and D5R, gaining a better understanding of the different protein complexes formed during dopamine receptor activation and how this is altered under pathophysiological conditions may postulate a new framework for the discovery of novel druggable receptor sites, thereby providing better ways to pharmacologically differentiate between the D1-class subtypes and offering more efficacious treatment of diseases.

The results from my project demonstrate that the truncation of the distal domains of the D1R CT, located between Val388 and Thr446, imparts a sequential negative regulatory impact on the phosphorylation of Thr354 and Ser372/Ser373, with greater truncation of the CT leading to greater loss of phosphorylation. Furthermore, the co-expression of PLZF with the D1R negatively impacts D1R phosphorylation of these specific residues. In addition, co-expression of PLZF with various truncated forms of the D1R CT alters the degree of phosphorylation imposed on Thr354 and Ser372/Ser373 by PLZF, suggesting that these downstream CT regions may mediate the regulatory effects of PLZF on D1R phosphorylation. Interestingly, I show that PLZF is recruited to the D1R regardless of the length of CT truncation, suggesting that PLZF may instead form a complex with the Helix 8/IL4 domain located proximally to the CT, as this region was part of the Y2H bait used for the D1R CT. I also demonstrate that PLZF interacts with both the CT and IL3 domains of the D1R, with PLZF forming a stronger interaction with the CT in the GST pulldown assays. Finally, the regions of the D1R IL3 mediate different effects on the binding of PLZF, with the removal of either the N-terminus or C-terminus shifting the degree of PLZF recruitment to the D1R between basal and agonist-stimulated states.

5.1 Phosphorylation of D1R CT residues may prime more upstream residues for phosphorylation

The findings show that the degree of phosphorylation of the D1R CT residues Thr354 and Ser372/Ser373 gradually decreases with progressive truncation of downstream CT domains. It is possible that the

removal of these domains alters the structural conformation of the D1R CT to restrict GRK access to Thr354 and Ser372/Ser373, thereby decreasing their phosphorylation levels. It is also possible that phosphorylation of the CT occurs in a sequential order, with phosphorylation of residues on the distal portion of the tail being of importance for the phosphorylation of more proximal residues like Thr354 and Ser372/Ser373. This hypothesis aligns with previous studies which showed that sequential truncation of the D1R CT, as well as mutation of specific residues of the CT, results in a consecutive loss of agonist-induced phosphorylation (Jackson et al., 2002; Lamey et al., 2002; Kim et al., 2004). It has also been demonstrated that receptor activation promotes phosphorylation in a hierarchical fashion, such that the CT must be phosphorylated first before the IL3 can be phosphorylated (Kim et al., 2004; Moritz et al., 2023). It has been well-established that β-arrestin associates with the IL3 during receptor desensitization. Studies show that phosphorylation sites in the proximal CT residues are critical for β-arrestin binding, whereas the phosphorylation sites in the IL3 bear responsibility for β-arrestin-mediated receptor internalization (Kaya et al., 2020; Moritz et al., 2023). Therefore, rather than creating a binding pocket, the role of phosphorylation is to alter the conformation of both the IL3 and CT to allow for the association and binding of β-arrestin (Kim et al., 2004). Altogether, phosphorylation of CT residues located downstream of Thr354 and Ser372/Ser373 may be an essential mediator to alter the structural conformation of D1R to allow for the recruitment of β-arrestin to the IL3 (**Fig. 32**).

The phosphorylation of these sites may also yield a structural conformation that repels the association of D1R with PLZF. As previously discussed, the Y2H screening performed in our lab showed that PLZF can form a complex with the CT of D1R. The “phosphorylation barcode” hypothesis implies that different receptor phosphorylation patterns dictate the probability of arrestin adopting a particular active conformation for the receptor (Kaya et al., 2020). Previous coimmunoprecipitation studies in our lab also unearthed that β-arrestin-2 levels decrease in the presence of D1R and PLZF. Based on this, the removal of phosphorylation sites downstream of Thr354 and Ser372/Ser373 may alter the phosphorylation barcode, reducing binding affinity for β-arrestin and allowing for the formation of a binding site that

prefers PLZF. Whereas phosphorylation of those downstream CT residues, alongside phosphorylation of Thr354 and Ser372/Ser373, may alter the receptor conformation in a way that impedes PLZF binding and increases the recruitment of β-arrestin. This theory also supports the subsequent results of this thesis, whereby phosphorylation of Thr354 and Ser372/373 is reduced in the presence of PLZF and becomes more reduced with removal of the distal CT domains.

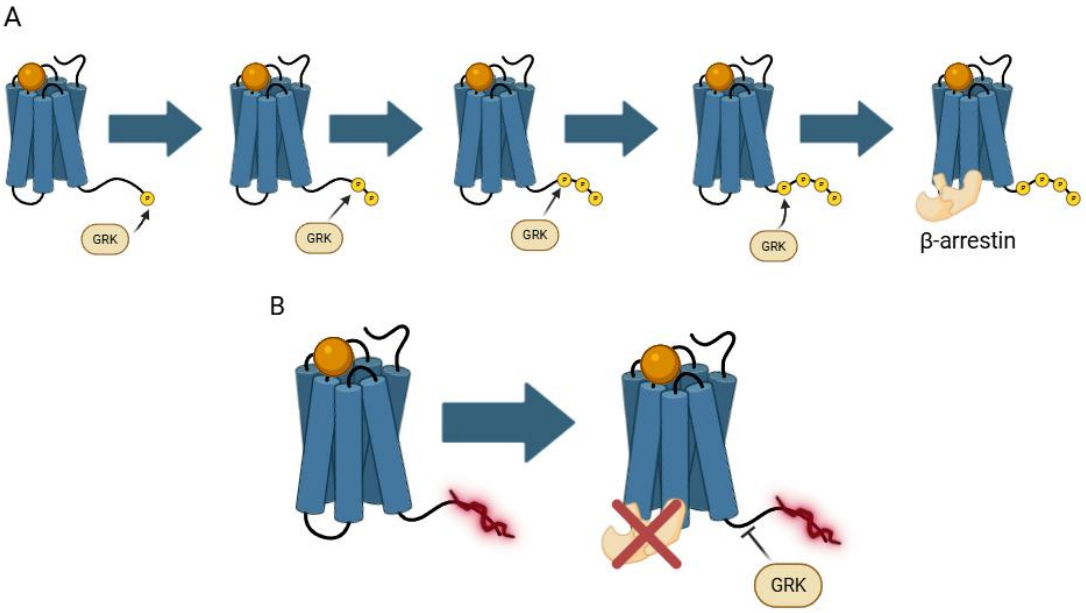

Figure 32. Phosphorylation of the D1R CT Occurs in a Sequential Manner. Schematic diagram of the gradual loss of D1R phosphorylation at residues Thr354 and Ser372/Ser373 with successive truncation of the D1R distal CT domains. Phosphorylation of the D1R CT potentially occurs in a sequential manner, starting with the most distal residues first. As phosphorylation of the CT has been shown to mediate the phosphorylation of the IL3 to confer binding of β-arrestin, phosphorylation of the D1R distal CT domains may regulate proper configuration of the receptor structure to increase the binding affinity of β-arrestin to the IL3. Created with BioRender.com.

5.2. PLZF may reduce the internalization of D1R through alterations in standard phosphorylation barcode, which may be regulated through its interaction with specific regions of the D1R CT

Prior unpublished results from the Tiberi lab have shown that PLZF inhibits internalization and accelerates recycling of D1R, prompting an investigation into whether PLZF mediates the regulation of D1R intracellular sorting through alterations in DA-induced phosphorylation. The results show that PLZF hinders phosphorylation of residues Thr354 and Ser372/Ser373, located on the proximal end of the CT. It is possible that PLZF, through its interaction on the CT, physically blocks GRK recruitment or triggers a change in structural conformation which may block GRK recruitment to these residues or other downstream residues that are essential for priming the phosphorylation of Thr354 and Ser372/Ser373, as I have shown in prior results. As previously discussed, receptor desensitization is governed by the phospho-barcode hypothesis, which states that downstream cellular events, such as the recruitment of β-arrestin, are facilitated through a unique phosphorylation pattern within the cytosolic domains (Kaya et al., 2020). Preliminary unpublished studies in the lab suggest that PLZF may hinder the recruitment of β-arrestin to the D1R. Therefore, the reduction in phosphorylation by PLZF may potentially interfere with this barcode, hindering the signal that is essential for β-arrestin to be recruited to the D1R. Additionally, this phosphorylation, in the presence of PLZF, is further altered through the deletion of the CT at Ser431 (Leu432-Thr446), with this truncation reducing phosphorylation of all three residues. On the other hand, CT truncations at Ser417 (Pro418-Val430) and Val388 (Tyr389-Leu416) increase phosphorylation of Thr354 and Ser372/Ser373, beyond that of wildtype D1R with PLZF. This shows that these regions play a role in the PLZF-mediated regulation of DA-induced phosphorylation, with a significant contribution from residues Tyr389-Val430.

We have shown that PLZF interacts primarily with the CT of D1R as well as the IL3 to a lesser extent. The idea that PLZF only interacts with one specific site on all D1Rs at a given time is unlikely. Rather, it can be assumed that the majority of D1Rs within a biological system form a complex with PLZF on the

CT whereas a smaller portion form a complex on the IL3 and this is determined by the current molecular conditions and needs of the cell at that given time. It is also possible that PLZF forms a complex with both the IL3 and CT of the D1R at the same time. It was previously discussed that the IL3 is the site of interaction for β-arrestin and that phosphorylation of the proximal CT residues is necessary to stimulate β-arrestin recruitment through changes in receptor conformation. Additionally, we previously hypothesized that Ser/Thr phosphorylation of the distal D1R CT residues is necessary to prime Thr354 and Ser372/Ser373 for phosphorylation. Therefore, PLZF may interact with the proximal CT to interfere with the binding of GRKs, impeding phosphorylation of those residues and preventing the conformational changes in the D1R that are important for the recruitment of β-arrestin. Alternatively, PLZF may interact with the distal CT residues to interfere with their phosphorylation and subsequently interfere with the phosphorylation of more upstream CT residues to block β-arrestin recruitment. Additionally, the complex formation between PLZF and the IL3 may impose a structural conformation of the receptor that hinders phosphorylation at this site, hindering the recruitment of β-arrestin to this domain on the receptor.

These findings also show a further decline in Thr354 and Ser372/Ser373 phosphorylation when PLZF is co-expressed with a form of D1R that is truncated at residue Ser431. In contrast, removal of the residues downstream of Val388 and Ser417 enhances phosphorylation of these sites relative to wildtype D1R with PLZF. This suggests that recruitment of PLZF to the Ser431 mutant alters the receptor conformation to expand the reduction of phosphorylation at Thr354 and Ser372/Ser373. There may also be residues downstream of Ser431 that are phosphorylated by GRKs to prime these residues for phosphorylation, as I showed in prior results. This may also lead to a downregulation in β-arrestin recruitment, though further studies are needed to confirm the impact of these mutants on the recruitment of β-arrestin when PLZF is co-expressed. In the case of the Val388 and Ser417 mutant receptors, the specific removal of CT residues between Ser417 and Ser431 may disrupt the regulation of Thr354 and Ser372/Ser373 phosphorylation by PLZF, either through a disturbance in PLZF interaction or a change in the receptor conformation mediated by PLZF that allows for greater GRK recruitment to Thr354 and Ser372/Ser373 or to other residues

whose phosphorylation is necessary to impart phosphorylation of these sites. Overall, these findings coincide with previous unpublished results in the Tiberi lab showing that co-expression of the D1R and PLZF results in a decreased β-arrestin interaction with D1R (Josephine Zein, 2022, Master's Thesis, University of Ottawa). This likely demonstrates that PLZF could be competing with β-arrestin for complex formation with the receptor, allowing it to stay on the membrane for a longer period. Therefore, the inhibition of D1R DA-induced phosphorylation by PLZF may potentially be a mechanism for the inhibition of DA-induced internalization seen with D1R when in the presence of PLZF (**Fig. 33**).

Also, it is possible that PLZF modulates the phosphorylation of D1R through mediation of GRK activity. While no studies have reported an interaction between PLZF and GRKs, a study showed that GIT1 and GIT2, which are part of a family of multifunctional zinc-finger proteins, were found to interact with GRK2, 3, 5 and 6 through a Y2H screen. Though the precise domains of interaction are yet to be identified, it was found that endogenous GIT1 is strictly required for receptor internalization, and its overexpression strongly impaired the endocytosis of several GPCRs (Premont et al., 1998; Premont et al., 2000; Ribas et al., 2007). Therefore, the downregulation of phosphorylation observed in HEK293 cells overexpressing D1R with PLZF may arise in part from PLZF-mediated impedance of GRK activity. In other words, PLZF may create unfavourable conditions for GRKs to phosphorylate the Ser and Thr residues of the CT of D1R or it may form a complex with GRK, hindering its ability to access phosphorylation sites on the D1R.

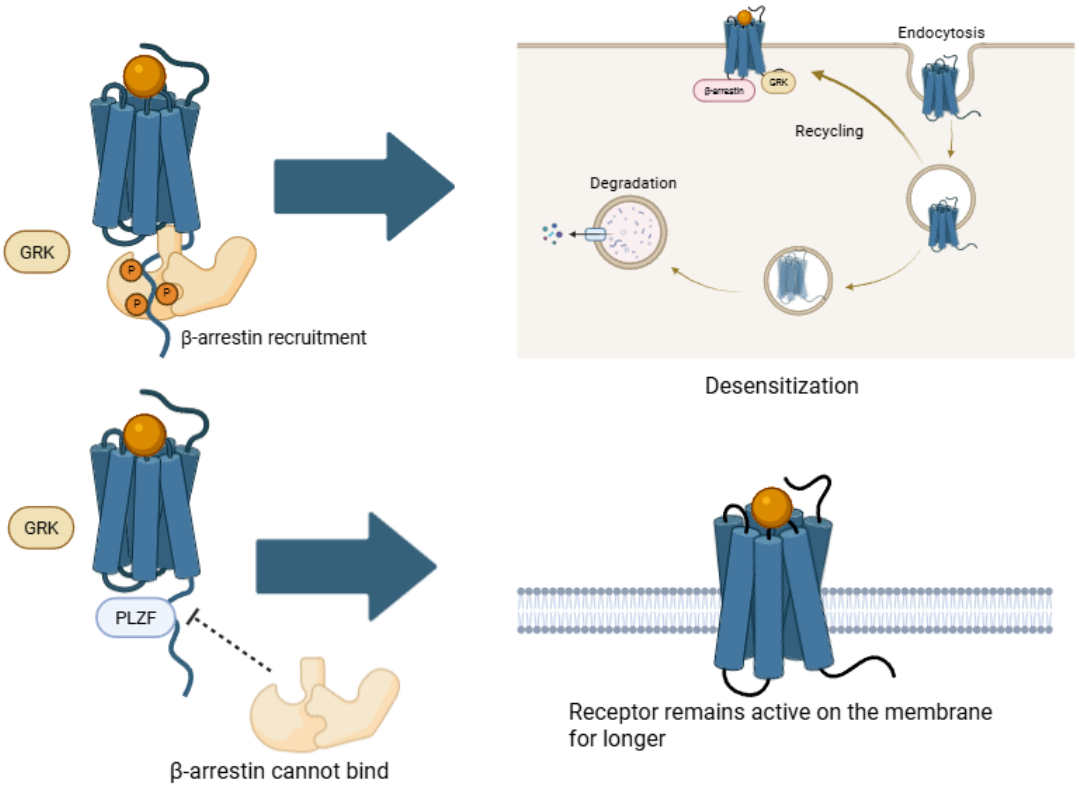

Figure 33. PLZF-Mediated Reduction in DA-Induced Phosphorylated Could Be a Factor in PLZF-Mediated Attenuation of D1R Internalization. Schematic diagram of the possible mechanism of PLZF-mediated reduction in D1R internalization. As GRK-mediated phosphorylation of the CT increases the binding affinity of β-arrestin to stimulate receptor endocytosis, a reduction in D1R phosphorylation at residues Thr354 and Ser372/Ser373 by PLZF may be a mediating factor in the decline of DA-mediated D1R internalization regulated by PLZF. Created with BioRender.com.

5.3. PLZF-D1R complex formation may be dynamic and interchangeable through fluctuations in the structural composition and chemical environment of the receptor

PLZF was first identified as a novel interactor of the D1R through a Y2H screen, where the use of the CT as bait pulled out PLZF as a positive match among several other potential interactors. On the contrary, the IL3 of D1R only isolated SAP102 as an interactor. Unpublished co-IP studies in the Tiberi lab have confirmed PLZF as an interactor in vitro. Additionally, preliminary data in our lab suggests that PLZF and D1R form a complex in-vivo, specifically within the hippocampus, striatum and cortex. Treatment with the natural agonist DA and the inverse agonist cis-flupentixol, respectively, enhanced and diminished PLZF recruitment to the receptor. As described in the ternary complex model, receptors can interchange between an inactive R conformation with low agonist affinity and an active R* conformation with high agonist affinity, whereby binding of an agonist stabilizes the receptor in the R* state while inverse agonists shift the equilibrium towards the R state (De Lean et al., 1980; Samama et al., 1993). This demonstrates that PLZF is likely rapidly associating and disassociating with the D1R under the basal state, however, PLZF recruitment appears to be rapidly enhanced when in contact with the active R* state of the D1R.

We previously demonstrated that PLZF alters the phosphorylation status of Ser and Thr residues on the D1R CT. Additionally, prior unpublished studies have found that PLZF downregulates D1R internalization. Given that phosphorylation of the CT is an important mediating step for the recruitment of β-arrestin to the cytosolic domains, whereby it can then stimulate receptor endocytosis, it is important to understand how the physical interaction between PLZF and the D1R is implicated in this phenomenon by mapping the precise interaction domains of PLZF on the D1R. A GST-pulldown assay was performed to confirm that the CT is the site of interaction. Interestingly, both the CT and IL3 of the D1R serve as interacting domains for PLZF, albeit the CT appears to mediate a stronger complex formation relative to the IL3. Although the IL3 had not been previously detected as a domain of interest during the preliminary Y2H screen, it is important to note that the accuracy of this approach is inherently limited and has been

known to generate a high rate of false negatives and even some false positives. This stems from many issues including protein misfolding or steric hindrance of the two proteins in yeast as well as the lack of post-translational modifications that are necessary for the interaction to occur (Rajagopala and Uetz, 2009; Galletta and Rusan, 2016). It is also possible that there may be intermediary proteins interacting with the GPCR in a cellular context that are required for the recruitment of PLZF to the IL3, hence its lack of positive results on the Y2H screen. In contrast, given that the bait in a Y2H screen is fused to the DNA-binding domain for the β-galactosidase gene, it cannot be ruled out that a positive interaction with a particular prey may be impacted by that domain. Therefore, using different protein-protein interaction approaches such as GST-pulldown assays and co-IPs are warranted to determine the interaction modalities of D1R with PLZF.

Interestingly, PLZF was found to interact with the receptor regardless of the truncation location of the CT, signifying that there are likely other domains involved in this interaction. It is also worth mentioning that the helix 8 (H8) was included as part of the CT bait that pulled out PLZF during the Y2H screen. H8 is a cytoplasmic domain located between the 7TM domain and the proximal CT portion of nearly all class A GPCRs (Sensoy and Weinstein, 2015). Studies have shown that this domain acts as a membrane-dependant conformational switch, meaning that it only adopts a helical structure when in the presence of membranes or membrane mimetics (Krishna et al., 2002). This suggests that PLZF may form a complex with H8, also known as the fourth intracellular domain (IL4), and this may explain why truncation of the CT does not impact the recruitment of PLZF to the D1R. Though high-resolution structures have not visualized this domain to the same degree as the rest of the receptor, many biochemical and biophysical studies have suggested that the H8 plays an important role in ligand binding, G-protein activation and receptor internalization (Tumova et al., 2004; Yang et al., 2019). Tumova et al demonstrated that swapping of H8 between the D1-class results in a switch in basal activity as well as dopamine affinity. Additionally, Yang et al found that swapping of the D1R H8 with that of D2R abolished β-arrestin-1/2-mediated desensitization. However, this was not the case when the D2R H8 was swapped for that of D1R,

showcasing that H8 alone is not sufficient in mediating the effects of desensitization. It is possible then that the recruitment of PLZF to the H8 of D1R may play a role in the downregulation of CT phosphorylation observed when PLZF is recruited to the D1R.

Additionally, the degree of recruitment changed under dopamine stimulation depending on the domain of IL3 that was cleaved. Specifically, cleavage of the IL3 N-terminus resulted in decreased recruitment of PLZF under agonist stimulation relative to basal state. Contrarily, cleavage of the IL3 C-terminus proceeded to increase PLZF recruitment during agonist stimulation relative to basal state, as was the case for truncation of any of the CT domains as well as with the wild-type receptor. Nonetheless, one of the most defining features from these results is that PLZF complex formation is always stronger with the mutated receptors than with the wildtype, regardless of the location of truncation.

It is possible that PLZF interacts with both the IL3 and CT at the same time, as the domains of PLZF that are involved in PLZF-D1R complex formation have not yet been investigated. Though the BTB/POZ domain is widely known to be the site of protein-protein interactions with PLZF, some studies have shown that the zinc-finger domain can form complexes with proteins in addition to DNA promotors. PLZF-mediated APL is caused by a reciprocal chromosomal translocation, fusing the retinoic acid receptor alpha (RARα) with PLZF to create two fusion protein products: PLZF-RARα and RARα-PLZF, whereby RARα forms a complex with the zinc fingers of PLZF in both proteins (Chen et al., 1993). A study by Sadler et al introduced small organic fluorophores at residues L258, located at the C-terminal domain of IL3, and Y350, located at the CT of the B2-AR to investigate the conformational dynamics of the IL3. FRET studies showed that these probes were relatively far apart under basal state. However, agonist stimulation resulted in increased FRET efficiency, suggesting that GPCR activation causes conformational changes within the IL3 and that these probes may be brought closer together during activation (Sadler et al., 2023; Wess, 2024). It is possible that PLZF forms a complex with both the D1R CT and the C-terminus of the IL3, and the decrease in distance between the two domains during receptor activation allows for more efficient recruitment of PLZF to the D1R. Removal of either the CT or IL3

may destabilize the protein complex, resulting in a compensatory effect by PLZF to form a tighter complex with the remaining domain so that PLZF can remain bound, hence the increase in PLZF binding under dopamine stimulation when these domains are removed.

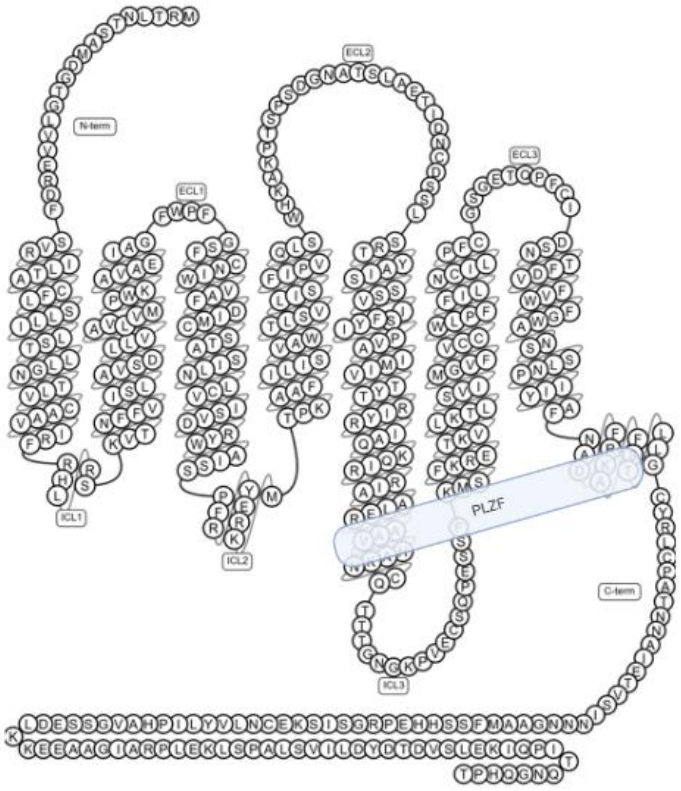

Figure 34. Working Model of PLZF-D1R Complex Formation. Schematic diagram of the potential D1R domains involved with the recruitment of PLZF. Based on results from the coimmunoprecipitation studies and GST-pulldown assays, PLZF appears to form a complex with both the IL3 and CT. As it is not yet known which domains of PLZF are involved in this interaction, it is possible that PLZF interacts with both D1R sites at the same time. Complete truncation of the D1R CT did not yield a loss of PLZF interaction, therefore PLZF may form a complex at the proximal H8 domain. Created with BioRender.com.

6. Limitations

Despite the many strengths of my MSc project, there are several limiting factors that should be considered, as they could potentially impact the interpretations of my obtained results. First off, the sample sizes of several of my studies were relatively modest, leading to reduced statistical power and a lower ability to detect smaller effect sizes. Nevertheless, some of these effects may be biologically meaningful, so performing future studies with larger sample sizes may help to confirm the reproducibility of these observed effects. Additionally, while many efforts were taken to control experimental conditions, it is possible that certain factors may have influenced the results and contributed to differences in the interpreted effect between samples numbers. For example, as previously described in some of the figure legends, detecting the immunoprecipitated receptor was unsuccessful for many of my samples, likely due to a combination of protein loss from repetitive stripping of the Western blot membrane or incomplete transfer of the gel proteins onto the membrane. Regardless, I conducted radioligand binding assays alongside all my co-immunoprecipitation studies to confirm the total level of receptor present, which sometimes differed between samples. Individual variability in receptor expression may alter the phosphorylation levels of residues Thr354 and Ser372/Ser373 on the D1R or the amount of receptor that can interact with PLZF. Given that these receptors are overexpressed in HEK293 cells, this may not fully recapitulate the effects of PLZF on endogenous receptor levels in native neuronal systems. Therefore, performing future studies in neuronal models or using inducible gene expression systems such as tetracycline (Fujimoto et al., 2010) to tightly regulate receptor expression could control these variabilities and improve the physiological relevance of my project. Another limitation I encountered in my project was due to the boiling of my IP samples when preparing them for my Western blots, resulting in the presence of additional higher-molecular bands when detecting the phosphorylation levels of Thr354 and Ser372/Ser373. Boiling samples at 100°C for 5 minutes is thought to be a critical step for Western blot preparation to denature proteins within the sample to allow the antibody better access to its specific epitope. However, boiling is not always necessary and, in some cases, can be detrimental to the proper migration of proteins on the SDS gel. Incomplete denaturation during boiling can cause exposed

hydrophobic domains in the protein structure to clump together and aggregate, resulting in bands that migrate at different molecular weights. I determined that boiling my samples was causing this issue as my samples migrated to their correct size once I stopped boiling them before loading. Finally, it could be considered a limitation that my project only analyzes the phosphorylation of three D1R residues. As I've previously discussed, there are 32 different serine and threonine residues on the D1R (Tiberi et al., 1996; Moritz et al., 2023). Though it is not known if all the serine and threonine residues can be phosphorylated, it is possible that PLZF could regulate the phosphorylation of some residues, which may contribute to its regulation of DA-induced D1R internalization. Future studies using antibodies that detect other phosphorylation sites or even performing whole-cell phosphorylation assays in the presence of PLZF may help to decipher the role of PLZF in regulating the rest of the D1R phosphorylation barcode.

7. Future directions

Through my M.Sc. project, we have identified PLZF as a novel interactor with the IL3 and CT of D1R. It remains to be known as to the exact domains of PLZF that interact with D1R. Both the BTB/POZ domain located at the N-terminus as well as the zinc fingers located at the C-terminus have been shown to confer protein-protein interactions. As previously stated in earlier sections, PLZF may form a complex with both domains at the same time or it may only be bound through either the BTB/POZ or zinc finger domain, interchanging its recruitment between the IL3 and CT. It is even possible that the centre RD2 domain, even though it has been formally regarded as a site for post-translational modifications, may be involved in this complex formation. A prior study by Hyman et al showed that both the RD2 and zinc finger domains were required for the association of PLZF with epsin, with epsin interaction being undetectable when only the zinc finger domain of PLZF was expressed (Hyman et al., 2000). Therefore, the RD2 domain may regulate complex formation between PLZF and D1R.

Additionally, exploring the role of PLZF in neurons expressing the D1R may help to elucidate how DA-mediated behaviours are modified by this complex. A study by Usui et al focused on the role of PLZF in the adult brain and found that not only does Zbtb16 regulate specific genes known to be involved in autism spectrum disorder and schizophrenia, but Zbtb16-knockout mice exhibit behaviours that are relevant to each of these disorders (Usui et al., 2021). Given that schizophrenia is well-associated with abnormalities in the dopaminergic system and that alterations in D1R expression within the prefrontal cortex and parieto-temporal cortex have been implicated in schizophrenia patients (Brisch et al., 2014), it is possible that complex formation between PLZF and D1R may play a role in the etiology of schizophrenia. Additionally, it has been shown that increased D1R signaling in the dorsal striatum promotes autistic-like behaviours (Lee et al., 2018). As prior studies in our lab have found that PLZF increases D1R-mediated cAMP production and ERK1/2 activation, recruitment of PLZF to the D1R may also be implicated in the behaviour of autistic patients.

As mentioned in the introduction section, studies show that PLZF plays a role in regulating the autophagy process, with mGluR5 activation promoting the inhibitory phosphorylation of ZBTB16 by GSK3-β, leading to activation of its ubiquitination activity through complex formation with Cullin3 and subsequent proteasomal degradation of the Atg14 protein (Zhang et al., 2015; Ibrahim et al., 2021). It is possible that PLZF may regulate D1R signaling through its ubiquitination activity or it may target the D1R itself for ubiquitination. Additionally, there are numerous autophagy-related proteins that are regulated by the D1R and PLZF, one of the most well-studied being the mechanistic Target of Rapamycin Complex 1 (mTORC1). A study found that inhibition of mTORC1 activity regulates autophagosome formation through the phosphorylation of ATG14 by the unc-51 like autophagy activating kinase 1 (ULK1) (Park et al., 2016). As well, increased mTORC1 activity during cocaine use was shown to be mediated by the D1R (Sutton and Caron, 2015). Additionally, a study demonstrated that PLZF regulates SPC maintenance through the repression of mTORC1 activity (Hobbs et al., 2011). Finally, inhibition of mTORC1 was found to prevent LID in mouse models of PD (Santini et al., 2009). As previously discussed, the pharmacological targeting of PLZF may aid in the development of novel therapies for LID, given that prior unpublished studies in our lab show that the co-expression of PLZF with D1R or D5R enacts differential and opposite modulation of functional activity between the subtypes. Specifically, PLZF reduces the recycling activity of the D5R while increasing that of D1R, causing D1R to be returned to the membrane more quickly. Therefore, PLZF may act on this protein to mediate the signaling and trafficking effects of the D1-class. PLZF may also act on mTORC1 to target the D5R to the autophagy machinery. Epsin may also be involved in the regulation of D1-class internalization by PLZF, as studies can show that it can directly interact with PLZF and together, can shuttle in and out of the nucleus (Hyman et al., 2000). Epsin has also been implicated in the internalization and autophagic destruction of Drosophila proteins (Csikós et al., 2009). Therefore, it could also play a role in PLZF-mediated regulation of D1-class internalization.

Unpublished studies in the lab have confirmed through immunoprecipitation that PLZF forms an interaction in-vitro with both the D1R and D5R (Josephine Zein 2022 MSc Thesis). Additionally, functional assays conducted in the lab showed that PLZF differentially regulates the signaling and trafficking activity between the two receptors. Specifically, PLZF enhances D1R-mediated cAMP signaling and ERK1/2 activity while decreasing that of D5R. PLZF also decreases internalization of D1R while increasing the internalization of D5R. It remains to be known the exact site of PLZF recruitment on the D5R as well as the molecular mechanisms underlying the regulation of D5R by PLZF. As we have demonstrated from the results of this study, PLZF regulates the internalization of D1R through modulation of phosphorylation on the CT, likely achieved through its dynamic binding pattern on the CT and to a lesser extent, the IL3. PLZF may interchange recruitment to the IL3 or CT depending on the current needs of the cell, or it may form a complex with both domains at the same time. Therefore, it is possible that alterations in the D5R phosphorylation pattern by PLZF may mediate its effects on internalization and this may be achieved through its recruitment to the IL3. PLZF-D5R interactions may allow for an increase in phosphorylation to the CT, thereby increasing the receptor's affinity for binding of β-arrestin. Alternatively, the binding of PLZF to the IL3 of D5R may increase the phosphorylation of the IL3 or alter the conformational structure of the receptor to allow for increased binding of β-arrestin. It is also possible that just like the D1R, PLZF may also form a complex with both the IL3 and CT of the D5R to mediate these effects. Therefore, further studies are needed to better understand the underlying molecular mechanisms surrounding the impact of PLZF on D5R activity.

8. Conclusion

The findings of my M.Sc. thesis have provided a clearer understanding of the underlying molecular mechanisms surrounding the regulation of D1R CT phosphorylation in addition to the PLZF-mediated regulation of D1R activity. The results of this project reveal the impact of the distal and central CT domains of the D1R on the phosphorylation of upstream residues, as well as the impact of PLZF recruitment on D1R phosphorylation and how this regulation is modulated through the distal and central domains. Specifically, the results demonstrate that phosphorylation of the distal and central residues of the D1R convey importance in mediating the phosphorylation of the proximal residues, with consecutive removal of these domains reducing phosphorylation of the upstream residues. These findings suggest that the CT is phosphorylated in a sequential manner, starting with the most distal residues, and this step may be important to phosphorylate the proximal residues, thereby mediating the correct structural conformation for b-arrestin to bind and initiate endocytosis of the receptor. This effect may also be regulated through changes in the recruitment of GRKs and other second messenger kinases.

The findings from this thesis also show that in the presence of PLZF, there is an observed decrease in DA-mediated phosphorylation at the proximal residues of the D1R. Interestingly, phosphorylation was further downregulated when PLZF was co-expressed with mutated forms of the D1R, whereby portions of the CT were truncated at various residues along the distal and central domains. As prior unpublished results in our lab have found that the presence of PLZF downregulates D1R internalization, these findings may be due to a downregulation in b-arrestin recruitment mediated by the decrease in phosphorylation. The removal of the distal and central CT domains, combined with the expression of PLZF, may further alter the structural conformation necessary for GRKs to bind and phosphorylate the CT. Moreover, the decrease in DA-induced D1R phosphorylation with PLZF may impact the level of GRK functional activity.

Finally, the results show that PLZF mediates a dynamic binding profile on the D1R, with PLZF interacting predominantly with the CT as well as the IL3 to a lower extent. Removal of either domain of

the IL3 conveys opposing patterns of recruitment between basal and dopamine-stimulated states. Complex formation between PLZF and any truncated form of the D1R was always stronger than with its wildtype counterpart, potentially hinting at a compensatory mechanism by PLZF to remain bound to the receptor. Future studies should further explore the effects of PLZF on the D5R as well as study the complex formation between PLZF and the D1-class in-vivo, specifically in brain tissues like the hippocampus and striatum where PLZF has been previously localized in other studies. Additionally, given the role of PLZF in regulating autophagy, future studies should look further at the link between PLZF and ubiquitination and regulation of other autophagy-related proteins and how this may mediate D1R functional activity. This project reveals that the functional relationship between PLZF and the D1R is much more complicated than previously thought, and further details about the molecular mechanisms underlying this complex formation may aid in a better understanding of the PLZF-mediated regulation of D1R.

Bibliography

Abd-Elrahman KS, Hamilton A, Vasefi M, Ferguson SSG. Autophagy is increased following either pharmacological or genetic silencing of mGluR5 signaling in Alzheimer's disease mouse models. Mol Brain. 2018 Apr 10;11(1):19. doi: 10.1186/s13041-018-0364-9. PMID: 29631635; PMCID: PMC5892040.

Abd-Elrahman, K.S., Hamilton, A. and Ferguson, S.S.G. (2019), mGluR5 regulates ZBTB16 pathway of autophagy in Alzheimer's disease in a sex-specific manner. The FASEB Journal, 33: 810.5-810.5. https://doi.org/10.1096/fasebj.2019.33.1_supplement.810.5

Abd-Elrahman KS, Albaker A, de Souza JM, Ribeiro FM, Schlossmacher MG, Tiberi M, Hamilton A, Ferguson SSG. Aβ oligomers induce pathophysiological mGluR5 signaling in Alzheimer's disease model mice in a sex-selective manner. Sci Signal. 2020 Dec 15;13(662):eabd2494. doi: 10.1126/scisignal.abd2494. PMID: 33323410.

Ahmad KF, Engel CK, Privé GG. Crystal structure of the BTB domain from PLZF. Proc Natl Acad Sci U S A. 1998 Oct 13;95(21):12123-8. doi: 10.1073/pnas.95.21.12123. PMID: 9770450; PMCID: PMC22795.

Andersson E, Tryggvason U, Deng Q, Friling S, Alekseenko Z, Robert B, Perlmann T, Ericson J. Identification of intrinsic determinants of midbrain dopamine neurons. Cell. 2006 Jan 27;124(2):393-405. doi: 10.1016/j.cell.2005.10.037. PMID: 16439212.

Aubert I, Guigoni C, Håkansson K, Li Q, Dovero S, Barthe N, Bioulac BH, Gross CE, Fisone G, Bloch B, Bezard E. Increased D1 dopamine receptor signaling in levodopa-induced dyskinesia. Ann Neurol. 2005 Jan;57(1):17-26. doi: 10.1002/ana.20296. PMID: 15514976.

Avantaggiato V, Pandolfi PP, Ruthardt M, Hawe N, Acampora D, Pelicci PG, Simeone A. Developmental analysis of murine Promyelocyte Leukemia Zinc Finger (PLZF) gene expression: implications for the neuromeric model of the forebrain organization. J Neurosci. 1995 Jul;15(7 Pt 1):4927-42. doi: 10.1523/JNEUROSCI.15-07-04927.1995. PMID: 7623123; PMCID: PMC6577856.

Barna M, Hawe N, Niswander L, Pandolfi PP. Plzf regulates limb and axial skeletal patterning. Nat Genet. 2000 Jun;25(2):166-72. doi: 10.1038/76014. PMID: 10835630.

Barna M, Merghoub T, Costoya JA, Ruggero D, Branford M, Bergia A, Samori B, Pandolfi PP. Plzf mediates transcriptional repression of HoxD gene expression through chromatin remodeling. Dev Cell. 2002 Oct;3(4):499-510. doi: 10.1016/s1534-5807(02)00289-7. PMID: 12408802.

Beaulieu JM, Gainetdinov RR. The physiology, signaling, and pharmacology of dopamine receptors. Pharmacol Rev. 2011 Mar;63(1):182-217. doi: 10.1124/pr.110.002642. Epub 2011 Feb 8. PMID: 21303898.

Beaulieu JM, Espinoza S, Gainetdinov RR. Dopamine receptors - IUPHAR Review 13. Br J Pharmacol. 2015 Jan;172(1):1-23. doi: 10.1111/bph.12906. PMID: 25671228; PMCID: PMC4280963.

Bergson C, Levenson R, Goldman-Rakic PS, Lidow MS. Dopamine receptor-interacting proteins: the Ca(2+) connection in dopamine signaling. Trends Pharmacol Sci. 2003 Sep;24(9):486-92. doi: 10.1016/S0165-6147(03)00232-3. PMID: 12967774.

Bermak JC, Li M, Bullock C, Zhou QY. Regulation of transport of the dopamine D1 receptor by a new membrane-associated ER protein. Nat Cell Biol. 2001 May;3(5):492-8. doi: 10.1038/35074561. PMID: 11331877.

Bernardo MV, Yelo E, Gimeno L, Campillo JA, Parrado A. Identification of apoptosis-related PLZF target genes. Biochem Biophys Res Commun. 2007 Jul 27;359(2):317-22. doi: 10.1016/j.bbrc.2007.05.085. Epub 2007 May 24. PMID: 17537403.

Bezard E, Brotchie JM, Gross CE. Pathophysiology of levodopa-induced dyskinesia: potential for new therapies. Nat Rev Neurosci. 2001 Aug;2(8):577-88. doi: 10.1038/35086062. PMID: 11484001.

Bohm A, Gaudet R, Sigler PB. Structural aspects of heterotrimeric G-protein signaling. Curr Opin Biotechnol. 1997 Aug;8(4):480-7. doi: 10.1016/s0958-1669(97)80072-9. PMID: 9265729.

Brisch R, Saniotis A, Wolf R, Bielau H, Bernstein HG, Steiner J, Bogerts B, Braun K, Jankowski Z, Kumaratilake J, Henneberg M, Gos T. The role of dopamine in schizophrenia from a neurobiological and evolutionary perspective: old fashioned, but still in vogue. Front Psychiatry. 2014 May 19;5:47. doi: 10.3389/fpsyt.2014.00047. Erratum in: Front Psychiatry. 2014;5:110. Braun, Anna Katharina [corrected to Braun, Katharina]; Kumaritlake, Jaliya [corrected to Kumaratilake, Jaliya]. PMID: 24904434; PMCID: PMC4032934.

Buaas FW, Kirsh AL, Sharma M, McLean DJ, Morris JL, Griswold MD, de Rooij DG, Braun RE. Plzf is required in adult male germ cells for stem cell self-renewal. Nat Genet. 2004 Jun;36(6):647-52. doi: 10.1038/ng1366. Epub 2004 May 23. PMID: 15156142.

Calebiro D, Koszegi Z, Lanoiselée Y, Miljus T, O'Brien S. G protein-coupled receptor-G protein interactions: a single-molecule perspective. Physiol Rev. 2021 Jul 1;101(3):857-906. doi: 10.1152/physrev.00021.2020. Epub 2020 Dec 17. PMID: 33331229.

Charpentier S, Jarvie KR, Severynse DM, Caron MG, Tiberi M. Silencing of the constitutive activity of the dopamine D1B receptor. Reciprocal mutations between D1 receptor subtypes delineate residues underlying activation properties. J Biol Chem. 1996 Nov 8;271(45):28071-6. doi: 10.1074/jbc.271.45.28071. PMID: 8910419.

Chen Z, Brand NJ, Chen A, Chen SJ, Tong JH, Wang ZY, Waxman S, Zelent A. Fusion between a novel Krüppel-like zinc finger gene and the retinoic acid receptor-alpha locus due to a variant t(11;17) translocation associated with acute promyelocytic leukaemia. EMBO J. 1993 Mar;12(3):1161-7. doi: 10.1002/j.1460-2075.1993.tb05757.x. PMID: 8384553; PMCID: PMC413318.

Cheng GL, Tang JC, Li FW, Lau EY, Lee TM. Schizophrenia and risk-taking: impaired reward but preserved punishment processing. Schizophr Res. 2012 Apr;136(1-3):122-7. doi: 10.1016/j.schres.2012.01.002. Epub 2012 Jan 27. PMID: 22285654.

Childers SR. Activation of G-proteins in brain by endogenous and exogenous cannabinoids. AAPS J. 2006 Mar 10;8(1):E112-7. doi: 10.1208/aapsj080113. PMID: 16584117; PMCID: PMC2751429.

Chun LS, Free RB, Doyle TB, Huang XP, Rankin ML, Sibley DR. D1-D2 dopamine receptor synergy promotes calcium signaling via multiple mechanisms. Mol Pharmacol. 2013 Aug;84(2):190-200. doi: 10.1124/mol.113.085175. Epub 2013 May 16. PMID: 23680635; PMCID: PMC3716318.

Cook M, Gould A, Brand N, Davies J, Strutt P, Shaknovich R, Licht J, Waxman S, Chen Z, Gluecksohn-Waelsch S, et al. Expression of the zinc-finger gene PLZF at rhombomere boundaries in the vertebrate hindbrain. Proc Natl Acad Sci U S A. 1995 Mar 14;92(6):2249-53. doi: 10.1073/pnas.92.6.2249. PMID: 7892256; PMCID: PMC42461.

Costoya JA, Hobbs RM, Barna M, Cattoretti G, Manova K, Sukhwani M, Orwig KE, Wolgemuth DJ, Pandolfi PP. Essential role of Plzf in maintenance of spermatogonial stem cells. Nat Genet. 2004 Jun;36(6):653-9. doi: 10.1038/ng1367. Epub 2004 May 23. PMID: 15156143.

Csikós G, Lippai M, Lukácsovich T, Juhász G, Henn L, Erdélyi M, Maróy P, Sass M. A novel role for the Drosophila epsin (lqf): involvement in autophagy. Autophagy. 2009 Jul;5(5):636-48. doi: 10.4161/auto.5.5.8168. Epub 2009 Jul 16. PMID: 19305132.

David G, Alland L, Hong SH, Wong CW, DePinho RA, Dejean A. Histone deacetylase associated with mSin3A mediates repression by the acute promyelocytic leukemia-associated PLZF protein. Oncogene. 1998 May 14;16(19):2549-56. doi: 10.1038/sj.onc.1202043. PMID: 9627120.

D'Aoust JP, Tiberi M. Role of the extracellular amino terminus and first membrane-spanning helix of dopamine D1 and D5 receptors in shaping ligand selectivity and efficacy. Cell Signal. 2010 Jan;22(1):106-16. doi: 10.1016/j.cellsig.2009.09.020. Epub 2009 Sep 26. PMID: 19786093.

Dearry A, Gingrich JA, Falardeau P, Fremeau RT Jr, Bates MD, Caron MG. Molecular cloning and expression of the gene for a human D1 dopamine receptor. Nature. 1990 Sep 6;347(6288):72-6. doi: 10.1038/347072a0. PMID: 2144334.

De Lean A, Stadel JM, Lefkowitz RJ. A ternary complex model explains the agonist-specific binding properties of the adenylate cyclase-coupled beta-adrenergic receptor. J Biol Chem. 1980 Aug 10;255(15):7108-17. PMID: 6248546.

Desmazières A, Charnay P, Gilardi-Hebenstreit P. Krox20 controls the transcription of its various targets in the developing hindbrain according to multiple modes. J Biol Chem. 2009 Apr 17;284(16):10831-40. doi: 10.1074/jbc.M808683200. Epub 2009 Feb 13. PMID: 19218566; PMCID: PMC2667770.

Diao J, Liu R, Rong Y, Zhao M, Zhang J, Lai Y, Zhou Q, Wilz LM, Li J, Vivona S, Pfuetzner RA, Brunger AT, Zhong Q. ATG14 promotes membrane tethering and fusion of autophagosomes to endolysosomes. Nature. 2015 Apr 23;520(7548):563-6. doi: 10.1038/nature14147. Epub 2015 Feb 9. PMID: 25686604; PMCID: PMC4442024.

Fan G, Ma J, Ma R, Suo M, Chen Y, Zhang S, Zeng Y, Chen Y. Microglia Modulate Neurodevelopment in Autism Spectrum Disorder and Schizophrenia. Int J Mol Sci. 2023 Dec 9;24(24):17297. doi: 10.3390/ijms242417297. PMID: 38139124; PMCID: PMC10743577.

Fang Q, Hu WW, Wang XF, Yang Y, Lou GD, Jin MM, Yan HJ, Zeng WZ, Shen Y, Zhang SH, Xu TL, Chen Z. Histamine up-regulates astrocytic glutamate transporter 1 and protects neurons against ischemic injury. Neuropharmacology. 2014 Feb;77:156-66. doi: 10.1016/j.neuropharm.2013.06.012. Epub 2013 Jun 18. PMID: 23791559.

Felice Reddy L, Green MF, Rizzo S, Sugar CA, Blanchard JJ, Gur RE, Kring AM, Horan WP. Behavioral approach and avoidance in schizophrenia: an evaluation of motivational profiles. Schizophr Res. 2014 Oct;159(1):164-70. doi: 10.1016/j.schres.2014.07.047. Epub 2014 Aug 19. PMID: 25153364; PMCID: PMC4177267.

Ferguson SS, Downey WE 3rd, Colapietro AM, Barak LS, Ménard L, Caron MG. Role of beta-arrestin in mediating agonist-promoted G protein-coupled receptor internalization. Science. 1996 Jan 19;271(5247):363-6. doi: 10.1126/science.271.5247.363. PMID: 8553074.

Ferguson SS. Evolving concepts in G protein-coupled receptor endocytosis: the role in receptor desensitization and signaling. Pharmacol Rev. 2001 Mar;53(1):1-24. PMID: 11171937.

Flower DR. Modelling G-protein-coupled receptors for drug design. Biochim Biophys Acta. 1999 Nov 16;1422(3):207-34. doi: 10.1016/s0304-4157(99)00006-4. PMID: 10548717.

Frederick AL, Yano H, Trifilieff P, Vishwasrao HD, Biezonski D, Mészáros J, Urizar E, Sibley DR, Kellendonk C, Sonntag KC, Graham DL, Colbran RJ, Stanwood GD, Javitch JA. Evidence against dopamine D1/D2 receptor heteromers. Mol Psychiatry. 2015 Nov;20(11):1373-85. doi: 10.1038/mp.2014.166. Epub 2015 Jan 6. PMID: 25560761; PMCID: PMC4492915.

Fredriksson R, Lagerström MC, Lundin LG, Schiöth HB. The G-protein-coupled receptors in the human genome form five main families. Phylogenetic analysis, paralogon groups, and fingerprints. Mol Pharmacol. 2003 Jun;63(6):1256-72. doi: 10.1124/mol.63.6.1256. PMID: 12761335.

Fujimoto K, Araki K, McCarthy DM, Sims JR, Ren JQ, Zhang X, Bhide PG. A transgenic mouse model of neuroepithelial cell specific inducible overexpression of dopamine D1-receptor. Neuroscience. 2010 Oct 27;170(3):961-70. doi: 10.1016/j.neuroscience.2010.07.036. Epub 2010 Jul 29. PMID: 20674683; PMCID: PMC2946832.

Furukawa M, He YJ, Borchers C, Xiong Y. Targeting of protein ubiquitination by BTB-Cullin 3-Roc1 ubiquitin ligases. Nat Cell Biol. 2003 Nov;5(11):1001-7. doi: 10.1038/ncb1056. Epub 2003 Oct 5. PMID: 14528312.

Furusho M, Kaga Y, Ishii A, Hébert JM, Bansal R. Fibroblast growth factor signaling is required for the generation of oligodendrocyte progenitors from the embryonic forebrain. J Neurosci. 2011 Mar 30;31(13):5055-66. doi: 10.1523/JNEUROSCI.4800-10.2011. PMID: 21451043; PMCID: PMC3086363.

Gaber ZB, Butler SJ, Novitch BG. PLZF regulates fibroblast growth factor responsiveness and maintenance of neural progenitors. PLoS Biol. 2013 Oct;11(10):e1001676. doi: 10.1371/journal.pbio.1001676. Epub 2013 Oct 8. PMID: 24115909; PMCID: PMC3792860.

Galletta BJ, Rusan NM. A yeast two-hybrid approach for probing protein-protein interactions at the centrosome. Methods Cell Biol. 2015;129:251-277. doi: 10.1016/bs.mcb.2015.03.012. Epub 2015 May 27. PMID: 26175443; PMCID: PMC5029858.

Gardner B, Liu ZF, Jiang D, Sibley DR. The role of phosphorylation/dephosphorylation in agonist-induced desensitization of D1 dopamine receptor function: evidence for a novel pathway for receptor dephosphorylation. Mol Pharmacol. 2001 Feb;59(2):310-21. doi: 10.1124/mol.59.2.310. PMID: 11160868.

Gerfen CR. Segregation of D1 and D2 dopamine receptors in the striatal direct and indirect pathways: An historical perspective. Front Synaptic Neurosci. 2023 Jan 19;14:1002960. doi: 10.3389/fnsyn.2022.1002960. PMID: 36741471; PMCID: PMC9892636.

Geyer R, Wee S, Anderson S, Yates J, Wolf DA. BTB/POZ domain proteins are putative substrate adaptors for cullin 3 ubiquitin ligases. Mol Cell. 2003 Sep;12(3):783-90. doi: 10.1016/s1097-2765(03)00341-1. PMID: 14527422.

Ghasemi N, Azizi H, Razavi-Amoli SK, Skutella T. The Role of Plzf in Spermatogonial Stem Cell Maintenance and Differentiation: Mapping the Transcriptional Dynamics and Key Interactions. Cells. 2024 Nov 21;13(23):1930. doi: 10.3390/cells13231930. PMID: 39682679; PMCID: PMC11640652.

Giudicelli F, Taillebourg E, Charnay P, Gilardi-Hebenstreit P. Krox-20 patterns the hindbrain through both cell-autonomous and non cell-autonomous mechanisms. Genes Dev. 2001 Mar 1;15(5):567-80. doi: 10.1101/gad.189801. PMID: 11238377; PMCID: PMC312642.

Golbabapour S, Majid NA, Hassandarvish P, Hajrezaie M, Abdulla MA, Hadi AH. Gene silencing and Polycomb group proteins: an overview of their structure, mechanisms and phylogenetics. OMICS. 2013 Jun;17(6):283-96. doi: 10.1089/omi.2012.0105. PMID: 23692361; PMCID: PMC3662373.

Goldman-Rakic PS. The cortical dopamine system: role in memory and cognition. Adv Pharmacol. 1998;42:707-11. doi: 10.1016/s1054-3589(08)60846-7. PMID: 9327997.

Guillemot F, Zimmer C. From cradle to grave: the multiple roles of fibroblast growth factors in neural development. Neuron. 2011 Aug 25;71(4):574-88. doi: 10.1016/j.neuron.2011.08.002. PMID: 21867876.

Handwerger KE, Gall JG. Subnuclear organelles: new insights into form and function. Trends Cell Biol. 2006 Jan;16(1):19-26. doi: 10.1016/j.tcb.2005.11.005. Epub 2005 Dec 1. PMID: 16325406.

Hobbs RM, Seandel M, Falciatori I, Rafii S, Pandolfi PP. Plzf regulates germline progenitor self-renewal by opposing mTORC1. Cell. 2010 Aug 6;142(3):468-79. doi: 10.1016/j.cell.2010.06.041. PMID: 20691905; PMCID: PMC3210556.

Hong SH, David G, Wong CW, Dejean A, Privalsky ML. SMRT corepressor interacts with PLZF and with the PML-retinoic acid receptor alpha (RARαlpha) and PLZF-RARαlpha oncoproteins associated with acute promyelocytic leukemia. Proc Natl Acad Sci U S A. 1997 Aug 19;94(17):9028-33. doi: 10.1073/pnas.94.17.9028. PMID: 9256429; PMCID: PMC23013.

Huguet G, Temel Y, Kádár E, Pol S, Casaca-Carreira J, Segura-Torres P, Jahanshahi A. Altered expression of dopaminergic cell fate regulating genes prior to manifestation of symptoms in a transgenic rat model of Huntington's disease. Brain Res. 2019 Jun 1;1712:101-108. doi: 10.1016/j.brainres.2019.01.041. Epub 2019 Jan 31. PMID: 30711400.

Hyman J, Chen H, Di Fiore PP, De Camilli P, Brunger AT. Epsin 1 undergoes nucleocytosolic shuttling and its eps15 interactor NH(2)-terminal homology (ENTH) domain, structurally similar to Armadillo and HEAT repeats, interacts with the transcription factor promyelocytic leukemia Zn(2)+ finger protein (PLZF). J Cell Biol. 2000 May 1;149(3):537-46. doi: 10.1083/jcb.149.3.537. PMID: 10791968; PMCID: PMC2174850.

Ibrahim KS, McLaren CJ, Abd-Elrahman KS, Ferguson SSG. Optineurin deletion disrupts metabotropic glutamate receptor 5-mediated regulation of ERK1/2, GSK3β/ZBTB16, mTOR/ULK1 signaling in autophagy. Biochem Pharmacol. 2021 Mar;185:114427. doi: 10.1016/j.bcp.2021.114427. Epub 2021 Jan 26. PMID: 33513340.

Jackson A, Iwasiow RM, Tiberi M. Distinct function of the cytoplasmic tail in human D1-like receptor ligand binding and coupling. FEBS Lett. 2000 Mar 24;470(2):183-8. doi: 10.1016/s0014-5793(00)01315-6. PMID: 10734231.

Jean-Charles PY, Kaur S, Shenoy SK. G Protein-Coupled Receptor Signaling Through β-Arrestin-Dependent Mechanisms. J Cardiovasc Pharmacol. 2017 Sep;70(3):142-158. doi: 10.1097/FJC.0000000000000482. PMID: 28328745; PMCID: PMC5591062.

Jensen AA, Pedersen UB, Kiemer A, Din N, Andersen PH. Functional importance of the carboxyl tail cysteine residues in the human D1 dopamine receptor. J Neurochem. 1995 Sep;65(3):1325-31. doi: 10.1046/j.1471-4159.1995.65031325.x. PMID: 7643110.

Jin H, Xie Z, George SR, O'Dowd BF. Palmitoylation occurs at cysteine 347 and cysteine 351 of the dopamine D(1) receptor. Eur J Pharmacol. 1999 Dec 15;386(2-3):305-12. doi: 10.1016/s0014-2999(99)00727-x. PMID: 10618483.

Jones-Tabah J, Mohammad H, Paulus EG, Clarke PBS, Hébert TE. The Signaling and Pharmacology of the Dopamine D1 Receptor. Front Cell Neurosci. 2022 Jan 17;15:806618. doi: 10.3389/fncel.2021.806618. PMID: 35110997; PMCID: PMC8801442.

Kang SI, Chang WJ, Cho SG, Kim IY. Modification of promyelocytic leukemia zinc finger protein (PLZF) by SUMO-1 conjugation regulates its transcriptional repressor activity. J Biol Chem. 2003 Dec 19;278(51):51479-83. doi: 10.1074/jbc.M309237200. Epub 2003 Oct 3. PMID: 14527952.

Kang K, Song MR. Diverse FGF receptor signaling controls astrocyte specification and proliferation. Biochem Biophys Res Commun. 2010 May 7;395(3):324-9. doi: 10.1016/j.bbrc.2010.03.174. Epub 2010 Apr 1. PMID: 20362555.

Kaya AI, Perry NA, Gurevich VV, Iverson TM. Phosphorylation barcode-dependent signal bias of the dopamine D1 receptor. Proc Natl Acad Sci U S A. 2020 Jun 23;117(25):14139-14149. doi: 10.1073/pnas.1918736117. Epub 2020 Jun 5. PMID: 32503917; PMCID: PMC7321966.

Kelly E, Bailey CP, Henderson G. Agonist-selective mechanisms of GPCR desensitization. Br J Pharmacol. 2008 Mar;153 Suppl 1(Suppl 1):S379-88. doi: 10.1038/sj.bjp.0707604. Epub 2007 Dec 3. PMID: 18059321; PMCID: PMC2268061.

Kim OJ, Ariano MA, Lazzarini RA, Levine MS, Sibley DR. Neurofilament-M interacts with the D1 dopamine receptor to regulate cell surface expression and desensitization. J Neurosci. 2002 Jul 15;22(14):5920-30. doi: 10.1523/JNEUROSCI.22-14-05920.2002. PMID: 12122054; PMCID: PMC6757921.

Kim OJ, Gardner BR, Williams DB, Marinec PS, Cabrera DM, Peters JD, Mak CC, Kim KM, Sibley DR. The role of phosphorylation in D1 dopamine receptor desensitization: evidence for a novel mechanism of arrestin association. J Biol Chem. 2004 Feb 27;279(9):7999-8010. doi: 10.1074/jbc.M308281200. Epub 2003 Dec 4. PMID: 14660631; PMCID: PMC4743542.

Kim E, Sheng M. PDZ domain proteins of synapses. Nat Rev Neurosci. 2004 Oct;5(10):771-81. doi: 10.1038/nrn1517. PMID: 15378037.

Klein MO, Battagello DS, Cardoso AR, Hauser DN, Bittencourt JC, Correa RG. Dopamine: Functions, Signaling, and Association with Neurological Diseases. Cell Mol Neurobiol. 2019 Jan;39(1):31-59. doi: 10.1007/s10571-018-0632-3. Epub 2018 Nov 16. PMID: 30446950; PMCID: PMC11469830.

Koken MH, Reid A, Quignon F, Chelbi-Alix MK, Davies JM, Kabarowski JH, Zhu J, Dong S, Chen S, Chen Z, Tan CC, Licht J, Waxman S, de Thé H, Zelent A. Leukemia-associated retinoic acid receptor alpha fusion partners, PML and PLZF, heterodimerize and colocalize to nuclear bodies. Proc Natl Acad Sci U S A. 1997 Sep 16;94(19):10255-60. doi: 10.1073/pnas.94.19.10255. PMID: 9294197; PMCID: PMC23349.

Kolesnichenko M, Vogt PK. Understanding PLZF: two transcriptional targets, REDD1 and smooth muscle α-actin, define new questions in growth control, senescence, self-renewal and tumor suppression. Cell Cycle. 2011 Mar 1;10(5):771-5. doi: 10.4161/cc.10.5.14829. Epub 2011 Mar 1. PMID: 21311223; PMCID: PMC3100790.

Kong MM, Hasbi A, Mattocks M, Fan T, O'Dowd BF, George SR. Regulation of D1 dopamine receptor trafficking and signaling by caveolin-1. Mol Pharmacol. 2007 Nov;72(5):1157-70. doi: 10.1124/mol.107.034769. Epub 2007 Aug 15. PMID: 17699686.

Krikov M, Thone-Reineke C, Müller S, Villringer A, Unger T. Candesartan but not ramipril pretreatment improves outcome after stroke and stimulates neurotrophin BNDF/TrkB system in rats. J Hypertens. 2008 Mar;26(3):544-52. doi: 10.1097/HJH.0b013e3282f2dac9. PMID: 18300867.

Krishna AG, Menon ST, Terry TJ, Sakmar TP. Evidence that helix 8 of rhodopsin acts as a membrane-dependent conformational switch. Biochemistry. 2002 Jul 2;41(26):8298-309. doi: 10.1021/bi025534m. PMID: 12081478.

Lamey M, Thompson M, Varghese G, Chi H, Sawzdargo M, George SR, O'Dowd BF. Distinct residues in the carboxyl tail mediate agonist-induced desensitization and internalization of the human dopamine D1

receptor. J Biol Chem. 2002 Mar 15;277(11):9415-21. doi: 10.1074/jbc.M111811200. Epub 2001 Dec 31. PMID: 11773080.

Lee Y, Kim H, Kim JE, Park JY, Choi J, Lee JE, Lee EH, Han PL. Excessive D1 Dopamine Receptor Activation in the Dorsal Striatum Promotes Autistic-Like Behaviors. Mol Neurobiol. 2018 Jul;55(7):5658-5671. doi: 10.1007/s12035-017-0770-5. Epub 2017 Oct 12. PMID: 29027111.

Lefkowitz RJ, Cotecchia S, Samama P, Costa T. Constitutive activity of receptors coupled to guanine nucleotide regulatory proteins. Trends Pharmacol Sci. 1993 Aug;14(8):303-7. doi: 10.1016/0165-6147(93)90048-O. PMID: 8249148.

Lewis MM, Watts VJ, Lawler CP, Nichols DE, Mailman RB. Homologous desensitization of the D1A dopamine receptor: efficacy in causing desensitization dissociates from both receptor occupancy and functional potency. J Pharmacol Exp Ther. 1998 Jul;286(1):345-53. PMID: 9655879.

Li X, Lopez-Guisa JM, Ninan N, Weiner EJ, Rauscher FJ 3rd, Marmorstein R. Overexpression, purification, characterization, and crystallization of the BTB/POZ domain from the PLZF oncoprotein. J Biol Chem. 1997 Oct 24;272(43):27324-9. doi: 10.1074/jbc.272.43.27324. PMID: 9341182.

Li Z, Benard O, Margolskee RF. Ggamma13 interacts with PDZ domain-containing proteins. J Biol Chem. 2006 Apr 21;281(16):11066-73. doi: 10.1074/jbc.M600113200. Epub 2006 Feb 10. PMID: 16473877.

Li Y, Li XH, Yuan H. Angiotensin II type-2 receptor-specific effects on the cardiovascular system. Cardiovasc Diagn Ther. 2012 Mar;2(1):56-62. doi: 10.3978/j.issn.2223-3652.2012.02.02. PMID: 24282697; PMCID: PMC3839167.

Lin HC, Ching YH, Huang CC, Pao PC, Lee YH, Chang WC, Kao TJ, Lee YC. Promyelocytic leukemia zinc finger is involved in the formation of deep layer cortical neurons. J Biomed Sci. 2019 Apr 26;26(1):30. doi: 10.1186/s12929-019-0519-8. PMID: 31027502; PMCID: PMC6485146.

Liu TM, Lee EH, Lim B, Shyh-Chang N. Concise Review: Balancing Stem Cell Self-Renewal and Differentiation with PLZF. Stem Cells. 2016 Feb;34(2):277-87. doi: 10.1002/stem.2270. Epub 2016 Jan 5. PMID: 26676652.

Logothetis DE, Kurachi Y, Galper J, Neer EJ, Clapham DE. The beta gamma subunits of GTP-binding proteins activate the muscarinic K+ channel in heart. Nature. 1987 Jan 22-28;325(6102):321-6. doi: 10.1038/325321a0. PMID: 2433589.

Luttrell LM, Roudabush FL, Choy EW, Miller WE, Field ME, Pierce KL, Lefkowitz RJ. Activation and targeting of extracellular signal-regulated kinases by beta-arrestin scaffolds. Proc Natl Acad Sci U S A. 2001 Feb 27;98(5):2449-54. doi: 10.1073/pnas.041604898. Epub 2001 Feb 20. PMID: 11226259; PMCID: PMC30158.

Luttrell LM. Reviews in molecular biology and biotechnology: transmembrane signaling by G protein-coupled receptors. Mol Biotechnol. 2008 Jul;39(3):239-64. doi: 10.1007/s12033-008-9031-1. Epub 2008 Feb 1. PMID: 18240029.

Ma XM, Blenis J. Molecular mechanisms of mTOR-mediated translational control. Nat Rev Mol Cell Biol. 2009 May;10(5):307-18. doi: 10.1038/nrm2672. Epub 2009 Apr 2. PMID: 19339977.

Marinissen MJ, Gutkind JS. G-protein-coupled receptors and signaling networks: emerging paradigms. Trends Pharmacol Sci. 2001 Jul;22(7):368-76. doi: 10.1016/s0165-6147(00)01678-3. PMID: 11431032.

Martin PJ, Delmotte MH, Formstecher P, Lefebvre P. PLZF is a negative regulator of retinoic acid receptor transcriptional activity. Nucl Recept. 2003 Sep 6;1(1):6. doi: 10.1186/1478-1336-1-6. PMID: 14521715; PMCID: PMC212040.

Mason JN, Kozell LB, Neve KA. Regulation of dopamine D(1) receptor trafficking by protein kinase A-dependent phosphorylation. Mol Pharmacol. 2002 Apr;61(4):806-16. doi: 10.1124/mol.61.4.806. PMID: 11901220.

Mathew R, Seiler MP, Scanlon ST, Mao AP, Constantinides MG, Bertozzi-Villa C, Singer JD, Bendelac A. BTB-ZF factors recruit the E3 ligase cullin 3 to regulate lymphoid effector programs. Nature. 2012 Nov 22;491(7425):618-21. doi: 10.1038/nature11548. Epub 2012 Oct 21. PMID: 23086144; PMCID: PMC3504649.

Matsunaga K, Saitoh T, Tabata K, Omori H, Satoh T, Kurotori N, Maejima I, Shirahama-Noda K, Ichimura T, Isobe T, Akira S, Noda T, Yoshimori T. Two Beclin 1-binding proteins, Atg14L and Rubicon, reciprocally regulate autophagy at different stages. Nat Cell Biol. 2009 Apr;11(4):385-96. doi: 10.1038/ncb1846. Epub 2009 Mar 8. PMID: 19270696.

Meda SA, Ruaño G, Windemuth A, O'Neil K, Berwise C, Dunn SM, Boccaccio LE, Narayanan B, Kocherla M, Sprooten E, Keshavan MS, Tamminga CA, Sweeney JA, Clementz BA, Calhoun VD, Pearlson GD. Multivariate analysis reveals genetic associations of the resting default mode network in psychotic bipolar disorder and schizophrenia. Proc Natl Acad Sci U S A. 2014 May 13;111(19):E2066-75. doi: 10.1073/pnas.1313093111. Epub 2014 Apr 28. PMID: 24778245; PMCID: PMC4024891.

Missale C, Nash SR, Robinson SW, Jaber M, Caron MG. Dopamine receptors: from structure to function. Physiol Rev. 1998 Jan;78(1):189-225. doi: 10.1152/physrev.1998.78.1.189. PMID: 9457173.

Moreira IS. Structural features of the G-protein/GPCR interactions. Biochim Biophys Acta. 2014 Jan;1840(1):16-33. doi: 10.1016/j.bbagen.2013.08.027. Epub 2013 Sep 7. PMID: 24016604.

Moritz AE, Madaras NS, Rankin ML, Inbody LR, Sibley DR. Delineation of G Protein-Coupled Receptor Kinase Phosphorylation Sites within the D_1 Dopamine Receptor and Their Roles in Modulating β-Arrestin Binding and Activation. Int J Mol Sci. 2023 Apr 1;24(7):6599. doi: 10.3390/ijms24076599. PMID: 37047571; PMCID: PMC10095280.

Mukouyama YS, Deneen B, Lukaszewicz A, Novitch BG, Wichterle H, Jessell TM, Anderson DJ. Olig2+ neuroepithelial motoneuron progenitors are not multipotent stem cells in vivo. Proc Natl Acad Sci U S A.

2006 Jan 31;103(5):1551-6. doi: 10.1073/pnas.0510658103. Epub 2006 Jan 23. PMID: 16432183; PMCID: PMC1345718.

Murphy TH, Miyamoto M, Sastre A, Schnaar RL, Coyle JT. Glutamate toxicity in a neuronal cell line involves inhibition of cystine transport leading to oxidative stress. Neuron. 1989 Jun;2(6):1547-58. doi: 10.1016/0896-6273(89)90043-3. PMID: 2576375.

Nanba D, Mammoto A, Hashimoto K, Higashiyama S. Proteolytic release of the carboxy-terminal fragment of proHB-EGF causes nuclear export of PLZF. J Cell Biol. 2003 Nov 10;163(3):489-502. doi: 10.1083/jcb.200303017. Epub 2003 Nov 3. PMID: 14597771; PMCID: PMC2173632.

Nguyen G, Delarue F, Burcklé C, Bouzhir L, Giller T, Sraer JD. Pivotal role of the renin/prorenin receptor in angiotensin II production and cellular responses to renin. J Clin Invest. 2002 Jun;109(11):1417-27. doi: 10.1172/JCI14276. PMID: 12045255; PMCID: PMC150992.

Oakley RH, Laporte SA, Holt JA, Barak LS, Caron MG. Association of beta-arrestin with G protein-coupled receptors during clathrin-mediated endocytosis dictates the profile of receptor resensitization. J Biol Chem. 1999 Nov 5;274(45):32248-57. doi: 10.1074/jbc.274.45.32248. PMID: 10542263

Oldham WM, Hamm HE. Heterotrimeric G protein activation by G-protein-coupled receptors. Nat Rev Mol Cell Biol. 2008 Jan;9(1):60-71. doi: 10.1038/nrm2299. PMID: 18043707.

Park JM, Jung CH, Seo M, Otto NM, Grunwald D, Kim KH, Moriarity B, Kim YM, Starker C, Nho RS, Voytas D, Kim DH. The ULK1 complex mediates MTORC1 signaling to the autophagy initiation machinery via binding and phosphorylating ATG14. Autophagy. 2016;12(3):547-64. doi: 10.1080/15548627.2016.1140293. PMID: 27046250; PMCID: PMC4835982.

Peppi M, Kujawa SG, Sewell WF. A corticosteroid-responsive transcription factor, promyelocytic leukemia zinc finger protein, mediates protection of the cochlea from acoustic trauma. J Neurosci. 2011

Jan 12;31(2):735-41. doi: 10.1523/JNEUROSCI.3955-10.2011. PMID: 21228182; PMCID: PMC3274172.

Plouffe B, D'Aoust JP, Laquerre V, Liang B, Tiberi M. Probing the constitutive activity among dopamine D1 and D5 receptors and their mutants. Methods Enzymol. 2010;484:295-328. doi: 10.1016/B978-0-12-381298-8.00016-2. PMID: 21036239.

Premont RT, Claing A, Vitale N, Freeman JL, Pitcher JA, Patton WA, Moss J, Vaughan M, Lefkowitz RJ. beta2-Adrenergic receptor regulation by GIT1, a G protein-coupled receptor kinase-associated ADP ribosylation factor GTPase-activating protein. Proc Natl Acad Sci U S A. 1998 Nov 24;95(24):14082-7. doi: 10.1073/pnas.95.24.14082. PMID: 9826657; PMCID: PMC24330.

Premont RT, Claing A, Vitale N, Perry SJ, Lefkowitz RJ. The GIT family of ADP-ribosylation factor GTPase-activating proteins. Functional diversity of GIT2 through alternative splicing. J Biol Chem. 2000 Jul 21;275(29):22373-80. doi: 10.1074/jbc.275.29.22373. PMID: 10896954.

Prenzel N, Zwick E, Daub H, Leserer M, Abraham R, Wallasch C, Ullrich A. EGF receptor transactivation by G-protein-coupled receptors requires metalloproteinase cleavage of proHB-EGF. Nature. 1999 Dec 23-30;402(6764):884-8. doi: 10.1038/47260. PMID: 10622253.

Rajagopala SV, Uetz P. Analysis of protein-protein interactions using array-based yeast two-hybrid screens. Methods Mol Biol. 2009;548:223-45. doi: 10.1007/978-1-59745-540-4_13. PMID: 19521828.

Rehman S, Rahimi N, Dimri M. Biochemistry, G Protein Coupled Receptors. [Updated 2023 Jul 30]. In: StatPearls [Internet]. Treasure Island (FL): StatPearls Publishing; 2025 Jan-. Available from: https://www.ncbi.nlm.nih.gov/books/NBK518966/

Ribas C, Penela P, Murga C, Salcedo A, García-Hoz C, Jurado-Pueyo M, Aymerich I, Mayor F Jr. The G protein-coupled receptor kinase (GRK) interactome: role of GRKs in GPCR regulation and signaling.

Biochim Biophys Acta. 2007 Apr;1768(4):913-22. doi: 10.1016/j.bbamem.2006.09.019. Epub 2006 Sep 30. PMID: 17084806.

Ross EM, Wilkie TM. GTPase-activating proteins for heterotrimeric G proteins: regulators of G protein signaling (RGS) and RGS-like proteins. Annu Rev Biochem. 2000;69:795-827. doi: 10.1146/annurev.biochem.69.1.795. PMID: 10966476.

Sadler F, Ma N, Ritt M, Sharma Y, Vaidehi N, Sivaramakrishnan S. Autoregulation of GPCR signalling through the third intracellular loop. Nature. 2023 Mar;615(7953):734-741. doi: 10.1038/s41586-023-05789-z. Epub 2023 Mar 8. PMID: 36890236; PMCID: PMC10033409.

Samama P, Cotecchia S, Costa T, Lefkowitz RJ. A mutation-induced activated state of the beta 2-adrenergic receptor. Extending the ternary complex model. J Biol Chem. 1993 Mar 5;268(7):4625-36. PMID: 8095262.

Santini E, Heiman M, Greengard P, Valjent E, Fisone G. Inhibition of mTOR signaling in Parkinson's disease prevents L-DOPA-induced dyskinesia. Sci Signal. 2009 Jul 21;2(80):ra36. doi: 10.1126/scisignal.2000308. PMID: 19622833.

Schefe JH, Menk M, Reinemund J, Effertz K, Hobbs RM, Pandolfi PP, Ruiz P, Unger T, Funke-Kaiser H. A novel signal transduction cascade involving direct physical interaction of the renin/prorenin receptor with the transcription factor promyelocytic zinc finger protein. Circ Res. 2006 Dec 8;99(12):1355-66. doi: 10.1161/01.RES.0000251700.00994.0d. Epub 2006 Nov 2. PMID: 17082479.

Schefe JH, Unger T, Funke-Kaiser H. PLZF and the (pro)renin receptor. J Mol Med (Berl). 2008 Jun;86(6):623-7. doi: 10.1007/s00109-008-0320-8. Epub 2008 Mar 12. PMID: 18335187.

Schiöth HB, Fredriksson R. The GRAFS classification system of G-protein coupled receptors in comparative perspective. Gen Comp Endocrinol. 2005 May 15;142(1-2):94-101. doi: 10.1016/j.ygcen.2004.12.018. Epub 2005 Feb 5. PMID: 15862553.

Sedaghat K, Tiberi M. Cytoplasmic tail of D1 dopaminergic receptor differentially regulates desensitization and phosphorylation by G protein-coupled receptor kinase 2 and 3. Cell Signal. 2011 Jan;23(1):180-92. doi: 10.1016/j.cellsig.2010.09.002. Epub 2010 Sep 17. PMID: 20837135.

Seidel K, Kirsch S, Lucht K, Zaade D, Reinemund J, Schmitz J, Klare S, Li Y, Schefe JH, Schmerbach K, Goldin-Lang P, Zollmann FS, Thöne-Reineke C, Unger T, Funke-Kaiser H. The promyelocytic leukemia zinc finger (PLZF) protein exerts neuroprotective effects in neuronal cells and is dysregulated in experimental stroke. Brain Pathol. 2011 Jan;21(1):31-43. doi: 10.1111/j.1750-3639.2010.00427.x. PMID: 20731660; PMCID: PMC8094305.

Senbonmatsu T, Saito T, Landon EJ, Watanabe O, Price E Jr, Roberts RL, Imboden H, Fitzgerald TG, Gaffney FA, Inagami T. A novel angiotensin II type 2 receptor signaling pathway: possible role in cardiac hypertrophy. EMBO J. 2003 Dec 15;22(24):6471-82. doi: 10.1093/emboj/cdg637. PMID: 14657020; PMCID: PMC291832.

Sensoy O, Weinstein H. A mechanistic role of Helix 8 in GPCRs: Computational modeling of the dopamine D2 receptor interaction with the GIPC1-PDZ-domain. Biochim Biophys Acta. 2015 Apr;1848(4):976-83. doi: 10.1016/j.bbamem.2014.12.002. Epub 2015 Jan 12. PMID: 25592838; PMCID: PMC4336197.

Sha J, Zhang M, Feng J, Shi T, Li N, Jie Z. Promyelocytic leukemia zinc finger controls type 2 immune responses in the lungs by regulating lineage commitment and the function of innate and adaptive immune cells. Int Immunopharmacol. 2024 Mar 30;130:111670. doi: 10.1016/j.intimp.2024.111670. Epub 2024 Feb 18. PMID: 38373386.

Shaknovich R, Yeyati PL, Ivins S, Melnick A, Lempert C, Waxman S, Zelent A, Licht JD. The promyelocytic leukemia zinc finger protein affects myeloid cell growth, differentiation, and apoptosis. Mol Cell Biol. 1998 Sep;18(9):5533-45. doi: 10.1128/MCB.18.9.5533. PMID: 9710637; PMCID: PMC109138.

Shahjouei S, Cai PY, Ansari S, Sharififar S, Azari H, Ganji S, Zand R. Middle Cerebral Artery Occlusion Model of Stroke in Rodents: A Step-by-Step Approach. J Vasc Interv Neurol. 2016 Jan;8(5):1-8. PMID: 26958146; PMCID: PMC4762402.

Skaggs K, Martin DM, Novitch BG. Regulation of spinal interneuron development by the Olig-related protein Bhlhb5 and Notch signaling. Development. 2011 Aug;138(15):3199-211. doi: 10.1242/dev.057281. PMID: 21750031; PMCID: PMC3133912.

Slater PG, Yarur HE, Gysling K. Corticotropin-Releasing Factor Receptors and Their Interacting Proteins: Functional Consequences. Mol Pharmacol. 2016 Nov;90(5):627-632. doi: 10.1124/mol.116.104927. Epub 2016 Sep 9. PMID: 27612874.

Song W, Shi X, Xia Q, Yuan M, Liu J, Hao K, Qian Y, Zhao X, Zou K. PLZF suppresses differentiation of mouse spermatogonial progenitor cells via binding of differentiation associated genes. J Cell Physiol. 2020 Mar;235(3):3033-3042. doi: 10.1002/jcp.29208. Epub 2019 Sep 20. PMID: 31541472.

Sprang SR, Chen Z, Du X. Structural basis of effector regulation and signal termination in heterotrimeric Galpha proteins. Adv Protein Chem. 2007;74:1-65. doi: 10.1016/S0065-3233(07)74001-9. PMID: 17854654.

Stoffel RH 3rd, Pitcher JA, Lefkowitz RJ. Targeting G protein-coupled receptor kinases to their receptor substrates. J Membr Biol. 1997 May 1;157(1):1-8. doi: 10.1007/s002329900210. PMID: 9141353.

Suliman BA, Xu D, Williams BR. The promyelocytic leukemia zinc finger protein: two decades of molecular oncology. Front Oncol. 2012 Jul 17;2:74. doi: 10.3389/fonc.2012.00074. PMID: 22822476; PMCID: PMC3398472.

Sun Q, Fan W, Chen K, Ding X, Chen S, Zhong Q. Identification of Barkor as a mammalian autophagy-specific factor for Beclin 1 and class III phosphatidylinositol 3-kinase. Proc Natl Acad Sci U S A. 2008

Dec 9;105(49):19211-6. doi: 10.1073/pnas.0810452105. Epub 2008 Dec 2. PMID: 19050071; PMCID: PMC2592986.

Sun J, Jia P, Fanous AH, van den Oord E, Chen X, Riley BP, Amdur RL, Kendler KS, Zhao Z. Schizophrenia gene networks and pathways and their applications for novel candidate gene selection. PLoS One. 2010 Jun 29;5(6):e11351. doi: 10.1371/journal.pone.0011351. PMID: 20613869; PMCID: PMC2894047.

Sutton LP, Caron MG. Essential role of D1R in the regulation of mTOR complex1 signaling induced by cocaine. Neuropharmacology. 2015 Dec;99:610-9. doi: 10.1016/j.neuropharm.2015.08.024. Epub 2015 Aug 24. PMID: 26314207; PMCID: PMC4703076.

Syrovatkina V, Alegre KO, Dey R, Huang XY. Regulation, Signaling, and Physiological Functions of G-Proteins. J Mol Biol. 2016 Sep 25;428(19):3850-68. doi: 10.1016/j.jmb.2016.08.002. Epub 2016 Aug 8. PMID: 27515397; PMCID: PMC5023507.

Tanowitz M, von Zastrow M. Identification of protein interactions by yeast two-hybrid screening and coimmunoprecipitation. Methods Mol Biol. 2004;259:353-69. doi: 10.1385/1-59259-754-8:353. PMID: 15250504.

Thibault D, Loustalot F, Fortin GM, Bourque MJ, Trudeau LÉ. Evaluation of D1 and D2 dopamine receptor segregation in the developing striatum using BAC transgenic mice. PLoS One. 2013 Jul 2;8(7):e67219. doi: 10.1371/journal.pone.0067219. PMID: 23843993; PMCID: PMC3699584.

Tiberi M, Nash SR, Bertrand L, Lefkowitz RJ, Caron MG. Differential regulation of dopamine D1A receptor responsiveness by various G protein-coupled receptor kinases. J Biol Chem. 1996 Feb 16;271(7):3771-8. doi: 10.1074/jbc.271.7.3771. PMID: 8631993.

Tumova K, Iwasiow RM, Tiberi M. Insight into the mechanism of dopamine D1-like receptor activation. Evidence for a molecular interplay between the third extracellular loop and the cytoplasmic tail. J Biol

Chem. 2003 Mar 7;278(10):8146-53. doi: 10.1074/jbc.M208059200. Epub 2002 Dec 30. PMID: 12509438.

Tumova K, Zhang D, Tiberi M. Role of the fourth intracellular loop of D1-like dopaminergic receptors in conferring subtype-specific signaling properties. FEBS Lett. 2004 Oct 22;576(3):461-7. doi: 10.1016/j.febslet.2004.09.059. PMID: 15498581.

Uings IJ, Farrow SN. Cell receptors and cell signalling. Mol Pathol. 2000 Dec;53(6):295-9. doi: 10.1136/mp.53.6.295. PMID: 11193047; PMCID: PMC1186983.

Usui N, Berto S, Konishi A, Kondo M, Konopka G, Matsuzaki H, Shimada S. Zbtb16 regulates social cognitive behaviors and neocortical development. Transl Psychiatry. 2021 Apr 24;11(1):242. doi: 10.1038/s41398-021-01358-y. Erratum in: Transl Psychiatry. 2021 May 11;11(1):279. doi: 10.1038/s41398-021-01402-x. PMID: 33895774; PMCID: PMC8068730.

Vanhaesebroeck B, Leevers SJ, Panayotou G, Waterfield MD. Phosphoinositide 3-kinases: a conserved family of signal transducers. Trends Biochem Sci. 1997 Jul;22(7):267-72. doi: 10.1016/s0968-0004(97)01061-x. PMID: 9255069.

Wang M, Lee FJ, Liu F. Dopamine receptor interacting proteins (DRIPs) of dopamine D1-like receptors in the central nervous system. Mol Cells. 2008 Apr 30;25(2):149-57. Epub 2008 Mar 28. PMID: 18414018.

Wheatley M, Wootten D, Conner MT, Simms J, Kendrick R, Logan RT, Poyner DR, Barwell J. Lifting the lid on GPCRs: the role of extracellular loops. Br J Pharmacol. 2012 Mar;165(6):1688-1703. doi: 10.1111/j.1476-5381.2011.01629.x. PMID: 21864311; PMCID: PMC3372823.

Won JH, Park JS, Ju HH, Kim S, Suh-Kim H, Ghil SH. The alpha subunit of Go interacts with promyelocytic leukemia zinc finger protein and modulates its functions. Cell Signal. 2008 May;20(5):884-91. doi: 10.1016/j.cellsig.2007.12.022. Epub 2008 Jan 12. PMID: 18262754.

Xu D, Holko M, Sadler AJ, Scott B, Higashiyama S, Berkofsky-Fessler W, McConnell MJ, Pandolfi PP, Licht JD, Williams BR. Promyelocytic leukemia zinc finger protein regulates interferon-mediated innate immunity. Immunity. 2009 Jun 19;30(6):802-16. doi: 10.1016/j.immuni.2009.04.013. Epub 2009 Jun 11. PMID: 19523849; PMCID: PMC2711215.

Xu B, Hrycaj SM, McIntyre DC, Baker NC, Takeuchi JK, Jeannotte L, Gaber ZB, Novitch BG, Wellik DM. Hox5 interacts with Plzf to restrict Shh expression in the developing forelimb. Proc Natl Acad Sci U S A. 2013 Nov 26;110(48):19438-43. doi: 10.1073/pnas.1315075110. Epub 2013 Nov 11. PMID: 24218595; PMCID: PMC3845161.

Yang HS, Sun N, Zhao X, Kim HR, Park HJ, Kim KM, Chung KY. Role of Helix 8 in Dopamine Receptor Signaling. Biomol Ther (Seoul). 2019 Nov 1;27(6):514-521. doi: 10.4062/biomolther.2019.026. PMID: 30971061; PMCID: PMC6824627.

Yeyati PL, Shaknovich R, Boterashvili S, Li J, Ball HJ, Waxman S, Nason-Burchenal K, Dmitrovsky E, Zelent A, Licht JD. Leukemia translocation protein PLZF inhibits cell growth and expression of cyclin A. Oncogene. 1999 Jan 28;18(4):925-34. doi: 10.1038/sj.onc.1202375. PMID: 10023668.

Zhang J, Vinuela A, Neely MH, Hallett PJ, Grant SG, Miller GM, Isacson O, Caron MG, Yao WD. Inhibition of the dopamine D1 receptor signaling by PSD-95. J Biol Chem. 2007 May 25;282(21):15778-89. doi: 10.1074/jbc.M611485200. Epub 2007 Mar 16. PMID: 17369255; PMCID: PMC2649122.

Zhang T, Dong K, Liang W, Xu D, Xia H, Geng J, Najafov A, Liu M, Li Y, Han X, Xiao J, Jin Z, Peng T, Gao Y, Cai Y, Qi C, Zhang Q, Sun A, Lipinski M, Zhu H, Xiong Y, Pandolfi PP, Li H, Yu Q, Yuan J. G-protein-coupled receptors regulate autophagy by ZBTB16-mediated ubiquitination and proteasomal degradation of Atg14L. Elife. 2015 Mar 30;4:e06734. doi: 10.7554/eLife.06734. PMID: 25821988; PMCID: PMC4421748.

Zollman S, Godt D, Privé GG, Couderc JL, Laski FA. The BTB domain, found primarily in zinc finger proteins, defines an evolutionarily conserved family that includes several developmentally regulated

genes in Drosophila. Proc Natl Acad Sci U S A. 1994 Oct 25;91(22):10717-21. doi: 10.1073/pnas.91.22.10717. PMID: 7938017; PMCID: PMC45093.